POLITECNICO DI MILANO

School of Industrial and Information Engineering
Master of Science in Materials Engineering and Nanotechnology
Department of Chemistry, Materials and Chemical Engineering "Giulio Natta"

SURFACE MODIFICATION TREATMENT OF

CARDIOVASCULAR TITANIUM STENT

Supervisors: Prof. Roberto Chiesa
                Dr. Monica Moscatelli

                                        Arash Mazinani

                                        787636

Academic Year: 2013-2014

Table of contents

Chapter 4: Materials and methods   44

List of Figures

x

List of tables

Abstract

Coronary artery disease is one of the leading cause of death worldwide.

Coronary angioplasty with deployment of stent is the most popular non-surgical treatment of cardiovascular disease which caused narrowing or occlusion (stenosis) of the affected vessel.

Unfortunately stenting is not a definitive answer to treatment of vessel occlusion symptoms. Deployment of stents combined with the balloon expansion is a traumatic event which result in inflammatory cells activation and vascular SMCs proliferation leading to the formation of a new neointimal tissue. In some cases, uncontrolled growth of this tissue leads to neointimal hyperplasia and re-occlusion of the treated vessel which is called In-Stent Restenosis (ISR).

In this work the possibility to coat titanium coronary stents by Anodic Spark Deposition (ASD) technique with a layer of anodized titanium doped by different elements such as Ca, P, Na and Si is investigated. The aim of this project is to obtain a biocompatible stent coating technology able to reduce the incidence of ISR in a cost-effective manner, in comparison to other current technologies such as drug-eluting stents.

Samples in a wide range of final voltages (155 V to 295 V) were coated and mechanical and physicochemical characterization of coatings were investigated. The main results after three point bending test showed that no delamination occurred on the surface of coatings deposited in low-voltage range which had undergone relatively high plastic deformation (12% elongation).

Abstract

La malattia coronarica è una delle principali cause di morte nel mondo.

L'angioplastica coronarica con impiego di stent è il più popolare trattamento non chirurgico della malattia cardiovascolare che ha causato restringimento o occlusione (stenosi) della coronaria interessata.

Purtroppo gli attuali stent non forniscono una risposta definitiva per il trattamento di questa patologia. L'applicazione dello stent in combinazione con l'espansione del palloncino atto a riaprire il vaso è un evento traumatico che comporta fenomeni infiammatori con attivazione di fattori e proliferazione di cellule che porta alla formazione di un nuovo tessuto neointimale. In alcuni casi, la crescita incontrollata di questo tessuto porta a iperplasia neointimale e alla ri-occlusione del vaso trattato (in-stent ri-stenosi - ISR).

In questo lavoro viene studiata la possibilità di utilizzare stent coronarici in titanio opportunamente trattati mediante tecnica di modifica superficiale Anodic Spark Deposition (ASD). Questa tecnica consente di modificare lo strato superficiale di titanio mediante anodizzazione ad alto voltaggio e di drogarlo con diversi elementi quali Ca, P, Na e Si. Lo scopo di questo progetto è quello di mettere a punto una tecnica di rivestimento su titanio adatta all'applicazione su stent, al fine di ottenere una superficie di titanio altamente biocompatibile e in grado di ridurre l'incidenza di ISR in modo economico, soprattutto in confronto alle altre costose tecniche attuali oggi possibili, che prevedono l'utilizzo di stent rivestiti con farmaci antiproliferativi (Drug-Eluting Stents).

Sono stati sviluppati diversi trattamenti di anodizzazione ad alto voltaggio tipo ASD, considerando una vasta gamma di voltaggi (155 V a 295 V). Tali trattamenti sono stati studiati e caratterizzati mediante test meccanici e analisi chimico-fisiche. Le analisi hanno consentito di individuare dei trattamenti utilizzabili per queste applicazioni, che consentono un'elevata deformazione plastica (fino al 12% di allungamento), necessaria per l'espansione dello stent, senza mostrare effetti di distacco e delaminazione dei rivestimenti superficiali dal substrato in titanio.

Summary

Introduction

The main role of the cardiovascular system is maintaining homeostasis, controlling continuous blood flow through the countless capillaries, reaching to every organs to ensure their survival. Controlling such a precise system is carried out by variant functions and component parts of cardiovascular system which serve all the cells according to their needs.

Unfortunately, this mechanism can be altered by pathological conditions. Cardiovascular disease which causes narrowing or occlusion (stenosis) of the affected vessel, is the leading cause of deaths worldwide. though, since the1970s, cardiovascular mortality rates have declined in many high-income countries due to impressive progress that has been achieved in recent decades .[2] Angioplasty is a non-invasive surgical technique to mechanically widen narrowed or obstructed arteries preferred by surgeons applied in atherosclerotic coronary vessels. Although angioplasty eliminates the atherosclerotic plaque, after a relatively short period of time, the tissue damage induced by the balloon expansion lead to an inflammatory response and finally restenosis.

Restenosis occurs when the treated vessel becomes re-narrowed or blocked again. The chance of restenosis in the case of alone balloon angioplasty is 40%.The only widely accepted method to reduce restenosis after angioplasty has been the deployment of a coronary stent combined with the balloon expansion. Stenting reduces the chance of restenosis to 25% and it is widely used in different centres in the United States and Europe in over 70% of PCI.

In 1986, Puel and Sigwart, invented the first coronary stent (an expandable lattice-shaped metal tubular mesh usually made of stainless steel) to prevent vessel closure during percutaneous transluminal coronary angioplasty (PTCA).Despite the widespread use of these devices, Bare Metal Stents (BMS) have been associated with a 20-30%

restenosis rate due to the stimulation occurs in formation of a neointimal tissue leading to neointimal hyperplasia, particularly in the small calibre vessels (under 2.5mm of diameter), where the incidence of in-stent restenosis (ISR) is approximately 15-30% [39] which requiring re-intervention.[42,44]

In the last few years many efforts have been performed to reduce the risk of ISR by developing new types of stents. In 2001, Drug-Eluting Stents (DES) were introduced as a new approach to minimize restenosis and requirement for re-intervention but factors such as high costs for the healthcare and the long-term results of some clinical trials, are two main problems related to DES [46,47] which seems to suggest that another direction should be set out.

In this work the possibility to coat titanium coronary stents with a layer of anodized titanium doped by different elements such as Ca, P, Na and Si is investigated, in the attempt of providing a titanium-core stent with a biocompatible coating, regarded as an alternative, cost-effective approach to drug-eluting stents for decreasing ISR.

Materials and methods

Specimen preparation and characterization

All the samples used for the mechanical, physical and chemical characterization were obtained from a plate of pure titanium grade 2 for biomedical use provided by Torresin Titanio Metalli S.r.l., Limena, Italy. Then the samples cut into 2 different shapes: the first set, rectangular shape (10cm x 1cm) with the average thickness of 0.8 mm ,for the assessment of mechanical characterization of coating, and the second one , titanium disks (diameter:12mm and 0.6 mm thickness), for the analysis of physicochemical properties of titanium samples.

Before undergoing any treatments, all of the samples were cleaned and rinsed in Millipore water and some etched in etching solution (HF 5%-HNO3 30%) for 15 seconds and rinsed in water Millipore again for further 10 minutes. Finally the samples were dried in a thermostat oven at 37°C for 4 hours.

Anodic Spark Deposition (ASD) technique has been used to coat titanium samples with an electrolytic solution (SIB) at 0°C. For the coating process, were used wide range of final voltage from 155V to 295V and current of 12 and 10 [mA/cm2] for rectangular and disk shape samples respectively.

The electrolytic solution (SIB) developed in the Politecnico di Milano. [101] (Na2SiO3*2H2O 0.03M, β-GP 0.1M, C4H6CaO4*H2O 0.3M, NaOH 0.036M)

During the process the temperature of the refrigerant fluid is automatically controlled and kept between -1°C and 0°C and the anti-freezing fluid also added in some cases which is composed from half Millipore water and half (v/v) Paraflu .All the treatments were performed in galvano-static conditions.

After the ASD treatments some surfaces were subjected to an alkali treatments in 5M NaOH for 2h at 60 ± 2°C. Finally after alkali treatment, samples rinsed with distilled water and were dried in a thermostat oven at 37°C for 4 hours.

For nominated sample (175V) electropolishing of titanium in an alcoholic solution-based electrolyte before ASD treatment also has been carried out. A non-aqueous electrolyte comprising ethyl alcohol (700 ml/L), isopropyl alcohol (300 ml/L), aluminum chloride (60 g/L), and zinc chloride (250 g/L) was prepared. Electropolishing was performed under an electrolytic condition of 70－75 V, 2.0 kA/m2, and 30℃ for 15 to 20 minutes.

Then the mechanical, physicochemical and morphological characterizations of the surfaces obtained by ASD treatments were investigated by means of the following techniques:

SEM: all the samples were analyzed by ZEISS-EVO 50 EP or Cambridge – Stereo scan 360

The samples were analyzed at different magnifications after the surface treatments, electropolishing and TiO2 delamination tests.

EDS: the EDS analysis carried out on 500X and, in some cases, on 2k.X magnification (Oxford, Inca energy 200) that correspond to micrometric surface (170m x 230m and 17m x 23m respectively) have permitted to assess the qualitative and semi-quantitative chemical composition of oxide layer.

Profilometry: To study the surfaces roughness 6 measurement on base lines of 4mm and points density of 500/mm per each sample were performed with laser profilometer (UBM Microfocus, 5600).

Contact angle: The contact angle measurements were performed according to the static sessile drop method, by an optical device (Data physics Instruments Mod. OCA 15 plus) and a related software (32-bit software SCA20); was used a water drop of a 2μl of volume, deposed in 1μl/s (medium speed) on the samples surface.

At least 4 different water drop depositions at room temperature were performed for each nominate disk shape and rectangular sample.

ICP-OES: surface of 3 disk shape samples, treated in final nominated voltage (175 V) were investigated by ICP-OES analysis to calculate the amount of Na, Ca, P and Si on their surfaces. Two of the samples, treated by alkali solution in 5M NaOH for 2h at 60 ± 2°C in advance.

Before analysis the samples were treated with nitric acid 1: 1 and ultrasounded for 2 hours; the quantitative determination was carried out with a tool model Perkin Elmer Optima 8300.

TiO2 delamination tests:

To analyze the coating susceptibility to delamination, a three-point bending test was carried out on coated rectangular shape (10cm x 1cm) samples with thickness of 0.75 to 0.85

mm by applying high plastic deformation around 12% to 13% on coated samples.

The evaluated coating was on the convex side, and the span and max bend-displacement were set to 20 mm and 10 mm respectively. Max bend-displacement equal to samples flexion of 110°was attained. Besides for nominated samples (175 V), bend-displacement also in 4mm were performed.

Results and Discussion

SEM Result

First observation of surfaces after ASD treatment by SEM demonstrates pore size with circular shape and bigger in dimension for coating treated in higher voltage set. Pores are distributed more homogenously across the surface. Besides some micro cracks are detectable on the surface of treated samples in high voltage range particularly on 295 V to 265 V. Meanwhile by lowering the voltage, pore size becomes smaller.

Different morphology is reported in lower voltage range which depicts elongated shape pores stretched out along the coated surface in a less homogeneous distribution pattern. Similarly by lowering the voltage, less regular pores with lower density are detectible.

SEM results after three point bending test

The SEM analyses after bending test showed sever delamination of coating on high final voltage range; while no peeling and delaminating occurred on the Ti–O film on the lower voltage set from 175 V downward which had undergone relatively high plastic deformation. It demonstrates better adhesion of coating on 175V ASD treated substrate than other deposition method such as Sol-Gel coating method, which the maximum acceptable plastic deformation without any sign of Ti-O film delamination is less than 8% [110]. This behavior can be justified regarding to this fact that, by increasing the ASD treatment voltage, the thickness of brittle oxide layer increases which makes the coating more prone to delaminate during bending test.

Besides, since by leveling up the voltage, the amount of doped elements on the oxide layer increases so 175 V can be regarded as nominated maximum final voltage in a way that final coating serves the best both mechanical and physicochemical aspect of the project.
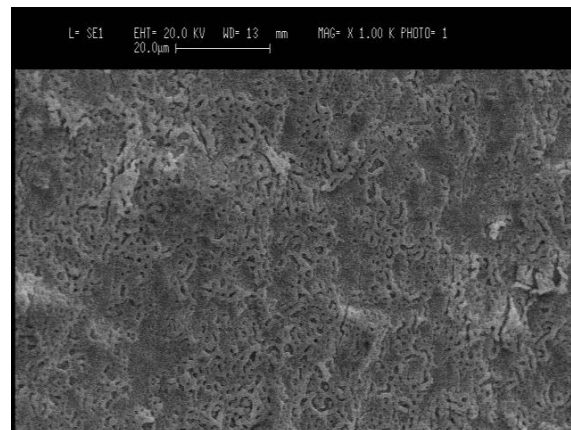
Fig S.1 SEM Image at 1K.X of Bended sample 175.R (12%)
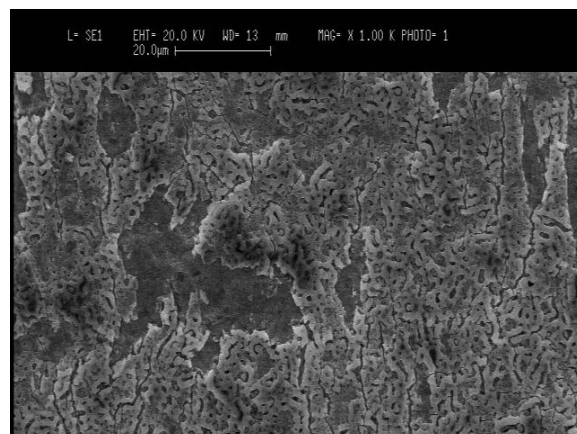
Fig S.2 SEM Image at 1K.X of Bended sample 195.R (12%)

For the sample which first electropolished and then deposited in nominated voltage (175V), in comparison with 175V treated sample without electropolishing ,no notable alteration in surface morphology has been observed by SEM analysis.

EDS

Figure S.3 depicts semi-quantitative result of EDS in which, all elements analysed (Normalised) and all results represented in weight%:
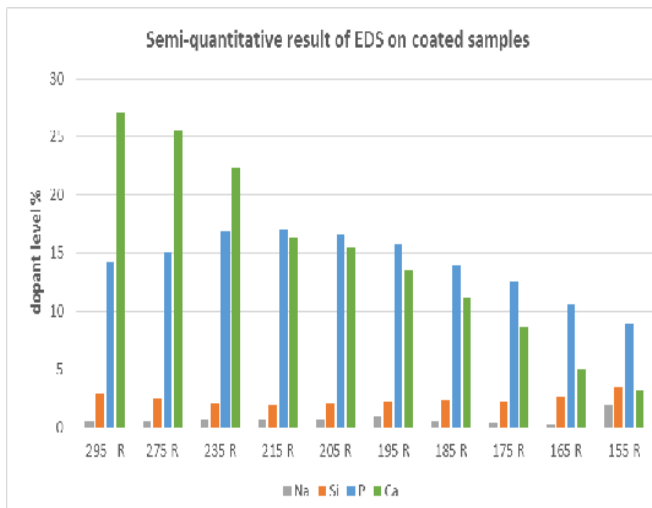
Fig S.3 Semi-quantitative result of EDS

The EDS results demonstrate a decreasing trend for Ca level on the coating as treatment final voltage decreases.

On the other side, P level shows slight fluctuation. It increases by increasing the treatment voltage and reaches to its peak at 205V then remains stable till 275 V where it follows by slight fall in P level.

It is important to mention that at around 215 V (treatment voltage), minimum difference between Ca and P level on the coating has been observed, so at 215 V, Ca/P ratio tends to almost 1.

Besides, Si level doesn't alter significantly by changing final treatment voltage. However, EDS results are semi-quantitative and are not precise so further analysis with ICP-OES has been carried out to calculate precise amount of dopants on the coating.

Contact angle

The measurements of the static contact angle shows that surfaces of all the samples which treated by alkali solution have water contact angle values lower than untreated titanium grade 2 indicating that the alkali treatment after ASD leads to an increase in surface hydrophilicity. Among applied voltages, 175 V ,185 V,255 V and 295 V (which followed by alkali treatment)showed better wettability properties with contact angle less than 55°(Berg's threshold) which is considered to limit the denaturation of adsorbed plasma proteins. (P<0.01)

So the surface of titanium dioxide in these voltages show higher hydrophilic properties and regarding to this fact that hydrophilic surfaces enhance interactions with biological fluids, cells and tissues and have a better resistance to bacterial adhesion it is expected to lead to better biocompatibility in body environment. [126,127]
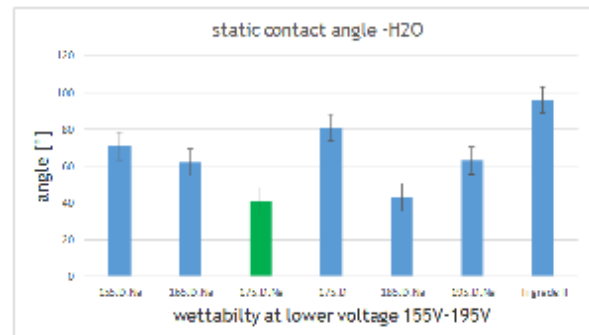
Fig S.4 Wettability of treated surface in lower voltages range (195V to 155V)

The ICP-OES

ICP-OES analyses indicates the effect of NaOH alkali treatment on alteration of Ca/P ratio for 175V ASD treated sample.

For 175 V non alkali treated sample Ca/P ratio is almost 2.69 while, after alkali treatment in 5M NaOH for 2h at 60 °C, Ca/P ratio increase and is equal to 3.6.

Besides, due to the nature of this kind of treatment, level of Na has been raised sharply on the alkali treated coatings.

Comparison between our ICP-OES results with the results for Ca and Si release from ASD treated sample at 295 V, (regarding to the previous work which has been done with the same electrolytic solution [124]) exhibit notable decrease

in Ca level while Si level has not been changed remarkably.
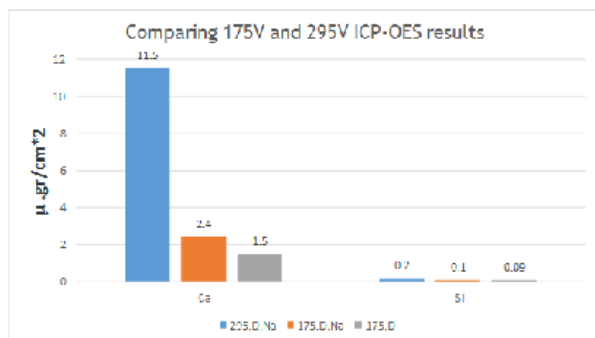
Fig S.5 ICP-OES results for samples 295.D.Na, 175.D.Na and 175.D

Laser Profilometry

The results of profilometry analysis shows that average roughness parameter(Ra) for the electropolished sample which has not been treated by ASD is about 0.284 µm and is moderately higher than the similar sample which firstly electropolished and then coated by ASD technique with Ra parameter 0.242 µm. (P<0.05)

Conclusion and Future work

In this project the possibility to coat titanium coronary stents with a layer of anodized titanium doped by different elements such as Ca, P, Na and Si by ASD treatment method was investigated, in the attempt of providing a Ti-core stent with a new biocompatible coating.

One of the main challenge of this project was to find maximum ASD treatment voltage needed to guarantee appropriate adherence of coating on titanium substrate at approximately high level of applied plastic deformation (12 %-13%).

The results of SEM analysis showed, 175 V was the optimum voltage which could be applied on the titanium rectangular

shape sample by ASD treatment, which result in (bended) coating without any trace of delamination or peeling. Although lower voltages (below 175V) also satisfy mechanical aspect of the project, EDS analysis demonstrated that level of dopants deposited on their surfaces were much lower compared to 175V coating .

Besides , 175V and 185V ASD treated samples which followed by chemical NaOH etching treatment showed better wettability characterization than other samples with contact angle less than 55°(Berg's threshold) which is expected to lead to better biocompatibility in body environment. (P<0.01) [126,127]

Average micro roughness (Ra) of the available coronary stents covers range of 0.11 µm to 0.6 µm, [130] besides, results of laser profilometry analysis for all the ASD treated samples exhibited Ra values lower than 0.36 µm which are in the acceptable range of surface roughness for the stent production.(P<0.05)

In light of these considerations, the ASD treatments on titanium with SIB electrolytic solution (Na2SiO3*2H2O 0.03M, β-GP 0.1M, C4H6CaO4*H2O 0.3M, NaOH 0.036M) which previously developed for dental and orthopaedic application can also be applicable (in term of mechanical and physiochemical aspects) in stent related fields such as endovascular surgery and stent placement in hemodialysis access. [129]

Since this work, deals only with mechanical and physiochemical terms of stent production, further in vitro investigations are required for a better understanding of body biological response to this new kind of stent coating.

.

Chapter 1

In-stent restenosis, biology and mechanisms

1.1 Introduction

Cardiovascular system is a bodily system, Responsible for transporting oxygen, nutrients, and blood to the billions of body cells and carries away wastes such as carbon dioxide from them, which with its unique and precise architecture assures the vital function of the whole human body.

The Cardiovascular System is divided into three main parts:

Body's hardest-working organ the heart, blood and the blood Vessels.

Veins and coronary arteries are the body's highways which allow blood to flow speedily and efficiently from the heart to every region of the body and back again.

Coronary artery includes three united layers: Tunica Intima, Media and Adventitia.

Tunica intima : the innermost layer, consisting of thin and simple endothelial cells providing the blood vessel wall, surrounded by a thin layer of sub endothelial with anti-coagulant properties. (Figure 1.1)

Media : This layer lies between the tunica on the inside and the adventitia on the outside ,is a multi-layered tissue , rich in vascular smooth muscle cells (SMCs), surrounded by an extra-cellular matrix (ECM) that brings flexibility especially in contraction mode both in radial and axial direction and controls the caliber of the veins.[1]

Tunica adventitia: also known as tunica externa, entirely made of collagen. It also contains nerves that supply the muscular layer, this is the outer tissue layer, which assures a strong structural function to the whole vessel.

As previously cited due to periodic contraction and relaxation of SMC's , coronary wall acquires best possible flexibility which guarantee constant flow through the veins in the whole circulatory system.
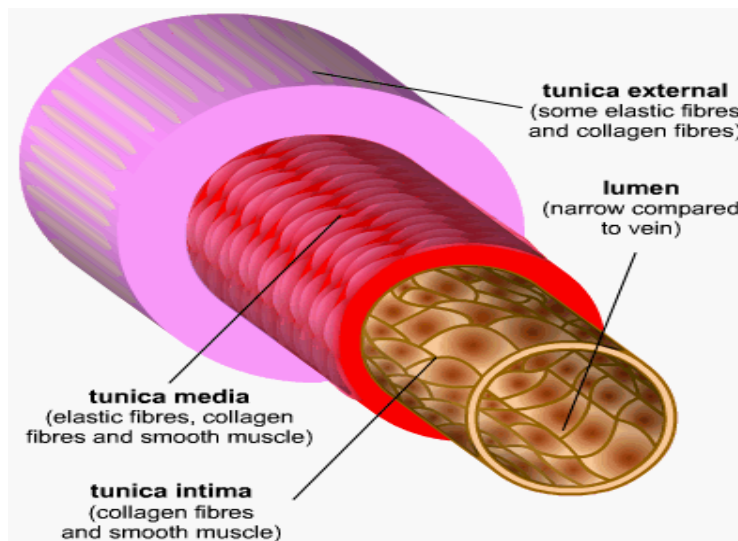
Fig 1.1 Schematic view of Coronary artery [116]

Besides, endothelium produced by vascular endothelial cells is the thin layer of cells that are in direct contact with blood flow in vessel, these cells have unique functions in vascular biology, possessing high hydrophilic nature which Inhibit coagulation of the blood , named thrombus, (or blood clot) and also they have important role in fluid filtration, such as in the glomeruli of the kidney, infiltration of plasma components as well as inflammatory cells from the blood to the surrounding tissue in case of injuries.

Pathological problems and conditions can significantly affect the balance of these functions and may lead to coronary artery diseases such as narrowing or occlusion (stenosis) of the vessel.

Cardiovascular disease is the leading cause of deaths worldwide, though, since the1970s, cardiovascular mortality rates have declined in many high-income countries due to impressive progress that has been achieved in recent decades .[2]

1.2 Coronary artery disease: atherosclerosis

Atherosclerosis is a process responsible for many heart disease, is typically hardening of arterial blood vessels mainly due to pathological conditions which disrupt balance of functions leads to the intima's endothelial layer failure (the deposition of lipoproteins, plasma proteins that carry cholesterol and triglycerides),thus increasing adhesiveness of the endothelium to platelets and leukocytes. The endothelial layer acquires a pro-coagulant tendency and starts to synthesize cytokines and growth factors.

In the case of atherosclerosis, infiltration of inflammatory cells to the space separating the endothelial layer (intima) from the SMC layer (media) occurs, in the next step, high activity of the occupied inflammatory cells result in initiation of the proliferation of SMCs into the vessel lumen. As a consequence of this action, a partial, or in some cases a complete stenosis occurs.

Blood fellow blockage particularly in a coronary artery would be deadly regarding to this fact that, when stenosis develops to the certain point, the area of cardiac muscle tissue is deprived of oxygen and nutrients.[3][4]

The most common cause of coronary occlusion is the progressive development of atherosclerosis, It also can be caused by normal aging, by high blood pressure, high LDL cholesterol, oxidative stress secondary to various genetic by diseases such as diabetes, smoking, lack of physical activity, and a combination of them. [31]

When the blockage is limited, chest pain or pressure called Angina Pectoris, may occur; whereas, in case of complete stenosis, the quantity of blood is not enough to the need of the supplied district, the result is a heart attack (Myocardial Infarction or heart muscle death).

Atherosclerosis is a type of arteriosclerosis that affects only the inner lining of an artery which is the result of an excessive and prolonged inflammatory condition. It is characterized by plaque deposits that block the flow of blood. Moreover in the cardiac district, atherosclerosis can lead to an aneurysm: An aneurysm is an abnormal widening or ballooning of a portion of an artery due to weakness in the wall of the blood vessel. Large aneurism are prone to burst or rupture. (Fig 1.2)

Rupture of aneurysm in the wall of aorta, causing life-threatening internal bleeding and may lead to death. More than 15000 American die each year due to ruptured aortic aneurysms. [66]
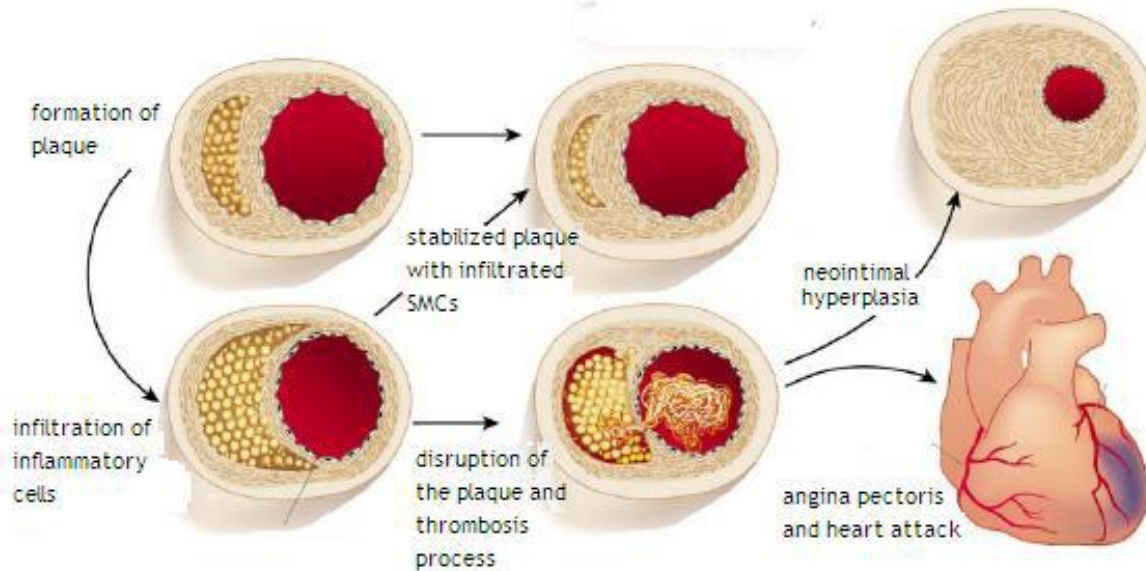
Figure 1.2   Schematic view of the atherosclerosis process [128]

1.3 The definition and mechanisms of In-Stent Restenosis

Scientists suggest that regular physical exercise and diet control can reduce the chance of occlusion of vessels, but in patients suffering critical stenosis problem, In addition, non-pharmaceutical kind of treatment is usually required.

Recent advances in surgical technique and equipment allow the surgeon to perform coronary artery bypass surgery in a less traumatic way. These types of procedures are called "Minimally Invasive" which can be done without stopping the heart and putting a patient on a heart-lung machine.

Angioplasty is a non-invasive surgical technique to mechanically widen narrowed or obstructed arteries preferred by surgeons applied in atherosclerotic coronary vessels.

During an angioplasty, surgeon expands a small balloon inside a narrowed blood vessel. The balloon helps to widen your blood vessel and improve blood flow. After widening the vessel with angioplasty the balloon is then deflated and withdrawn.

Angioplasty is often combined with the permanent placement of a stent to help prop the artery open and decrease its chance of narrowing again. Stents are usually tiny metal mesh tubes that support artery walls to keep vessels open. (Figure 1.3)

Stenting after angioplasty is widely used in different centers in the United States and Europe in over 70% of PCI. However, despite their advantages it suffers from some disadvantages like complications of stent thrombosis and in-stent restenosis. [12][13]

Angioplasty and stenting are usually done through a small puncture, in the skin, called the Access Site. The tip of the catheter is equipped with a balloon which is guided by X-ray guidance to the site of the blocked area where it is expanded to remove mechanically the plaque obstructing the vessel lumen.
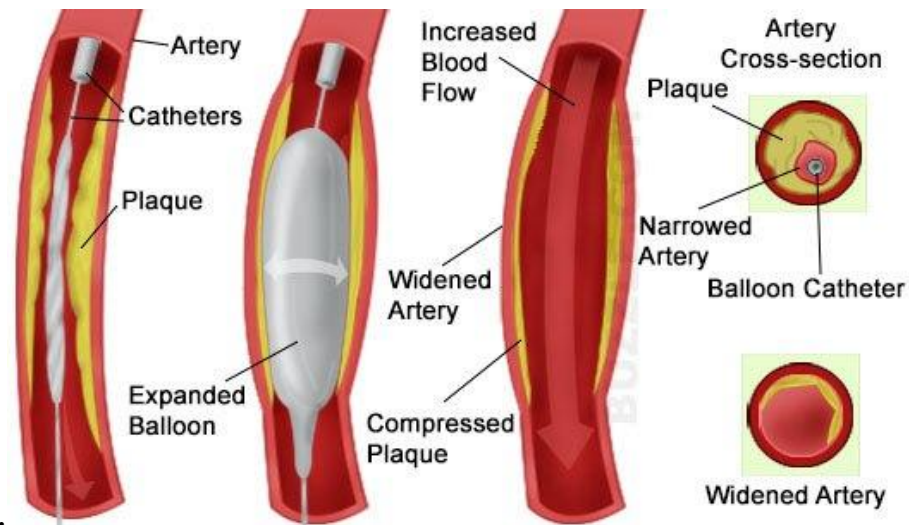
Fig 1.3 Schematic view of angioplasty with expansion of the balloon [120]

Angioplasty and stenting techniques are widely used all over the world and considered as an alternative option to medical therapy and bypass surgery for improving blood flow in cardiovascular system. Although "Restenosis" Is one of the limitation related to angioplasty and stenting. [5]

Restenosis occurs when the treated vessel becomes re-narrowed or blocked again. It usually occurs within 6 months after the initial surgery. The chance of restenosis in the case of alone balloon angioplasty is 40%, where stents reduce the chance of restenosis to 25%. That is the reason, stent insertion is widely applied in patients having angioplasty. Restenosis can occur after the use of stents, and physicians refer to this as "In-Stent Restenosis or ISR."[6], [7] and [8]

ISR is considered to occur through five phases (Figure 1.4): [9] [10]

- Elastic recoil, at the early stage of restenosis, elastic recoil takes place due to the mechanical response of the elastic fibers of vascular wall to overstretching by balloon catheter. The recoil occurs within minutes following balloon deflation; the recoil may cause up to a 40% lumen loss

The biological response to the procedure is more complicated to eliminate, and it may consist of the following four phases, as following:

- Platelet Aggregation: Immediately after stent placement, endothelial denudation and medial dissection results due to the mechanical injury of percutaneous coronary intervention (PCI).The injury causes platelets aggregation and activation, producing a countless number of various cell-signaling factors initiating an inflammatory cascade and releasing adhesion molecules that cause a thrombus formation.

- Inflammatory Phase: Over the next few days to weeks, a variety of white cells will gather at the injury site, secrete their own factors, and exert their own influence on the healing tissue. The inflammatory response can persists for months.

- Proliferation phase and Neointimal hyperplasia: The inflammatory phase stimulates smooth muscle cells (SMCs) migration and proliferation, in an attempt to repair the wound. This process is enabled by leukocytes cells releasing and activating tissue-digesting enzymes, forming a path for the SMCs to move. SMCs migrate to the thrombus that acts as a scaffold, providing the substrate for neointimal formation. The migrating SMCs form an overgrown, obstructing scar.

- Late Remodeling Phase or Negative remodeling: The final mechanism of restenosis response is the late remodeling of the vessel. This produces a neointimal layer, which is mainly formed by proliferating SMC and extracellular matrix (ECM). Inflammatory mediators and cellular elements contribute to trigger complex array of events that modulates matrix production and cellular proliferation. As the amount of scar develops blood flow is gradually reduced. Additionally, there is evidential reendothelialization of partial segments of the injured vessel surface.[11]
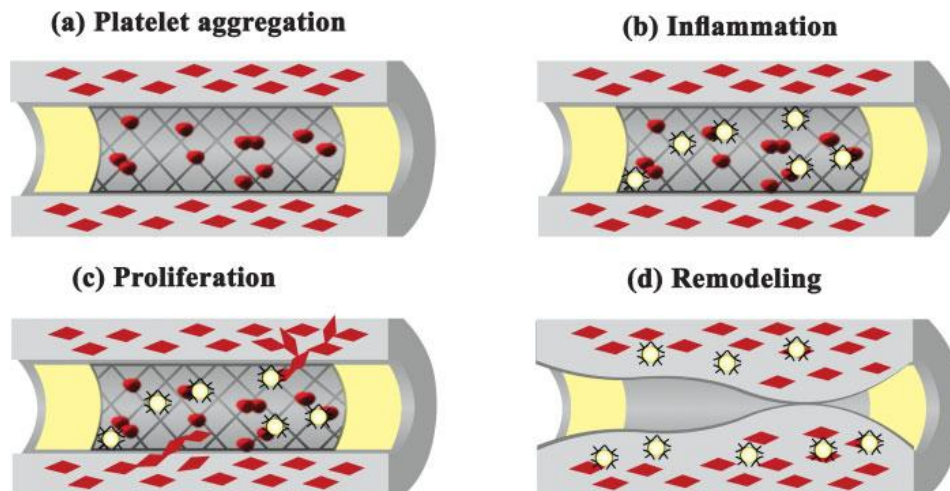
Figure 1.4 Schematic representation of the restenosis process. (a) Platelet aggregation: Immediate result of stent placement with endothelial denudation and platelet/fibrinogen (not shown) deposition. (b) Inflammatory Phase: A variety of white cells will gather at the injury site. (c) Proliferation Phase: Smooth muscle cells migrate and proliferate, creating the neointima in an attempt to repair the wound. (d) Late Remodeling Phase: The neointima is changed from predominantly cellular to a less cellular and more extracellular matrix-rich plaque [122]

As previously cited, stent is a tubular mesh inserted into a obstructed vessel in the body to prevent or diminish localized flow constriction; this mechanical scaffold mainly stop elastic recoil and negative remodeling that has greatly reduced the risk of restenosis however intravascular ultrasound studies suggest that ISR can be regarded as a consequence of neointimal hyperplasia. [9][14]

In-stent restenosis exhibits different patterns (Figure 1.5) and it can be classified according to the length of restenosis in reference to the implanted stent:

1- Focal (<10mm length)

2- Diffuse (>10mm within the stent); can be subdivided into intra-stent and intra-lesional, depending on whether or not the lesion extends beyond the edges of the stent. (diffuse lesions have a higher recurrence rate after treatment with coronary angioplasty)

3- Proliferative (10mm extending outside the stent)

4- Occlusive
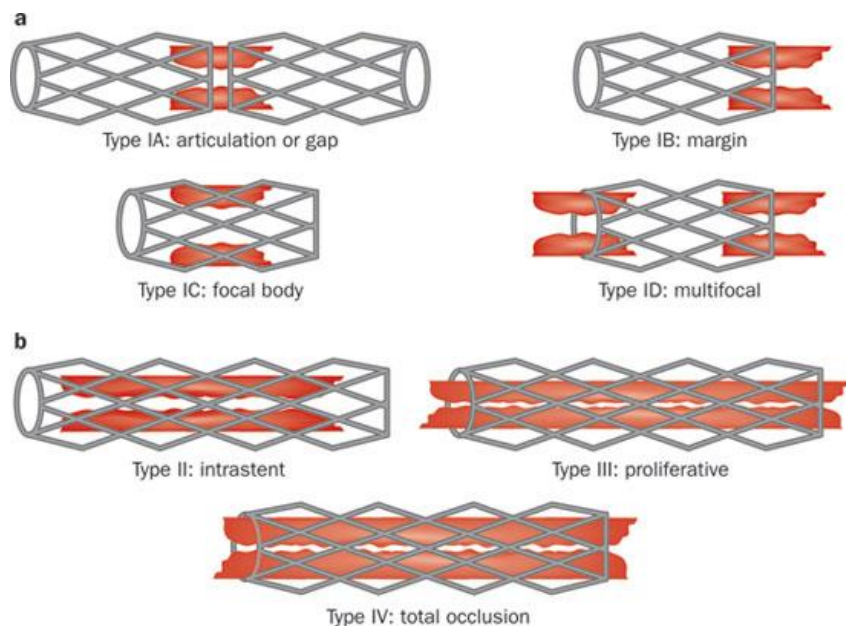
Figure 1.5 Schematic representation of ddifferent patterns of ISR [15]

Between different causes suggested by scientists to explain the recurrence of vessel stenosis after stent deployment, inflammation plays important role, it can be described by traumatic event which can change several parameters fundamental to the blood vessel physiology after endovascular stent deployment which lead to neointimal growth and lumen occlusion by alteration

of the vascular response to injury, causing a more intense and prolonged inflammatory state. [16]

Regarding to this fact that, primary balloon expansion sometimes would not be satisfactory to completely expand the stent, second inflating might be required which intensify the mechanical damage introduced by ballooning and stent deployment.

Besides, there is always a chance of blood flow alteration caused by improper stent placing which increases pressure gradients and affects blood laminar flow, considered as an important factors in formation of neointimal hyperplasia.

Due to stent deployment and the excessive ballooning, local artery extendibility is damaged and the vessel wall compliance is decreased.

Above all the damage mentioned, expansion of the stent to the vessel wall is considered the most important event leading to ISR: the destruction of the tissue integrity, added to the presence of a foreign body is likely to disturb the normal wound healing which instead develops into hyperplasia. [14,16]

Meanwhile, the presence of a foreign body in the vessel is disturbing injury healing process and it has been hypothesized that stenting sometimes cause more intense and prolonged inflammatory stat. [16]

1.4 Biology of ISR

After common injury which introduced by expansion of the coronary stent, Leukocyte recruitment and infiltration occur at sites of vascular injury where the lining endothelial cells have been denuded and platelets and fibrin have

been deposited. In vivo studies have shown that leukocytes and platelets localize at sites of bleeding, within atherosclerotic and post angioplasty restenosis lesions. [23]

Studies have supported a critical role of inflammatory cells in the restenosis process and have uncovered a critical role for the thrombotic cascade in the initial recruitment of these inflammatory cells which caused by changes in adhesion proteins interfacing with the foreign material. [24]

In other word, adherence of platelet and inflammatory cells on the surface of stent due to host response leads to proliferation of the smooth muscle cells followed by SMCs phenotypic change from contractile to synthetic, proliferate into the media and finally migrate from the media, forming the neointima with the consequent obstruction of the vessel lumen. (Figure 1.6)
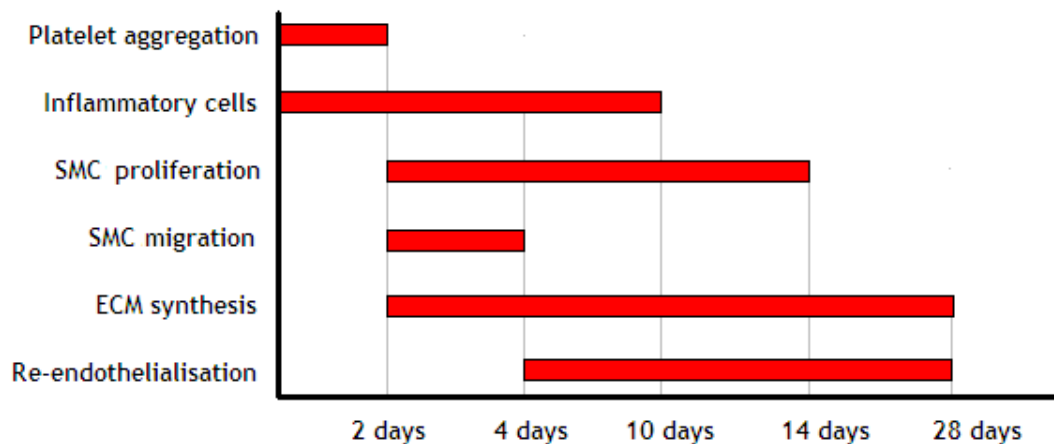
Fig 1.6 schematic representation of timeline of ISR [123]

Chapter 2

Stent, technology and materials

2.1 Introduction

Since the introduction of percutaneous transluminal coronary angioplasty (PTCA) by Gruntzig in the United States in 1977, vast effort have been done in the clinical practice of percutaneous coronary intervention (PCI).

PTCA is a non-surgical method for arterial revascularization which is a minimally invasive procedure to open up blocked coronary arteries, to restore arterial blood flow to the heart tissue without open-heart surgery.

It involves steering a guide wire, from an opening usually created in the femoral artery, then a special catheter (long hollow tube) is inserted into the coronary artery and past the blockage in the blockage through the vascular system and into the coronary arteries.

The catheter contains a tiny balloon, when the catheter is in the obstruction zone, pressure is applied and the balloon inflated in order to re-open the vessel and establish normal blood flow.

In few years PCI has become so common which more than one million percutaneous coronary intervention procedures are performed annually worldwide [39].

However regarding to vascular elastic recoil and negative remodeling of the vessel this procedure has caused restenosis in approximately 50% of patients, after revascularization [41].

In 1986, Puel and Sigwart, invented the first coronary stent (an expandable lattice-shaped metal tubular mesh usually made of stainless steel) to prevent

vessel closure during PTCA, and also to reduce the incidence of angiographic restenosis, which had an occurrence rate of 30-40%. [43, 42] (Figure 2.1)

Besides, recent reports have expanded the role of stents in different fields such as management of pseudoaneurysms associated with dialysis access. [129] Stenting, is widely improving PTCA performances and are more successful than balloon angioplasty alone, in preventing abrupt vessel closure, and also it decreases the occurrence of vessel re-coiling, thus reducing the incidence of restenosis.
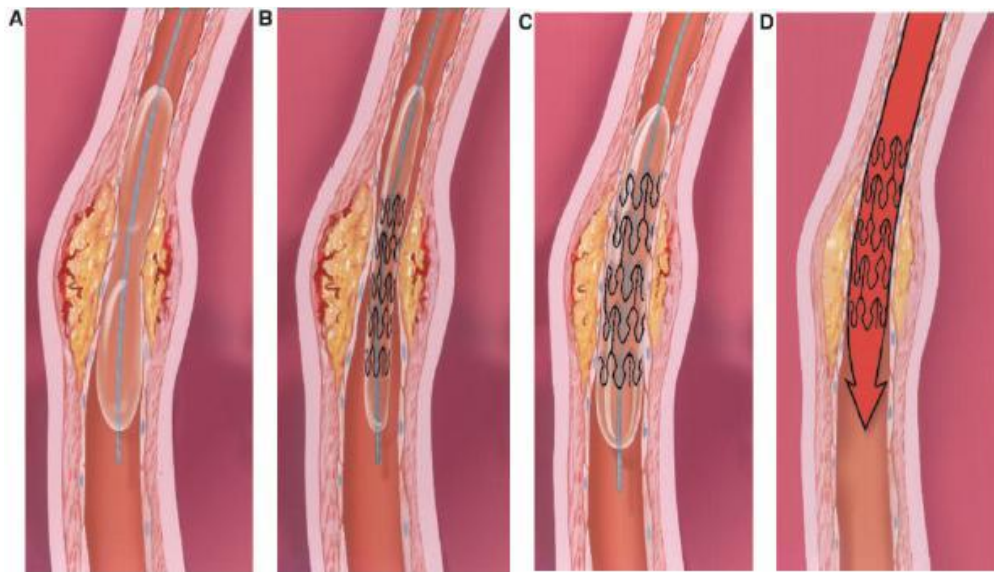
Fig 2.1 Scheme of PTCA with stent implantation: balloon-tipped catheter is positioned in the coronary artery narrowing and inflated (A). The stent is positioned at the site of the narrowing (B). When the balloon is inflated, the stent expands and presses against the arterial wall (C). The balloon is deflated and removed. The stent remains permanently in place (D) [100]

Despite the widespread use of these devices, bare metal stents (BMS) have been associated with a 20-30% restenosis rate due to the stimulation occurs in formation of a neointimal tissue leading to neointimal hyperplasia, particularly in the small caliber vessels (under 2.5mm of diameter), where the incidence of in-stent restenosis (ISR) is approximately 15-30% [39] which requiring reintervention.[42,44]

This restenosis is clinically evident within the first 6-9 months after stent placement, and occurs in response to strut-associated injury and inflammation [40].

In 2001, Drug-Eluting Stents (DES) were introduced as a new approach to minimize restenosis and requirement for re-intervention but factors such as high costs for

The healthcare and the long-term results of some clinical trials, are two main problems related to DES. [46, 47]

In the case of stent development, a lot of biomechanical, physiological aspects must be carefully noticed.

Mainly, mechanical properties are related to the bulk characteristics of the core of stent material which is commonly metallic, and those related to biocompatibility and haemocompatibility are linked to surface properties.

Primary mechanical concern of stent development is the need to reduce device profiles and to increase flexibility. Important factors required are the capability to cover any lesion, to guarantee acceptable radial support, and finally to prevent elastic recoil of the artery after angioplasty.

For balloon-expandable stents, a higher elastic modulus (E), prevents recoil after stent deployment .however, a low yield strength material is preferred because it allows better stent expansion at range of acceptable balloon pressures. Meanwhile, although High tensile properties after expansion help to achieve radial strength with a minimal volume of implanted foreign material but associated higher yield strength promotes the undesired acute recoil upon balloon deflation.

Besides, stent as foreign material challenges the vessel wall tissue and may considered as a threat for its integrity. For these reasons it is important also to investigate the biocompatibility of stents. Therefore, stent design and mechanical features need careful attention.

2.2 Biocompatibility aspects of stent technology

Biocompatibility represents the fundamental necessity in a biomaterial and it is general defined as the ability of a material to perform an appropriate host response in a specific application. The goal of early biomaterials research was to fulfill an appropriate combination of chemical and physical properties to fit those of the replaced tissue causing a minimal foreign body response in the host [48], which this goal has been changed over time, from former definition of it , to be an inert material.

Despite their popular clinical use of stents, an "ideal stent" with no adverse biological response does not exist. The two most common adverse biological responses are in-stent restenosis (IR), reduction in lumen size by neointima formation and stent thrombosis (ST), which is formation of a blood clot inside a treated vessel.

Such adverse effects are multi-factorial and depend on a number of factors including vessel injury caused during the stent implantation and alteration of haemodynamics in the treated vessel leading to early thrombus and late neointima development. [49]

Early biocompatibility problems with stents are associated with thrombosis, inflammation and neointima formation. Late problems with stents can be divided in two categories:

(1) Mechanical failure due to material fatigue resulting from the considerable stress imposed to stents by cardiac contractions in function

(2) Chemical failure related to potential toxic substances release such as nickel from stent [50].

Stent implantation by expansion leads to greater vessel injury than solely balloon angioplasty and it causes inflammation accompanied by alteration in wound healing process and sometimes foreign body response [51, 52]. Other

studies have concluded that stent geometry, specifically the strut thickness, is a key determinant of restenosis rates. [51]

Moreover, researches have shown that metallic stents deployment produced a rather limited inflammatory response, whereas coated stents have shown more severe responses with lymphocytic infiltrates, macrophages and giant cells typical of foreign body reaction. [25]

In addition, the accumulation of inflammatory cells in lumen may stimulate growth factor and accelerate SMCs migration leading to neointima formation [53].

The basic principle of blood-stent interactions is that circulating cells do not react directly with the metallic stent [54]. Within minutes after stent insertion, soluble proteins will adhere to it and rapidly form a film conditioning the surface of the foreign material so using a proper coating with a good hydrophilic properties on the surface of stent may lead to lower adhesion of these proteins and decrease the chance of ISR.

Changes in wall shear stress during stent implantation are believed to induce endothelial dysfunction, ultimately leading to neointimal hyperplasia and consequently to ISR. It has also been suggested that magnitude of the shear stress is of secondary importance to the spatial and temporal fluctuations of this quantity. [56]

Another factor which must be noticed is a corrosion properties of stent materials.

Although, oxide layer on the surface of many metals stop corrosion process, but in the sever condition, like interaction with blood, the oxide layer will be destabilized and passivation would not be effective.

This destabilization will lead to migration of corrosion particles from stent metallic surface to other parts of the body and these released ions can form

metallo-organic complexes with proteins, causing both immune response and cytotoxicity elicitation. [29]
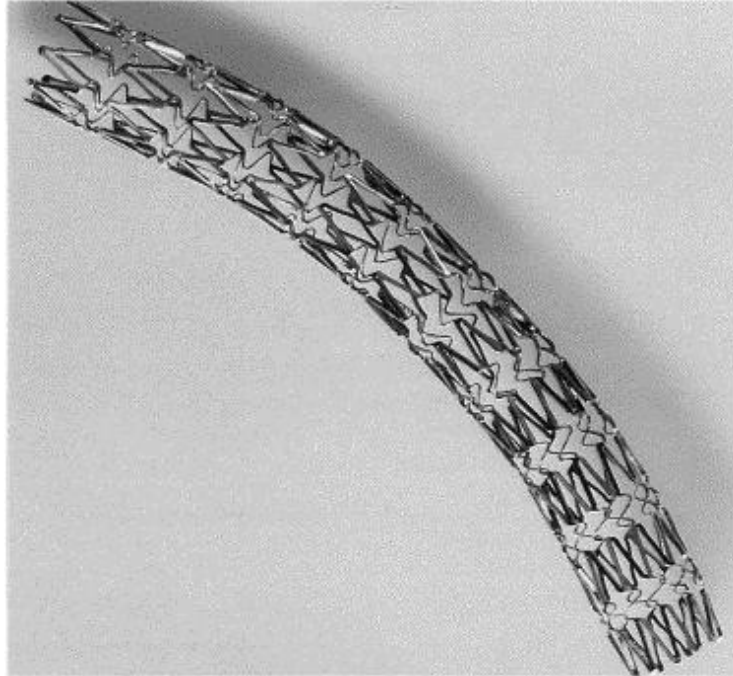
Fig 2.2 Image of a common coronary stent [55]

There are mainly 3 types of stents commonly employed in coronary angioplasty (Fig 2.2)

1- Metallic coronary stents

2- Coated coronary stents

3- Drug-eluting and Bio-absorbable coronary stents

2.3 Metallic coronary stents

Materials to be used as stent core must fulfil sever physical, mechanical and chemical properties.

First-generation stents were made of bare metal. Although bare-metal stents almost eliminated the risk of the artery collapsing, they only modestly reduced the risk of restenosis.

The metal of an expandable stent must have enough plasticity to remain at the required size when expanded. Self-expanding stents, in addition, must be prepared from metals with sufficient elasticity in order to be compressed and then expanded while retaining sufficient radial hoop strength to prevent vessel recoil or closure [4].

The two most common metals used in current-generation stent applications include titanium and various grades of vacuum-melted stainless steel.

316L stainless steel provides good resistance to corrosion, and excellent mechanical properties but biocompatibility remains limited by the thrombosis issue. [57, 58, and 59]

The primary advantages of titanium, is its weight and high biocompatibility. Weighing less than a third as much as stainless steel and exhibiting high strength, titanium is an attractive option for stent applications. That immune system will be less likely to reject this type of medical implant device.

However, stainless steel is more commonly used to manufacture stent tubing because it is less expensive and more readily available. [63]

Tantalum stent shows several theoretical advantages over stainless steel in terms of radiopacity, biocompatibility and mechanical properties.

In This kind of stents, inert tantalum peroxide creates an electrically negative charge that can reduce adhesion of negatively charged. However, in clinical practice, tantalum has not been shown to decrease stent thrombosis compared with stainless steel stents due to activation of the coagulation biochemical cascade that occurs when it is in contact with blood. [50]

Another alternative to 316L stainless steel for production of cardiovascular stents is a nickel/titanium memory alloy (nitinol) from which self-expandable implants can be obtained; this kind of stents represent superplastic

And thermal shape memory properties of that alloy, which minimize the vessel injury upon stent implantation.

Nitinol alloy has also proved to have good early biocompatibility. Some concern exists that nickel leakage from these alloys could lead to immunogenic reactions.

The dissolution is due to nickel migration towards the metal surfaces induced by the heating process required to manufacture these memory alloys. Progress has been made to avoid this problem, so in overall nitinol stents can reduce the chance of thrombosis and ISR. [50]

However, during handling and following deployment into the body, stents are subjected to cyclic stresses, e.g., from the expansion and contraction of the blood vessels, which can result in fatigue damage and curtail their useful life.

Therefore, coronary nitinol stents are no longer in widespread clinical use. [29] [60]

Cobalt/chromium stents assures a stronger elastic modulus than stainless steel, thus allowing the manufacture of thinner stent struts with the same radial strength and an acceptable plastic deformability [65].

2.4 Surface treatment and effect of dopants

In 1998, research made by Scheerder proved the decreasing effect of thrombogenicity and neointimal hyperplasia after surface treatment using electrochemical polishing on the surface of metallic stents. [61]

Besides , the nature of the metal surface is important for the sake of blood compatibility , a smooth surface can help to prevent the activation and aggregation of platelet ,which is recognized to be one of the crucial component of the thrombosis process .So generally surface treatment can improve the performance of stents .[62]

Moreover, in 2005 studies revealed the effect of doping elements such as Ca and P (on the surface of stents) in decreasing platelet adhesion which enhances surface blood compatibility. [64]

In their work the surface biocompatibility was assessed using in vitro

platelet adhesion tests. The statistical results show smaller numbers of adhered and inactivated platelets. Their results show strong adhesion of albumin with low conformational change of fibrinogen on both the Ca-DLC and P-DLC films demonstrate that either Ca or P doping alone can enhance the hemocompatibility.

Moreover, the addition of Si, over a range of doping levels was also observed to be beneficial to the bio response in different type of stent coatings.

Human micro vascular endothelial cell attachment was enhanced, which Shows that coatings with Si dopant, stimulate less inflammatory activity than uncoated materials. [73]

2.5 Coated coronary stents

The importance of coating stainless steel surface from the biological environment has led to the production of several types of coatings based on ceramic, metallic, polymeric and biological materials.

For instance, the titanium coating over stainless steel is offered, so that immune system will be less likely to reject the medical implant device.

Different metals react differently to magnetism, and titanium is one of the least magnetic of all metals. However, steel is much more strongly attracted to magnets, so the steel core of the stent would most definitely be affected

Even though the titanium coating reduces the steel's attraction to the magnets, It is believed that prolonged exposure to magnetic devices, such in cases of Magnetic Therapy reduces the quality of the stainless steel stent which coated by titanium and diminishes the stent's ability to prevent the clogging of the arteries .[67]

Gold as an element known to be resistant to corrosion previously used to coat stainless steel stents, however, patients treated with gold-coated stents had an increased incidence of acute cardiac events and ISR when compared with uncoated controls.

Stents have been also coated with amorphous silicon carbide with an expected anti-thrombotic effect. However, this coating has shown no significant difference when compared to stainless steel stents.

Heparin-coated stents have been shown to reduce sub-acute stent thrombosis, resulting in favorable long-term clinical and angiographic outcome. However, despite an anti-proliferative effect of heparin under in vitro conditions, no reduction in neointimal proliferation was observed in histopathological

examinations. Therefore, no clear benefit on ISR emerged with these types of stents.

Also, polymers with and without drug elution have been used as stent coatings, with various results. The major problem with these materials, which can be both biodegradable and non-biodegradable, is their marked inflammatory reactivity, mostly caused by the surface degradation in contact with biological fluids. Furthermore polymeric stents showed insufficient tensile and coil strength. [65], [66]

2.6 Drug-eluting coronary and biodegradable stents

A Drug-Eluting Stent (DES) is a coronary stent coated with an anti-proliferative drug, so that when is implanted in the narrowed coronary arteries , slowly allows drug elution into the coronary wall for weeks after stent implantation
And stop cell proliferation. (Figure 2.3)
By this approach the stent is used both as implant and as vehicle for local intra-vascular drug delivery. The drug may be absorbed into the stent material or incorporated into its coating.
Manufacturing technique involves, bare metal stents are generally coated with a direct layer of drug by means of grooves, wells and surface treatments.
Bare-metal or non-drug coated stents are usually fully coated by body tissue within a few weeks.
However, the drug-coated stents are significantly more costly than non-coated stents.
Moreover, ISR does not definitely disappear after DES deployment and stent failure tends to be dependent on the same factors causing restenosis after bare metal stenting; furthermore the delivery of drugs causes some weakness:

1- Late coronary thrombus

2- Localized hypersensitivity

3 -development of drug resistance by the SMCs

4- Late development of ISR [47]

For the above reasons and, and moreover, high initial burden to the healthcare system budget, drug-eluting stents are recommended only to patients who suffer a serious condition with predictable higher incidence of ISR.
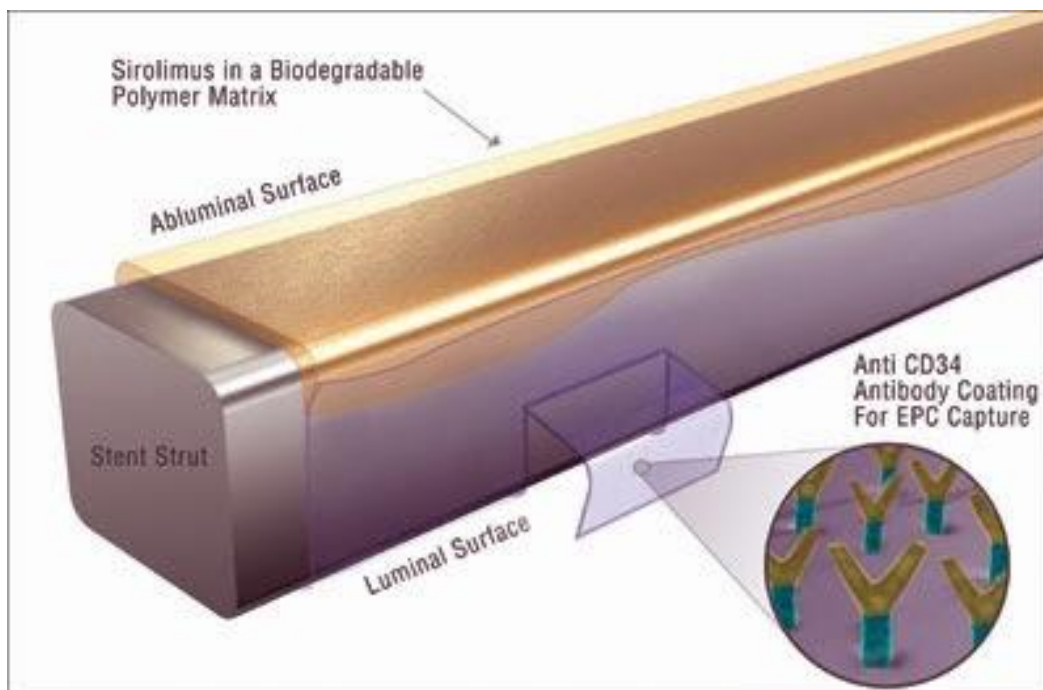
Fig 2.3 Schematic view of a drug eluting stent [68]

In the other branch, bio-absorbable stent is manufactured from a material that may dissolve or be absorbed in the body such as magnesium and specific polymers.

Bio-absorbable stents has created interest because the need for mechanical support for the healing artery is temporary, and beyond the first few months there are potential disadvantages of a permanent metallic prosthesis

potential advantages of having the stent disappear from the treated site include reduced or abolished late stent thrombosis, improved lesion imaging with computed tomography or magnetic resonance, facilitation of repeat treatments (surgical or percutaneous) to the same site, restoration of vasomotion, and freedom from side-branch obstruction by struts and from strut fracture-induced restenosis.[71][72]

Although the concept of bio-absorbable stents has created interest for more than 20 years, there are challenges in making a stent that has sufficient radial strength for an appropriate duration, that does not have improperly thick struts, that can be a drug delivery vehicle, and where degradation does not generate an unacceptable inflammatory response.[69][70]

2.7 The aim of the project

In this work the possibility to coat titanium coronary stent with a layer of anodized titanium doped by different elements such as Ca, P, Na and Si is investigated, in the attempt of providing a titanium-core stent with a biocompatible coating, regarded as an alternative, cost-effective approach to drug-eluting stents for decreasing ISR.

The starting-point of this work is the ASD silicon-based osteointegrative treatment developed and patented by Politecnico di Milano [101,102], which nowadays is used in production of Ti-implants as well as dental application,

With excellent results.

But it would be the first time which, the application of this coating deposited by Anodic Spark Deposition technique (ASD) in production of titanium stents is investigated.

The main challenge of this project is to determine, optimum technical parameters needed to be applied in the coating process with ASD technique, So that the final product can meet the mechanical and physicochemical

requirements, needed for the stent production, which will be discussed in the next chapters.

Chapter 3

Titanium, characteristics and treatments

3.1 Introduction

Biomaterials are the best solution to the human need of replacing and integrating tissues and organs in pathologic conditions. The number of applications vastly increased in the last years and the therapeutic innovations allow to restore different abilities and functions of the human body.

Nowadays, different biomaterials are available; metals, polymers, ceramics, and composites. They present different advantages and their choice depends on the specific medical application, on the specific case of needs, and on the special function required. Among them, titanium - pure or in alloys - is one of the most common material used, especially in cardiovascular and orthopaedic applications. Because, besides its common metallic-material properties (strength, toughness, impact resistance, stiffness), it also presents high biocompatibility and corrosion resistance.

Over the years the concept of biomaterial has been modified and this process is still ongoing. (Figure 3.1) [74]

Today , the biomaterials concept has been advanced trying to develop bioactive and biomimetic materials to create so called , "self platforms" able to make a better interface with the host tissue, try to mimic and reproduce nature's hierarchical structural assemblages and mechanisms which

stimulating a specific cellular response at the molecular level driving a fast regeneration process for improving the implant lifetime. [74, 75]
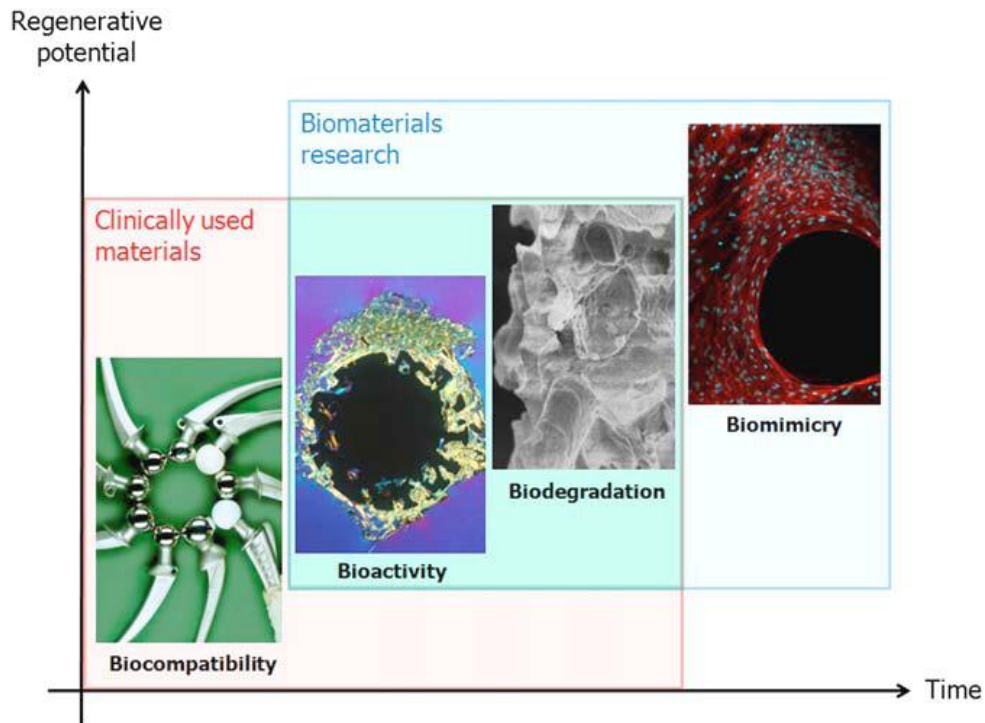
Fig 3.1 Evolution of biomaterials during the last decades [74]

3.2 Titanium

Titanium is the fourth most abundant structural metal on earth's crust and it is an element of transition with oxidation numbers 2, 3 and 4. . It is not found as a free element; rather it is present in igneous rocks and in their derived sediments. In nature it is chiefly found as ilmenite (FeTiO3), rutile (TiO2) and in titanates or metallic ores.

Historically, titanium has been used widely in aeronautical and marine fields, because of its high strength and stiffness it possess , its low density, and its ability to tolerate high temperatures as well as its corrosion resistivity. [9]

Today, the Kroll process is the main method for production of titanium.
 It involves the reaction of chlorine and carbon upon ilmenite (FeTiO₃) or rutile (TiO₂): the resultant titanium tetrachloride (TiCl4) is separated from the iron tri-chloride (FeCl3) by fractional distillation. Finally titanium tetrachloride (TiCl4) is reduced to metallic titanium by reduction with magnesium in high temperature atmosphere (1100°C). Therefore the Kroll's process is carried out with a two steps reaction (a, b), as illustrated below. (Figure 3.2)

$$a) \begin{cases} TiO_2 + 2C + 2Cl_2 \xrightarrow{700°C} TiCl_4 + 2CO \\ 2TiFeO_3 + 6C + 7Cl_2 \xrightarrow{900°C} 2TiCl_4 + 2FeCl_3 + 6CO \end{cases}$$

$$b)\ TiCl_4 + 2Mg \xrightarrow{1100°C} Ti(s) + 2MgCl_2$$
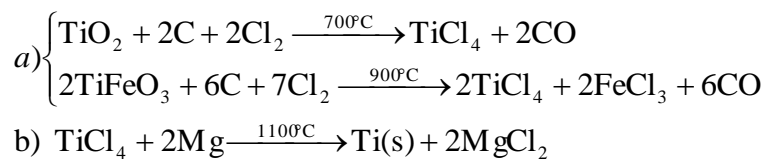
Figure 3.2 the Kroll's process and its two steps reaction (a, b)

Titanium is highly reactive with atmospheric elements such as oxygen and nitrogen, which is due to its oxidative nature and it burns readily in the presence of oxygen. It therefore requires an inert atmosphere for high-temperature processing (otherwise it is processed by vacuum melting).
Titanium and titanium alloys have replaced over the years the other commonly used metals (such as cobalt-chromium alloys, stainless steel) in vast implantable devices and now account the first choice materials for a significant number of biomedical applications. [76]

Although the cost of production of these Ti-based materials and their application in biomedical devises are high in comparison to stainless steel and Co-Cr-Mo alloys, Ti and Ti-based alloys are still preferred because they possess

a generalized and localized corrosion resistance in body environment, high mechanical resistance, high fatigue, wear resistance, moderate modulus (110 GPa), good workability, low density (approx. 4700 Kg m-3) and excellent biocompatibility. [77, 78 and 79]

These unique characteristics of titanium, made this metal in the center of attention over many years, which led to development of derived medical-grade titanium alloys which make them irreplaceable materials for numerous high-technology applications.

In table 1.1 is reported a brief overview of the application and the main properties of titanium and its alloys:

Material	Structure	Standard	Alloying elements (weight %)	Elastic modulus (GPa)	Yield strength (MPa)	Ultimate strength (MPa)	Biomedical applications
Ti	α	ASTM F67 ISO 5832–2	Balance Ti Max 0.4 O	105	692	785	Dental implants
Ti–6Al–4V	α-β	ASTM F1472 ISO 5832–3	Balance Ti 5.5–6.5 Al 3.5–4.5 V	110	850–900	960–970	Prostheses stems Hip and knee prostheses Screws and pins for bone fixation
Ti6Al7Nb (Protasul 100)	α-β	ASTM F1295 ISO 5832–11	Balance Ti 6 Al 7 Nb	105	921	1024	Prostheses stems Hip and knee prostheses
Ti35Nb5Ta7Zr (TNZT)	Metastable β		Balance Ti 35 Nb 5 Ta 7 Zr	55	530	590	Under investigation
NiTi		ASTM F2063	55.9–56.1 Ni Balance Ti	20–70 (martensite) 70–110 (austenite)	50–300 (martensite) 100–800 (austenite)	755–960	Internal fixator for long bone shafts Spinal correctors Vertebral spacer anchoring of prostheses and staples Stents, occlusion coils
TiNb			Balance Ti 25–40 Nb	60–85	–	–	Under investigation

Table 1.1 Structure and properties of titanium and its alloys in medical applications [14]

3.3 Compositional properties of titanium and titanium alloys

The American society for testing and materials (ASTM) introduced four classes of commercially pure (CP) titanium and of titanium alloys, on the basis of the maximum content of different elements, considered as maximum percentage of weight.

The four grades of unalloyed commercially pure titanium for surgical implant applications are shown in Table 1.2.

Titanium alloys are also known as Grade 5. Oxygen, iron, and nitrogen have to be controlled carefully. Oxygen in particular has a great influence on the ductility and strength.

	N	*C*	*H*	*O*	*Fe*
Grade 1	0.03	0.10	0.015	0.18	0.20
Grade 2	0.03	0.10	0.015	0.25	0.30
Grade 3	0.05	0.10	0.015	0.35	0.30
Grade 4	0.05	0.10	0.015	0.40	0.50

Table 1.2 Four classes of commercially pure (CP) titanium and of titanium alloys [117]

Grade 1 Is the most ductile and softest titanium alloy, due to a low content of oxygen, it is a good solution for cold forming and corrosive environments.

Grade 2 Unalloyed titanium, with standard oxygen. Presents a medium content of oxygen (0.25% of weight) and iron, thus showing a good compromise between tensile strength, ductility and weld ability. It is the most exploited CP titanium in engineering applications.

Grade 3 Unalloyed titanium, medium oxygen.

Grade 4 Presents a high content of oxygen (0.40% of weight); this pure titanium is widely exploited by aeronautic industry thanks to its enhanced tensile strength.

Grades 1-4 are unalloyed and considered commercially pure or "CP". Generally the tensile and yield strength increase with grade number. The difference in their physical properties is mainly due to the quantity of added elements. They are used for corrosion resistance applications where cost, ease of fabrication, and welding are important.

Grade 5 Also known as Ti6Al4V. It is significantly stronger than commercially pure titanium while having the same stiffness and thermal properties. [80]

The principal chemical-physical properties of titanium are listed in the table1.3

Symbol	*Ti*
Atomic number	22
Atomic weight	47.867
Group number	4
Period number	4
Electron configuration	$[Ar]3d^24s^2$
Oxidation number	+2, +3, +4
Standard state	Solid at 293K
Atomic radium	1.47Å
Electronegative	1.54 (Pauling electronegativity)
Density	4.51 gr/cm^3 at 293K
Melting point	1941K

Table 1.3 Main chemical-physical properties of titanium [80].

Additionally, titanium and titanium alloys show a significantly higher strength to weight ratio than any other metallic biomaterial because of their very low density (4.51 g/cm^3).

This metal has recently got a popular employment in biomedical applications.

In detail, the features which make titanium the benchmark in these applications are its relatively low elastic modulus, high fatigue strength, ductility, formability and corrosion resistance .[78]

Titanium is an allotropic material that exists in two different forms (Figure3.3):

1-Under 883°C: Hexagonal packed structure (α- phase), with high mechanical characteristics;

2-Above 883°C: Body-cantered cubic structure (β - phase), with improved ductility properties.

Crystal structure
of α-titanium.

Crystal structure
of β-titanium.
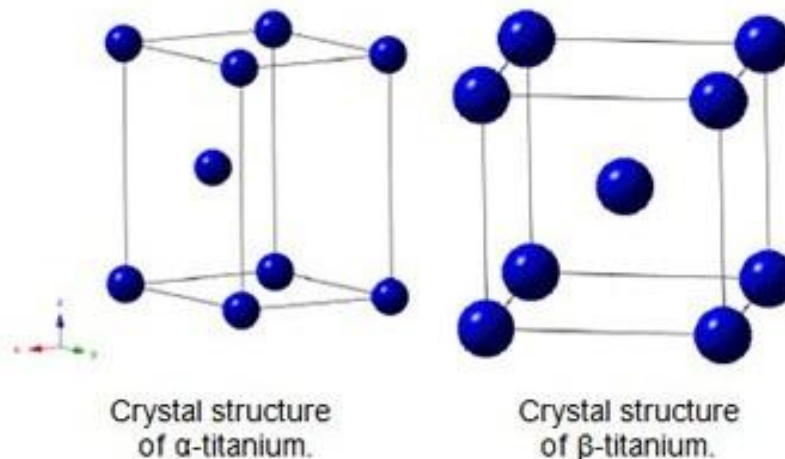
Figure 3.3 Allotropic forms of titanium. Left image α Phase; Right image β phase. [81]

3.4   Corrosion properties of titanium

The corrosion of metals – the primary cause of metal deterioration – is an electrochemical process between the metallic surface and the environment lead to release of metallic ions which tends to form metal oxides, dioxides and other compounds. From the enteric point of view, the oxide state is more favourable as they spontaneously tend to this state and become stable.

Human body fluids just like sea water is considered highly corrosive environments for metallic compounds due to presence of saline liquid.

Most metals corrode when in contact with aqueous environment (water and acids, bases or salts).

In fact, being an electrochemical process, corrosion results in a complex mechanism of charge transfer between the metal surface and the electrolyte, that is formed by the fluid and the released metal ions. An electrochemical circuit is established and its thermodynamic work is the difference between the reduction potential and the oxidation potential.

Standard Oxidation-Reduction Potential at 77 °F (25 °C)

MORE ACTIVE	Reaction	E_0 (volts)
	$Na \rightarrow Na^+ + e^-$	-2.71
	$Mg \rightarrow Mg^{++} + 2e^-$	-2.38
	$Al \rightarrow Al^{+++} + 3e^-$	-1.66
	$Zn \rightarrow Zn^{++} + 2e^-$	-0.763
	$Fe \rightarrow Fe^{++} + 2e^-$	-0.409
	$Ni \rightarrow Ni^{++} + 2e^-$	-0.250
	$Pb \rightarrow Pb^{++} + 2e^-$	-0.126
	$H \rightarrow 2H^+ + 2e^-$	0.00 Reference
	$Cu \rightarrow Cu^{++} + 2e^-$	$+0.34$
	$4OH^- \rightarrow O_2 + 2H_2O + 4e^-$	$+0.401$
	$Fe^{+2} \rightarrow Fe^{+++} + e^-$	$+0.771$
	$2Hg \rightarrow Hg_2^{++} + 2e^-$	$+0.905$
	$Ag \rightarrow Ag^+ + e^-$	$+0.799$
	$2Br^- \rightarrow Br_2 + 2e^-$	$+1.06$
	$2H_2O \rightarrow O_2 + 4H^+ + 4e^-$	$+1.23$
	$2Cl^- \rightarrow Cl_2 + 2e^-$	$+1.36$
	$Pt \rightarrow Pt^{++} + 2e^-$	$+1.2$
MORE NOBLE	$Au \rightarrow Au^{+++} + 3e^-$	$+1.498$

Table 1.4   Typical thermodynamic oxidation-reduction potentials of elements [82]

The above Table 1.4 is a listing of some useful oxidation-reduction potentials. These values represent the thermodynamic tendency for the indicated reaction to occur on a relative basis. All potential values are compared to an arbitrary value of 0.00 volts which is assigned to the hydrogen oxidation reaction. The more negative a value, the more likely the reaction will proceed in the direction shown.

The corrosion process consists of two semi-reactions (in aerobic environment):
- At the anode (metal), the metal oxidizes and liberates electrons:

$$Me \rightarrow Me^{z+} + ze^-$$

- At the cathode (electrolyte), the following reduction reactions occurs resulting in an electrons drawing from metal:

$$z(O_2) + 2z(H_2O) + 4ze^- \rightarrow 4z(OH^-)$$
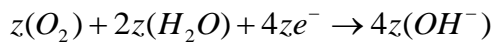
In the case of titanium, considering +4 as number of oxidation, the whole reaction can be written as:

$$Ti + O_2 + 2H_2O \rightarrow Ti^{4+} + 4(OH^-) \rightarrow Ti(OH)_4$$
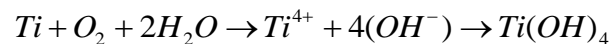
When the reduction potential is higher than the oxidation potential, the environment shows a high thermodynamic tendency to corrosion.

When the reduction potential is greater than the oxidation potential, the environment shows a high thermodynamic tendency to corrosion. Only noble metals, such as Pt and Au, do not undergo electrochemical corrosion in aqueous environment.

In this case, there are two types of metals, which show different corrosion resistance (Figure 3.4):

- Active metals, that have high corrosion rate (low kinetic dissipation of thermodynamic work)

- Active-passive metals, that have low corrosion rate (the presence of an adherent passivating oxide layer stops the further oxidation of the metal bulk)
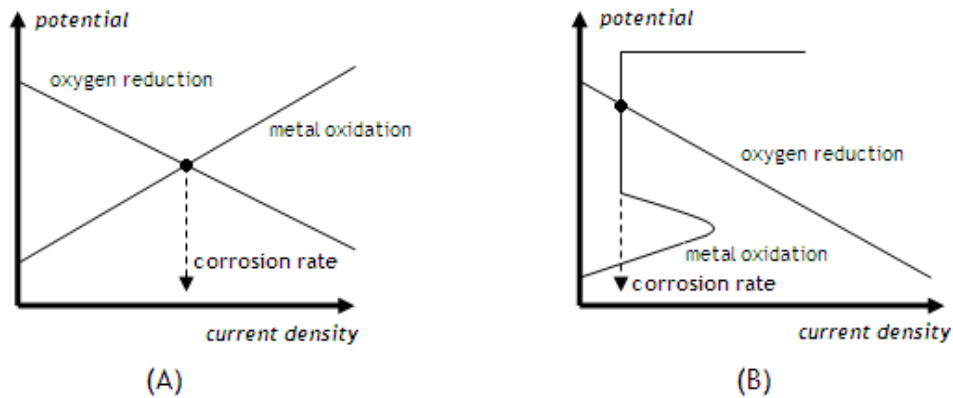
Figure 3.4 Corrosion process in active metals (a) and active-passive metals (b) [9]

As previously cited, titanium oxide layer can be efficiently passivate titanium surface , thus shows very low corrosion rates (less than 0.03 $\mu g/dm^2 \cdot day$) .

A clear method to illustrate the corrosion behaviour of titanium, in function of potential and PH of the environment, is the plot of regions (corrosion, passivity and immunity) called Pourbaix diagram.

It shows that the passivation of titanium surface is very efficient in human body environment (Figure 3.5)

The biological environment is very aggressive mainly due to the presence of high protein concentration [84]. In a protein-free solution the corrosion resistance of titanium is similar to stainless steel L316, the stainless steel shows high reactivity when incubated with protein solution when implanted in vivo [85]. A protein solution enhances the corrosion rate of stainless steel, compared to a saline solution .Meanwhile, the passive titanium oxide layer protect titanium and, the corrosion rate of titanium is not increased by the presence of proteins in the surrounding environment. [86]
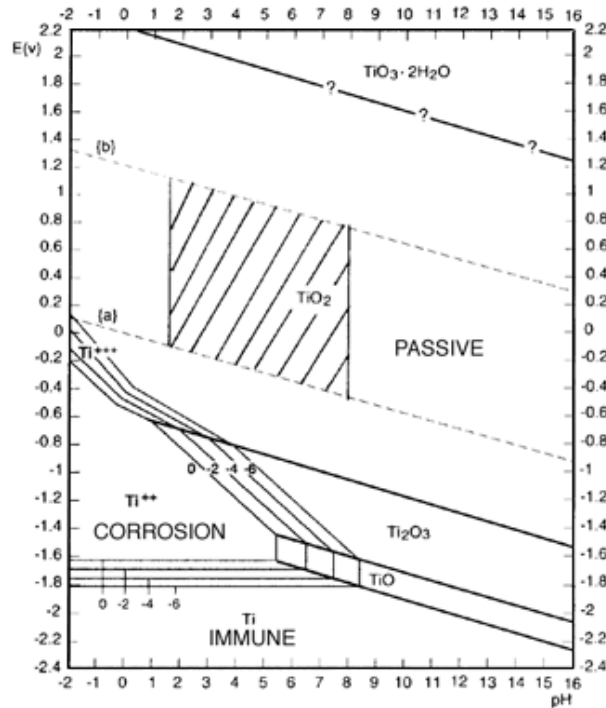
Figure 3.5 Pourbaix diagram of titanium; hatch marked region indicates human body environment [74]

3.5 Surface treatments to titanium and the oxide layer

Titanium and titanium alloys are naturally covered by a thin titanium oxide layer ,however titanium oxide shows a class of oxides with a wide range of Ti/O ratio namely TiO_3, Ti_3O_2, Ti_3O_5, TiO_2, Ti_2O_2 [89]:

Gradual change of the Ti/O ratio from the outer part on the surface (+IV oxidation state) to the bulk of the metal is due to oxygen solubility in titanium and different titanium oxidation states.

Nevertheless, TiO_2 considered as the main oxide on titanium alloys, and its properties control the biological interaction when a titanium-based device is implanted in the human body. It exists in three different crystallographic forms: Rutile, Anatase (Figure 3.6) and Brookite.

Regarding to thermodynamic stability, rutile possess the most thermodynamically stable phase among the three phases, while anatase and brookite are metastable and usually transform to rutile when the temperature is increased [90].

(A)   (B)
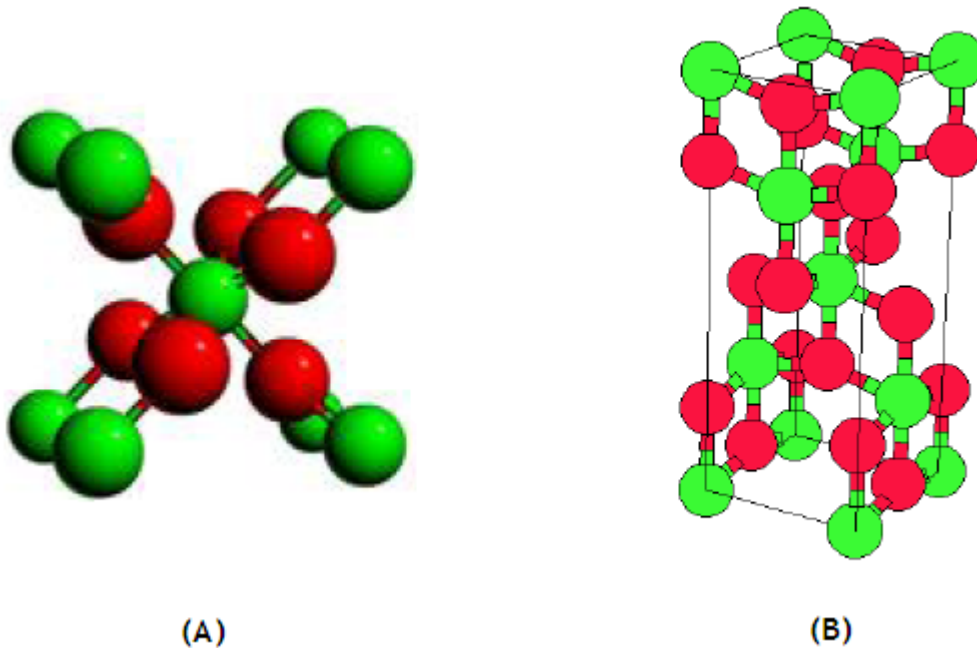
Fig 3.6 Structures of titanium dioxides: Ti (red)-O2 (green). **(A)** Rutile; **(B)** Anatase [63]

Generally surface modification approaches can be categorized in 3 main section: [91]

1. Mechanical modification treatments used to achieve specific topography and generally based on subtractive processes
2. Chemical modification treatments applied to the surface to make it clean, rough or smooth with subtractive processes, along with removal process of material from μm to mm scale. Additionally chemical treatments (such as electrochemical treatments, CVD, sol-gel) are beneficial to coat organic or inorganic films with favorable topographical and chemical properties.

3. Physical modification treatments usually is used to clean the surfaces, remove the native titanium oxide layer or to rough the surfaces.

Among surface treatment techniques, the chemical and electrochemical techniques appear particularly promising thanks to the possibility to treat very complex structure such as stents and implants, allowing a very thin and advanced controlling of chemical composition and topographical structure.

Besides this technique is moderately cheap and have relatively simple procedure.

The electrochemical treatments can be divided into three main branches: The anodic oxidation, the cathodic oxidation/polarization and the electrophoretic deposition.

Anodic oxidation is an electrolytic process which permits to increase oxide film thickness, that naturally forms on the surface of several metals, in order to improve the corrosion, abrasion resistance and to decrease ion release or to obtain oxide film with desired properties. These characteristics depend on bath composition (electrolyte) and operating condition (temperature and current density, in galvano static configuration).

In natural atmosphere, the surface of titanium is spontaneously covered with a 1–10 nm thick film of titanium oxide (TiO_2),

Titanium sample is immersed in an electrolytic solution and connected to the positive terminal of a direct current power supplier whose negative terminal is connected to a metallic counter-electrode made of stainless steel or titanium. When the circuit is closed, the titanium plate behaves as anode and the formed oxide film augments its thickness, which linearly depends on the potential applied (until the breakdown of the film occurs). A kind of setup for anodic oxidation is represented in Figure 3.7.

The electrophoretic deposition allows coating growth as a consequence of the charged particles deposition, previously suspended in an organic solvent-based electrochemical cell, and opportunely moved from electric field.
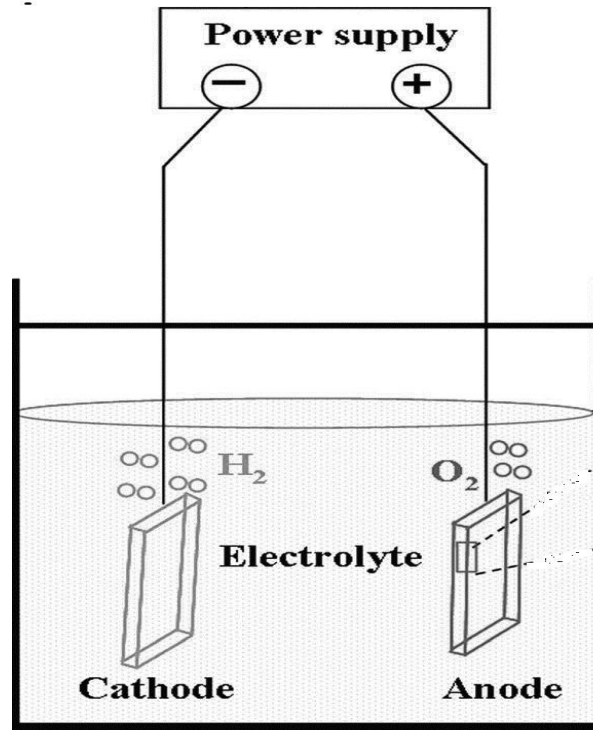
Figure 3.7 Set-up for anodic oxidation of titanium surface [84]

The main chemical reactions leading to anodization can be written as [84]:

At Ti/Ti oxide interface: $Ti \leftrightarrow Ti2+ + 2e-$ (1)

At Ti oxide/electrolyte interface: $2H2O \leftrightarrow 2O2- + 4 H+$ (2)

$2H2O \leftrightarrow O2$

(Gas) $+ 4 H+ + 4e-$ (3)

At both interfaces: $Ti2+ + 2O2- \leftrightarrow TiO2 + 2e-$ (4)
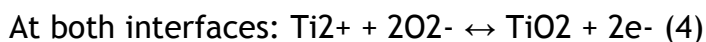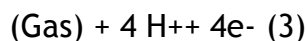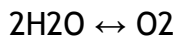
The TiO2 growth can be categorized in two stages: the first is a linear increase of the TiO2 layer thickness, depending on the applied voltage, with a correlate increase of the TiO2 resistivity until the breakdown of the film happens. It's

commonly observed that the growth of this dielectric film is linear up to 130-160 V, depending on the process conditions. [93]

When the dielectric breakdown occurs the surface is filled with large number of small sparks which is due to gas evolution at the anode anodized metal. [93] It is believed that the sparks produce thousands of micro-melting spots of the oxide layer lead to doping of chemical species present in the electrolytic solution on titanium surface and remix them with titanium oxide layer.

Consequently, the final oxide layer is characterized by a micro porous morphology and is enriched with chemical species of the electrolytic

Solution whit a concentration gradient across the oxide Figure 3.8. [93]
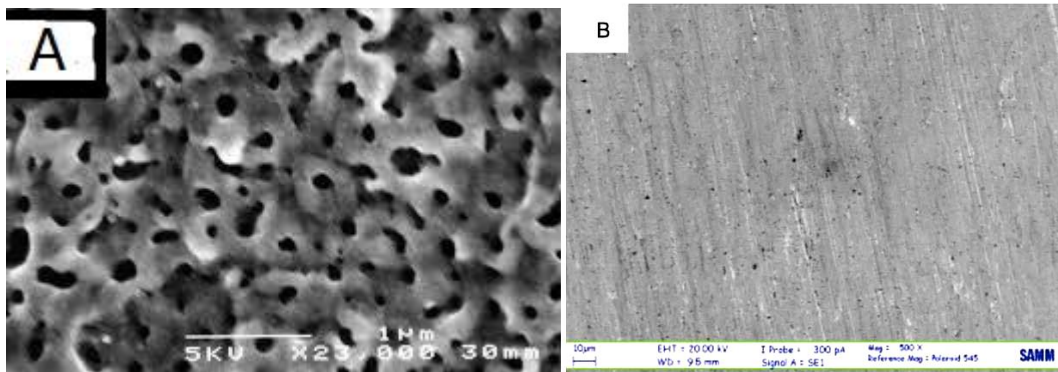
Fig 3.8 SEM images of titanium surface A) Magnification 23k.X after the anodic oxidation B) Before the anodic oxidation. [94, 95]

Anodic Spark Deposition (ASD) or Micro-Arc Oxidation (MAO) is one of the important surface treatment technique, involving above described phenomenon whit an appropriate electrolytes to dope specific elements on the surface of metal.

Altering the electrical variables and the electrolytic solution is possible to control the chemistry, topography and surface morphology of the titanium oxide layer. They can briefly summarized as follow:

3.5.1 Electrical variables

Film thickness is a function of the total current passed per area unit; so, higher voltage produce thicker oxide [94]. Moreover, porosity and roughness of the oxide layer is correlated to current density so that, pores may be round shaped, ellipsoidal or irregular, and with elongated shapes. Usually, the diameter of the pores and the roughness of the film increase with increasing current density.[94] The thickness of the oxide layer challenges it's adherence properties and density; In particular higher thickness are more prone to oxide delamination and crack growth.

3.5.2 Electrolytic solution

Electrolytic solution composition is directly influence the final chemical composition of oxide surface, resulting in different doping level of elements on the surface of titanium sample to stabilize the precipitation of chemical species, the stabilizing compound (such as coordination compound or chelating agents) is added to solution. [96]

Besides the electrolytic bath must be free from chloride ions, due to this fact that oxide layer is not stable in presence of these ions leading to dissolution of protective oxide layer and decrease its thickness.

Regarding to the mechanical properties, ASD produces inorganic glass-ceramic coating on the metallic surface with adhesive strength variable between 25 MPa and 40 MPa. Since ASD technique directly modify the pre-existing oxide layer and don't carry out a film deposition, it permits a better interaction between oxide and underlying substratum resulting in an increased mechanical stability of coating [97, 98]; In fact the anodic oxide in that the Interface of the oxide layer and the surface of metal does not show any discontinuity, and

the increased thickness of the layer improve the corrosion resistance of the titanium.

Above mentioned advantage of ASD along with high mechanical stability of the anodic film, as well as possibility to control the chemical and the topographical structure of the titanium surface, make ASD a powerful treatment method for different kind of bio-medical coating applications.

Here in this work the possibility to use this technique with proper solution also for production of titanium-core stents is investigated.

Chapter 4

MATERIALS AND METHODS

4.1 Introduction

In this chapter, morphological, physicochemical and mechanical characterization methods used to investigate the effect of the coatings on titanium will be represented.

Generally these methods can be divided as following:

- Topographical and micro-structural analysis of the modified titanium oxide layer;
- Mechanical characterization of the obtained surfaces;
- Qualitative and quantitative surface chemical characterization

A set of titanium samples were treated using Anodic Spark Deposition (ASD) method over the vast voltage range, then coated samples tested to assess their physiochemical and mechanical characteristics.

The main goal of this work is to find optimum voltage, required to assure sufficient adherence of coating on titanium substrate during mechanical deformation, regarding to its application as cardiovascular stent.

In the next step, further tests are carried out on the nominated samples which treated in proper voltages.

4.2 Materials

The procedures applied for the preparation of a ceramic coating on titanium is based on a patent of Politecnico di Milano [101,102] which was used as a starting point for the methodology of this project, followed by further investments.

4.2.1 Titanium samples

All the samples used for the mechanical, physical and chemical characterization were obtained from a plate of pure titanium grade 2 for biomedical use provided by Torresin Titanio Metalli S.r.l , Limena, Italy.

Then the samples cut into 2 different shapes: First rectangular shape (10 cm x 1cm) with the average thickness of 0.8 mm ,for the assessment of mechanical characterization of coating, and the second one , titanium disks (diameter: 12 mm), for the analysis of physicochemical properties .

Before undergoing any treatments, samples were rinsed with Millipore water and cleaned and some of them etched in etching solution (HF 5%-HNO3 30%) for 15 seconds from the time of reaction activation(represented by production of bubbles around the sample in corrosive solution) and rinsed in water Millipore for further 10 minutes. Finally the samples were dried in a thermostat oven at 37˚C for 4 hours.

4.2.2 Samples preparation using ASD technique

Figure 4.1 represents the scheme of electrochemical circuit used in this project to coat titanium samples with the specific electrolytic solutions.

Electrical setting such as the final voltage and the current intensity are the main parameters modifying surface morphology, thickness, chemical composition and physical properties of final oxide layer.
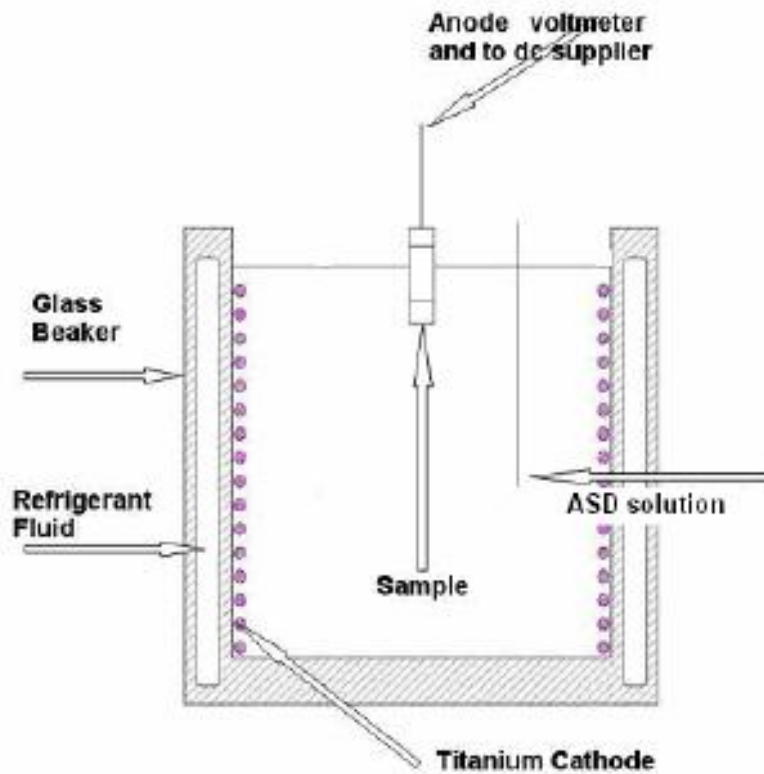
Fig 4.1 Scheme of electrochemical circuit for ASD treatment [103]

The electrolytic solution is poured in a jacketed beaker, while the chilling system provides refrigerating fluid to refrigerate the solution.

During the process the temperature of the refrigerant fluid is automatically controlled and kept between -1°C and 0°C by an automatic chiller (Julabo F32-HL Refrigerated/Heating Circulator with -35_200°C temperature working range to ensuring the flowing of the refrigerant fluid. (Fig 4.2)

Fig 4.2 Chiller used for refrigerating the solution

The anti-freezing fluid also added in some cases which is composed from half Millipore water and half (v/v) Paraflu and it was used to avoid the formation of ice in the refrigerating bath during treatment. The average temperature of the electrolytic solution is important because it has been observed that solutions at higher temperatures lead to formation of weak coatings. [104]

A cylindrical net of titanium grade 2 (same grade as the samples) is used as cathode and is placed in the inner of a beaker, so that covers the inner wall of beaker and connected with the negative pole. The cathode surface must be big enough in comparison to titanium sample (anode) surface to decrease the

Influence of anode dimension on the final coating and to get a more homogeneous distribution of the electrical field involved in the deposition process.

On the other side, the titanium samples used as the anode of the cell, are connected to the positive pole and are completely immersed in the

electrolytic solution by means of specific ad-hoc to allow the treatment of several samples in the same time.

4.2.3 Electrolytic solutions

To prepare the electrolytic solutions the reagents shown in Table 1.5, were used.

This milky-looking solution (so called SiB), already developed in a previous master thesis work, is nowadays clinically used to produce a biomimetic coating on dental implants with optimum control as well as excellent results. [94,105,106]

Besides, in 2005 studies carried out on the effect of doping elements such as Ca and P (on the surface of stents) in decreasing platelet adhesion which enhances surface blood compatibility. [64]

Moreover, the presence of Si, over a range of doping levels was also observed to be beneficial to the bio response in different type of stent coatings. [73]

Reagents	Chemical Formula	Molecular Weight [g/mol]
Sodium Silicate (Carlo Erba Reagenti, 373908)	$Na_2SiO_3*2H_2O$	182.13
Beta-glycerhophosphate (β-GP) Disodium Salt Pentahydrate (Fluka, 50020)	$C_3H_7Na_2O_6P*5H_2O$	306.12
Calcium Acetate (Fluka, 21052)	$C_4H_6CaO_4*H_2O$	158.7
Sodium Hydroxide (Fluka, 71690)	NaOH	40

Table 1.5 SiB solution

4.2.4 Parameters of ASD treatments

Programmable DC power supply (N5772A, Agilent Technologies, Everett, WA, USA, with a 600 V full-scale and a 2.6 A full-scale current intensity) was used to carry out the deposition. Using the electrical setting it was possible to modify the current intensity applied to the electrolytic solution and the final voltage necessary to reach during the ASD process. (Fig 4.3)

Fig 4.3 ASD experimental set-up (Left), DC power supply (Right)

Current intensity (I) and final voltage (V), are directly altering the properties of the resulting oxide layers in terms of titanium oxide layer thickness, surface chemical characterization (regarding to dopant deposition level and morphological aspect). All the different anodization treatments were carried out in galvano static conditions until the achievement of the set final voltage while the solution was kept stirred by magnetic stirring.

4.2.5 Chemical alkali treatment

After the ASD treatments some surfaces were subjected to an alkali treatments in 5M NaOH for 2h at $60 \pm 2°C$.

Finally after etching, samples rinsed with distilled water and were dried in a thermostat oven at 37°C for 4-5 hours.

This alkali etching aims to enrich the surface of oxide with Sodium which lead to higher hydrophilicity of oxide layer and to increase the Ca/P (calcium/phosphorous) ratio [107]. In particular the control treatments SiB after the ASD process is treated in this alkali solution. [94]

4.2.6 Experimental matrix

The table 1.6 shows all the samples treatments carried out during this project. For each treatment are indicated the current intensity and the final voltage set during the ASD treatment. The label "Na" after the treatment label means that was carried out the post-chemical etching according to part 4.2.5.

Besides, label "R" signifies rectangular shape samples while "D", represents disk shape sample.

For more accuracy, in each voltage 3 Rectangular shape samples tested.

Treatment Label	Current Intensity [mA/cm2]	Final Voltage [V]	Chemical NaOH treatment
295.R	12	295	
295.R.Na	12	295	•
285.R	12	285	
285.R.Na	12	285	•
275.R	12	275	

275.R.Na	12	275	•
265.R	12	265	
265.R.Na	12	265	•
255.R	12	255	
255.R.Na	12	255	•
245.R	12	245	
245.R.Na	12	245	•
235.R	12	235	
235.R.Na	12	235	•
225.R	12	225	
225.R.Na	12	225	•
215.R	12	215	
215.R.Na	12	215	•
205.R	12	205	
205.R.Na	12	205	•
195.R	12	195	

195.D.Na	10	195	•
185.R	12	185	
185.D.Na	10	185	•
175.R	12	175	
175.D	10	175	
175.D.Na	10	175	•
165.R	12	165	
165.D.Na	10	165	•
155.R	12	155	
155.D.Na	10	155	•

Table 1.6 samples treatments carried out during this project

4.2.7 Titanium Electropolishing

For nominated sample (175.D not chemically etched in HF-HNO3 solution) electropolishing in an alcoholic solution-based electrolyte before ASD treatment also has been carried out.

A non-aqueous electrolyte comprising ethyl alcohol (700 ml/L), isopropyl alcohol (300 ml/L), aluminum chloride (60 g/L), and zinc chloride (250 g/L) was prepared.

Titanium Disk samples placed as anode connected with the positive pole in the beaker while a cylindrical net of titanium grade 2 (same grade as the samples) is used as cathode and is placed in the beaker, so that covers the inner wall of beaker.(Figure 4.4)

Electropolishing was performed under an electrolytic condition of $70-75$ V, 2.0 kA/m2, and 30℃ for 15 to 20 minutes.
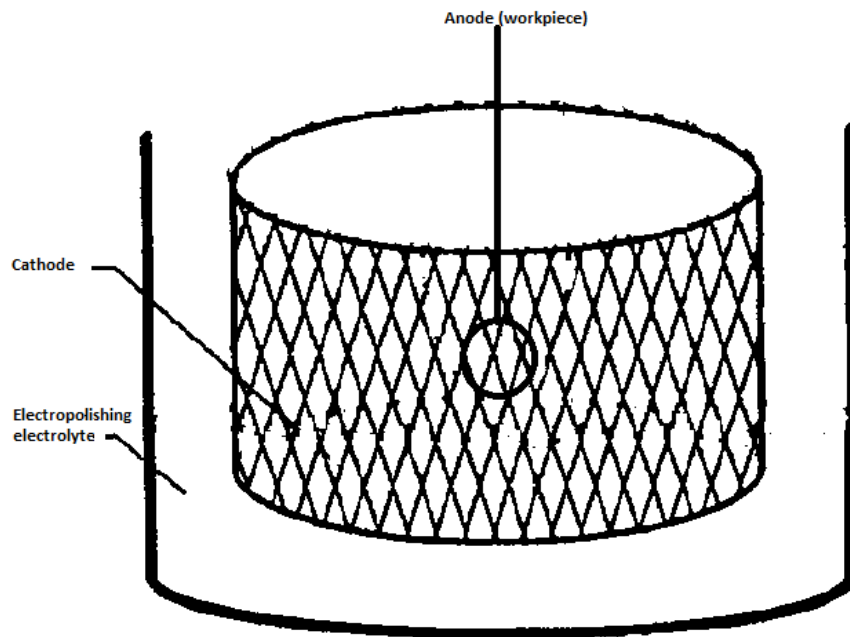

Fig 4.4 Scheme of circuit for electropolishing of samples

4.3 Methods

The mechanical, physicochemical and morphological characterizations of the surfaces obtained by ASD treatments were investigated by means of the following techniques:

- Scanning Electron Microscopy (SEM);

- Elemental Dispersive X-ray Spectrometry (EDS);

- Contact angle measurements;

- TiO2 delamination test (3 point bending test);

- Inductively Coupled Plasma Optical Emission Spectrometry (ICP-OES);

- Laser Profilometry (LP)

4.3.1 Scanning electron microscopy (SEM)

Scanning electron microscopy (SEM) is chiefly used to investigate the samples surface morphology at high magnification (from 100X to approximately 25000X, with a spatial resolution from 50 to 100 nm).

The scanning electron microscope uses a focused beam of high-energy electrons.

The electrons interact with atoms in the surface of sample, producing various signals that can be detected which, contain information about the sample including external morphology, chemical composition, crystalline structure and orientation of materials making up the sample.

Accelerated electrons in an SEM transport considerable amounts of kinetic energy, which is dissipated as a vast kind of signals produced by electron-sample interactions occurs.

These signals include secondary electrons (that produce SEM images), backscattered electrons (BSE), diffracted backscattered electrons (EBSD, used to determine crystal structures and orientations of minerals), photons (characteristic X-rays that are used for elemental analysis and continuum X-rays), visible light (cathodoluminescence-CL), and heat.

The SEM allows the analysis of conductive specimens; so for analysis of nonconductive surfaces, gold sputtering on the surfaces has to be performed.

The common electron gun source is the tungsten filament, which consists of a fine tungsten wire. The filament is connected to a source of current and electrons are passed through the wire.

As filament heats up, electron emission occurs from the tungsten bended filament, which produce a coherent source of electrons.

In this type of gun the outside source of electrons and the heating source are one in the same.

Secondary electrons and backscattered electrons are widely used for imaging samples, it worth notice that, secondary electrons are mainly used for depiction of morphology and topography of samples while backscattered

electrons are mainly useful in multiphase samples condition for illustration of contrasts in composition (i.e. for fast phase discrimination).

4.3.2 Elemental dispersive X-ray spectrometry (EDS)

EDS is an analytical technique uses the X-rays detection for the elemental analysis or chemical characterization on the surface of sample.

Every different element after being excited emits x-rays at particular frequencies.

Each element emission depends on its atomic number. X-ray generation is produced by inelastic collisions of the incident electrons with electrons in discrete orbitals (shells) of atoms in the sample.

As the excited electrons return to lower energy levels, they produce X-rays with specific wavelength in correlation with difference in energy levels of electrons in different shells for a given element. Thus, each element in material would have a characteristic X-rays after getting excited by electron beam.

EDS is generally a qualitative chemical analysis and is not a true quantitative method, but by performing EDS at different voltages and different degree of surface depth some semi-quantitative information can be obtained.

Although to obtain better precision in this project, Inductively Coupled Plasma Optical Emission Spectrometry (ICP-OES) test has been performed.

SEM and EDS analyses are considered to be "non-destructive"; that is, X-rays generated by electron interactions do not lead to volume loss of the sample, so it is possible to analyze the same materials repetitively. [108,103]

4.3.3 Samples SEM and EDS analysis

Samples surfaces were analyzed by two different SEM, ZEISS-EVO 50 EP able to work both in air and in high vacuum (10-6 mmHg), and Cambridge – Stereo scan 360 able to work only in high vacuum (10-5 mmHg). The samples were analyzed at different magnifications after the surface treatments, electropolishing and TiO2 delamination tests.

The samples were analyzed with EDS (Oxford, Inca energy 200, Politecnico di Milano) after the surface treatments.

4.3.3 Contact angle measurements

The contact angle θ is the quantitative measure of the wetting of a solid by a liquid. When a droplet of liquid is placed on a flat horizontal solid surface, the solid-air and liquid-air interfaces come together under the static contact angle (CA), θ which, in particular represents the angle formed by a liquid at the three phase boundary where a liquid, a gas and a solid intersect. The value of θ can be determined from the Young's equation, which express the minimization of the total free energy of the system during equilibrium: (Figure 4.5)
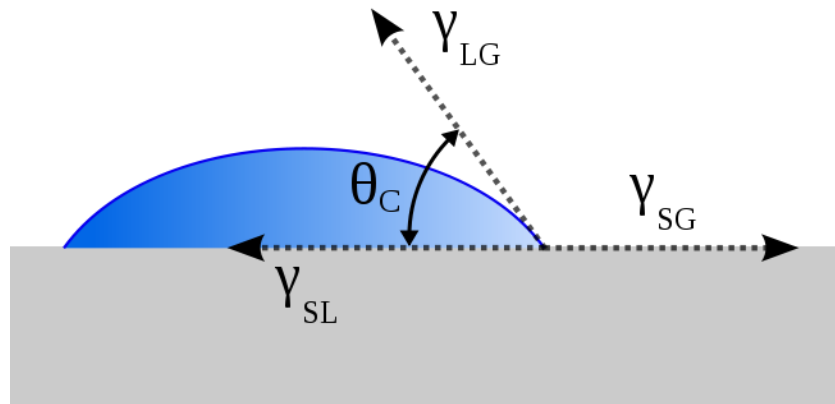
$$\gamma_{SV} = \gamma_{SL} + \gamma_{LV} \cos\theta$$

Fig 4.5 Scheme of liquid droplet in contact with a solid surface [115]

Where γ_{LG}, γ_{SG}, γ_{SL} are respectively liquid-air, solid-air and solid-liquid interface free energies. Both surface chemistry (i.e. functional groups) and morphology contribute to determine the wetting behavior of a material.

To measure the contact angle (static or dynamic) is used a device composed by an optic bench. A light source and an optical detector are used to take pictures of drops deposed on sample by a syringe perpendicular to the sample surface. Particular software elaborates the information from the picture and calculates the relative contact angle.

Measurements of contact angles permit to determine the wettability properties of sample surface.

In principal, the surface is considered hydrophilic if $0<\theta<90°$ while is considered hydrophobic if $\theta>90°$. The value of θ can be determined from the Young's equation, which express the minimization of the total free energy of the system.

Contact angles are extremely sensitive to contamination; values reproducible to better than a few degrees are generally only obtained under laboratory conditions with purified liquids and very clean solid surfaces.

4.3.4 Samples surfaces wettability analysis

The contact angle measurements were performed according to the static sessile drop method, by an optical device (Data physics Instruments Mod. OCA 15 plus) and a related software (32-bit software SCA20); was used a water drop of a 2µl of volume, deposed in 1µl/s (medium speed) on the samples surface.

At least 4 different water drop depositions at room temperature were performed for each nominated disk shape and rectangular sample.

Bended rectangular samples after 3 point bending test also were cut into smaller rectangular pieces and wettability test on the flat area of their surfaces (far form bended zone) carried out.

4.3.5 Three point bending test

In the clinical application, cardiovascular stents must undergo an extent of plastic deformation during installation which induced by balloon angioplasty, and finally the stents must withstand continuously cyclic deformation by the beating heart.

In the case of coated metallic stent, if the hemocompatible coating peels off, the exposed metal surface (usually stainless steel) owning lower blood-

compatibility will be exposed to the blood directly, and rapidly induce coagulation which lead to ISR.

In more seriously cases, the peeled fragments may flow with the

blood stream and reach to narrower locations in cardiovascular system and cause further occlusion.

Nevertheless, in our case, since, the core of the stent is made of titanium- a high biocompatible material- low level of coating delamination may not affect overall biocompatibility of the stent.[37,110]

In this work, to analyze the coating susceptibility to delamination, a three-point bending test was carried out on rectangular shape (10cm x 1cm) titanium grade 2 samples with thickness of 0.75mm to 0.85mm after ASD treatment in different voltages, as cited in sector 4.2.2 and 4.2.3.

Regarding to the previous work which has been done in a similar field, optimum strain of 12% to 13% was selected as the final elongation value. [110]

The test was performed on an electronic universal test machine (MTS 858 Mini Bionix working in position control method) by placing the coated specimens on a support span with two rollers and a single upper roller. The schematic of specimen during measurement is shown in Figure 4.6.

The evaluated coating was on the convex side, and the span and max bend-displacement were set to 20 mm and 10 mm respectively.

Besides for nominated samples (175 V), bend-displacement also in 4mm were performed.

A force was applied with a slow speed of 2 mm/min.

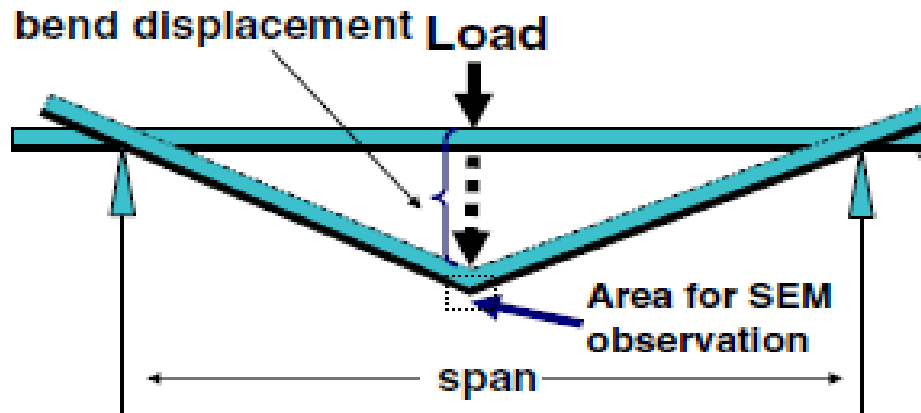Max bend-displacement equal to samples flexion of 110° was attained.

Fig 4.6 the schematic of samples in Three-point bending side view while testing [110]

Calculation of strain induced by 3 point bending test carried out regarding to ASTM document No.D790, Designation: E2769 – 13 as following: (Figure 4.7)
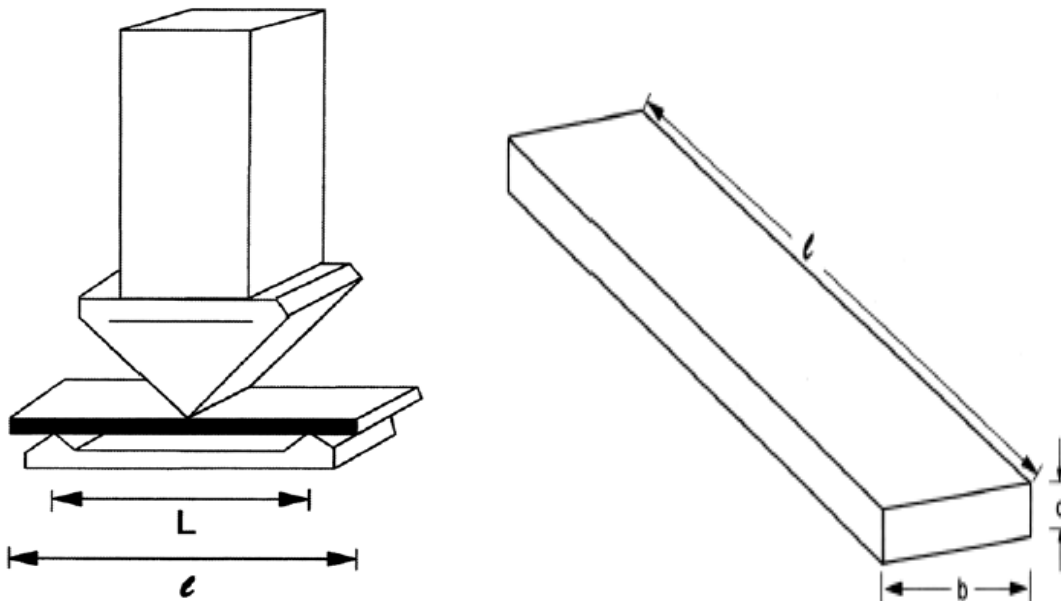

Fig 4.7 Test Specimen Geometry [111]

$$\text{strain} = \varepsilon = \frac{(6\,D\,d)}{(L^2)}$$

b = beam width, mm,
d = beam thickness, mm,
D = beam displacement, mm,
L = support span, mm, and
ε = strain, dimensionless.

So after above calculation, regarding to mentioned values for parameters, maximum final strain of about 12%- 13% was obtained.

After bending, the surface topography of the samples at the point of highest deformation was inspected by scanning electron microscopy.

4.3.6 ICP-OES

ICP-OES is one of the most powerful and popular analytical tools which permits the simultaneous detection of many chemical elements (up to 70) even if in a very low concentration (under 1g/L).

In the inductively coupled plasma optical emission spectrometry the liquid and gas samples may be injected directly into the instrument, while solid samples needed to be extracted so acid digestion is required.

Through a nebulization process, the sample solution is converted to an aerosol and directed into the central channel of the plasma.

At its core the inductively coupled plasma (ICP) sustains a temperature of approximately 10000 K, so the aerosol is quickly vaporized.

Meanwhile atoms and ions are excited and then excited state species may then relax to the ground state via the emission of a photon.

Each emitted electromagnetic radiation by its unique wavelengths signifies presence of a particular elements.

The intensity of this emission is indicative of the concentration of the element within the sample.

The resultant polychromatic emission is scanned in individual wavelength voiding the detection and measure of each single emission without interference.

The following conversion of the single detections in electrical signals allows the quantification of the relative concentrations. (Figure 4.8) [112, 113 and103]
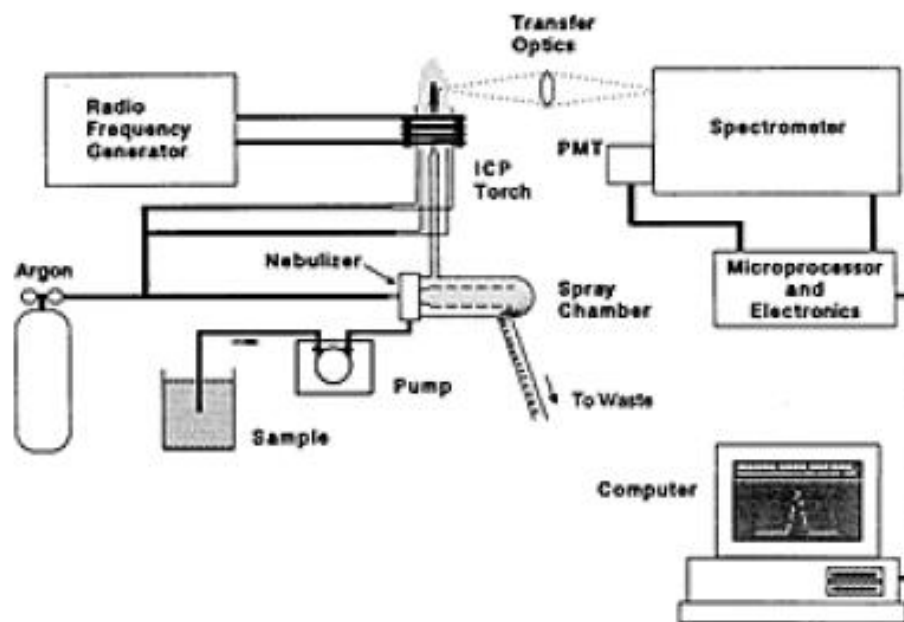
Fig 4.8 ICP-OES working scheme (114)

4.3.7 Sample ICP-OES analysis

Surface of 3 disk shape samples, (treated in nominated voltage 175 V) were investigated by ICP-OES analysis to calculate the level of Na, Ca, P and Si on their surfaces.

Two of the coated disk shape samples, also treated previously in alkali solution in 5M NaOH for 2h at $60 \pm 2 °C$ as cited in section 4.2.5.

Before analysis all the samples were treated with nitric acid 1: 1 and ultrasounded for 2 hours; then solutions were analyzed by optical emission spectrometry plasma.

The quantitative determination was carried out with a tool model Perkin Elmer Optima 8300.

4.3.8 LASER PROFILOMETRY (LP)

The laser profilometer is a non-contact device which allows us to determine the profile of the surface of samples.

It is based on the signal produced by a spot laser beam released by a source and reflected by the material surface under a scanning mode.

The reflected beam coming back to the source includes different optical paths regarding to the different morphology of the surface.

With this device it is possible to analysis both surfaces roughness and linear roughness. The optical signals are processed by a software and many different parameters related to different surface properties can be acquired and analyzed in order to characterize precisely the surface texture, roughness and morphology.

The limitations of this technique are the lateral resolution (1 **μ**) due to the width of the laser beam, and the vertical resolution (50nm) due to the instrument precision.

In this study three parameters were taken into account for surface investigation:

• Ra: Represents the arithmetic average of the absolute values of all points of the profile of the surface traced by the laser beam moving along a line. This is the main height value calculated and expressed in micrometers from the lower and the higher values of the detected areas (UBM parameters).

• Rz(DIN) or Rz :This is the mean of the 5 highest peaks and the 5 deepest valleys found in the 5 adjoining samples.

• K: The kurtosis is the comparison of the profile curve with a Gaussian amplitude and characterizes the density as "smooth" or "with peaks".

Kurtosis provides information about the profile morphology: K>3

Means a sharp morphology of the surface profile; K<3 Means a smoother morphology of the surface profile.
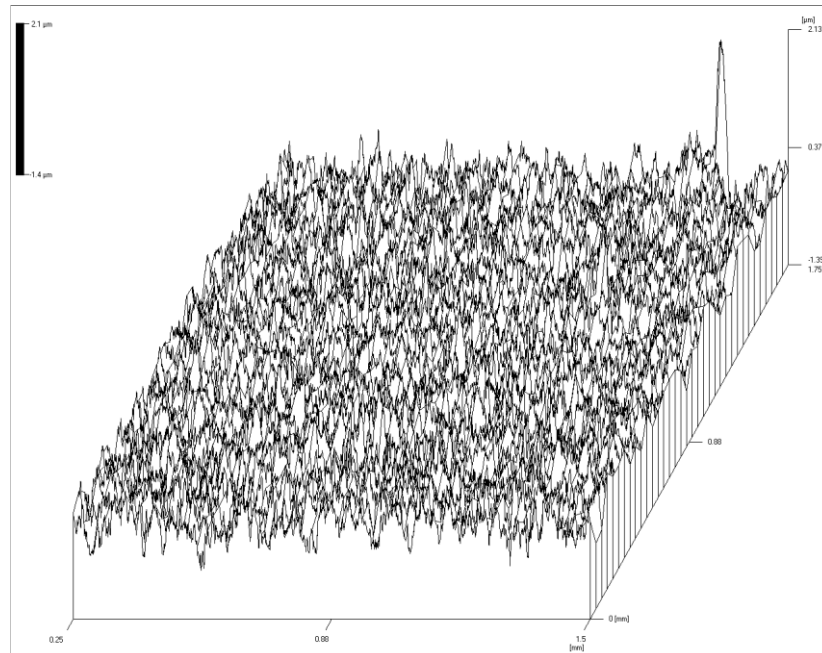
Fig 4.9 Surface profile detection during Laser Profilometry acquisition

4.3.9 Profilometric analyses on samples

The profilometric analyses were carried out with a laser profilometer (UBM Microfocus, 5600). 5 kind of samples analyzed with this method as following:

A) Ti disk grade II without primary (HF-HNO3) etching & without ASD treatment

B) 175.D sample primary (HF-HNO3) etched and ASD treated without alkali (NaOH) treatment

C) 175.D sample primary (HF-HNO3) etched and ASD treated followed by alkali (NaOH) treatment

D) 175.D sample primary electro-polished and then ASD treated without (HF-HNO3) and (NaOH) alkali treatment

E) Ti disk, electro-polished without ASD treatment, without (HF-HNO3) and (NaOH) alkali treatment

Each sample underwent 6 measures on base lines of 4mm and points density of 500/mm.

4.3.10 Statistical analysis

Statistical analysis was performed using Microsoft Excel software. By independent two-sample t Student-test to the data for group comparison (significance level p=0.05). The results were expressed as means ± standard deviation.

Chapter 5

Result and Discussion

5.1 Surface morphology analysis before bending test

Figure 5.1 shows SEM image of an untreated titanium surface.

While, in Figures 5.1.A to 5.1.G are reported the SEM images of the coatings obtained after the Anodic Spark Deposition ASD.
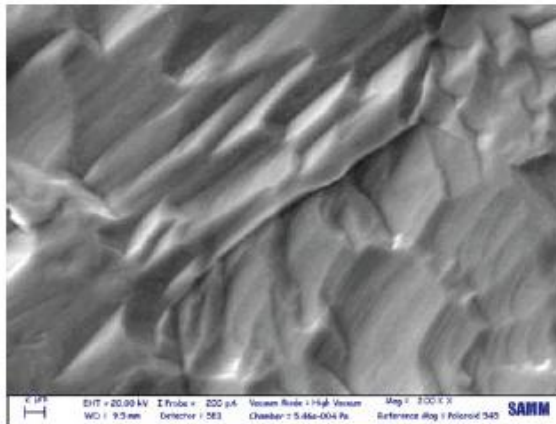
Fig 5.1 SEM image at 2k.X of untreated Ti
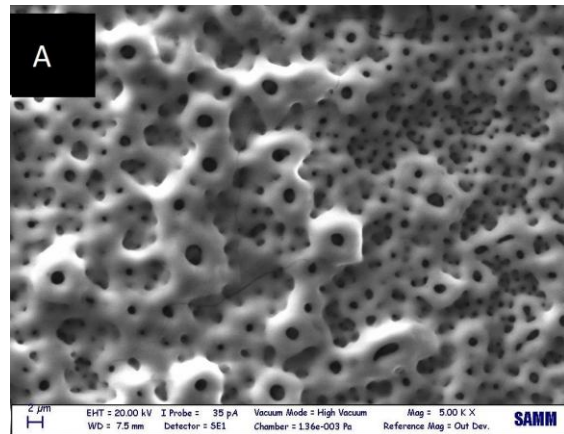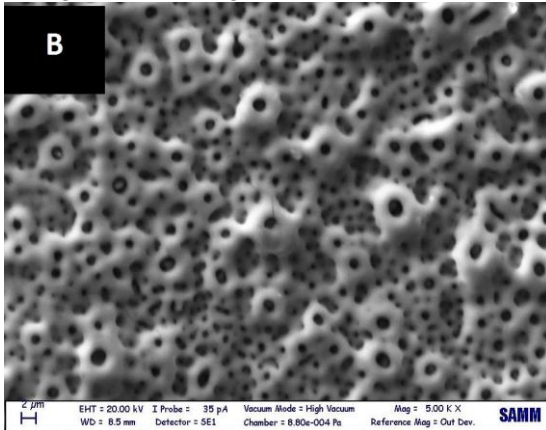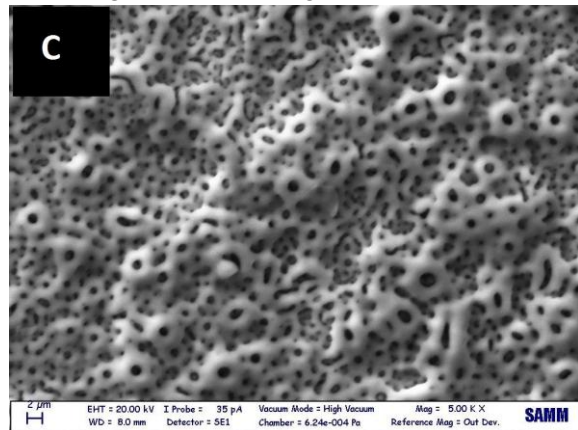

Fig 5.1.A SEM image at 5000X of 295.R

Fig 5.1.B SEM image at 5000X of 265.R

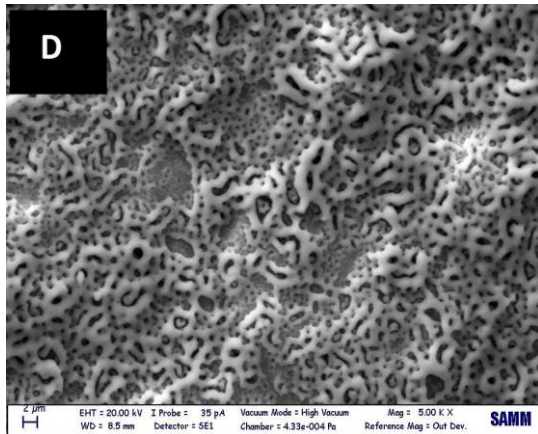**Fig 5.1.C** SEM image at 5000X of 235.R

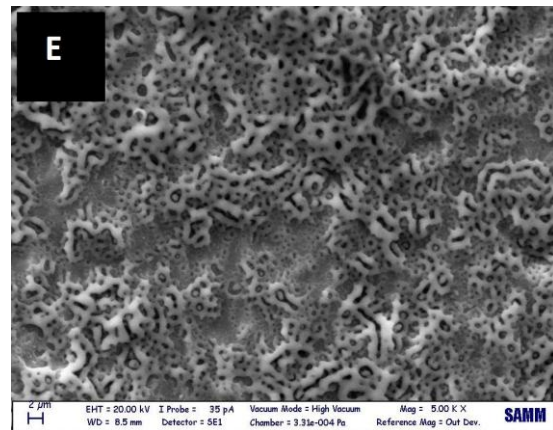**Fig 5.1.D** SEM image at 5000X of 215.R

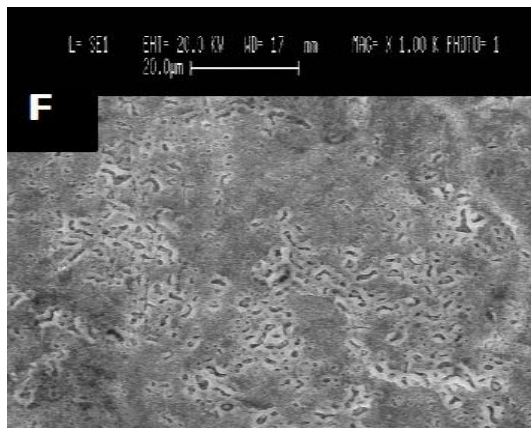**Fig 5.1.E** SEM image at 5000X of 205.R
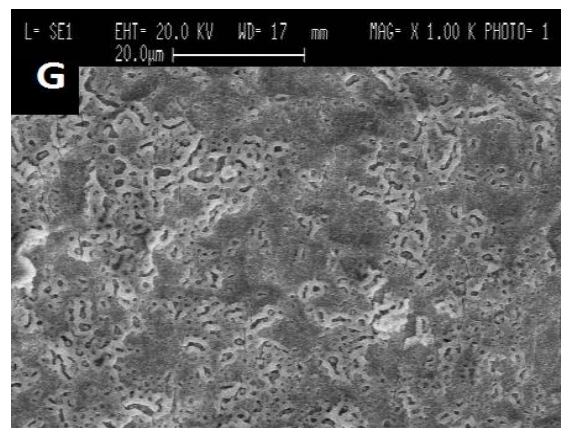

Fig 5.1.F SEM image at 1000X of 165.R

Fig 5.1.G SEM image at 1000X of 175.R

SEM image of untreated titanium before the ASD, shows that surface is not smooth and characterized by "flakes" morphology. (Figure 5.1)

As can be seen, higher voltage range ASD treated surfaces, demonstrate pore size with circular shape and bigger in dimension, which are distributed more homogenously across the surface.

Meanwhile by lowering the voltage, pore size becomes smaller. (Figure 5.1.A-5.1.B and 5.1.C)

It is worth pointing out that some micro cracks are detectable on the surface of treated samples in high voltage range particularly on 295 V to 265 V coated surfaces (Fig 5.1.A and 5.1.B) which are commonly present on the ASD treatments and not altering the coating adherence to the substrate.

Different morphology is observed in lower voltage range (Figure 5.1.D, 5.1.E, 5.1.F, 5.1.G) which depicts elongated shape pores stretched out along the coated surface in a less homogeneous distribution pattern.

Again by lowering the voltage, less regular pores with lower density are observable.

The result of SEM analysis for the nominated sample (175V) which has been electropolished before ASD treatment exhibits the same morphological pattern as 175V deposited sample without any electropolishing.(fig 5.1.H)
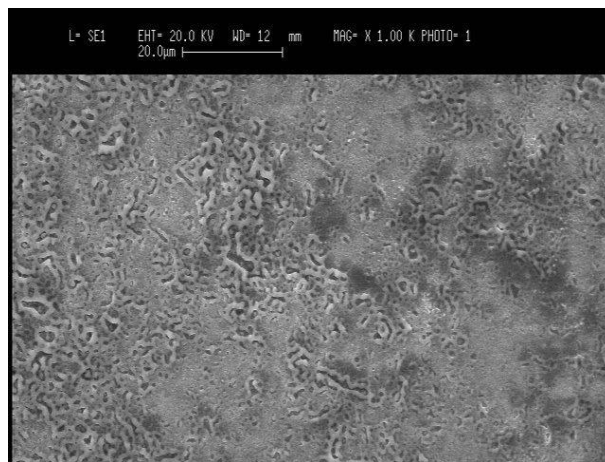

Fig 5.1.H SEM image at 1000X of 175.D coated after electropolishing

5.2 Chemical composition (EDS analysis)

The qualitative results of the chemical surface composition obtained by EDS analysis are reported in Figures (5.2.1 to 5.2.10) which divided in two categories of high final voltage and low final voltage treated samples.

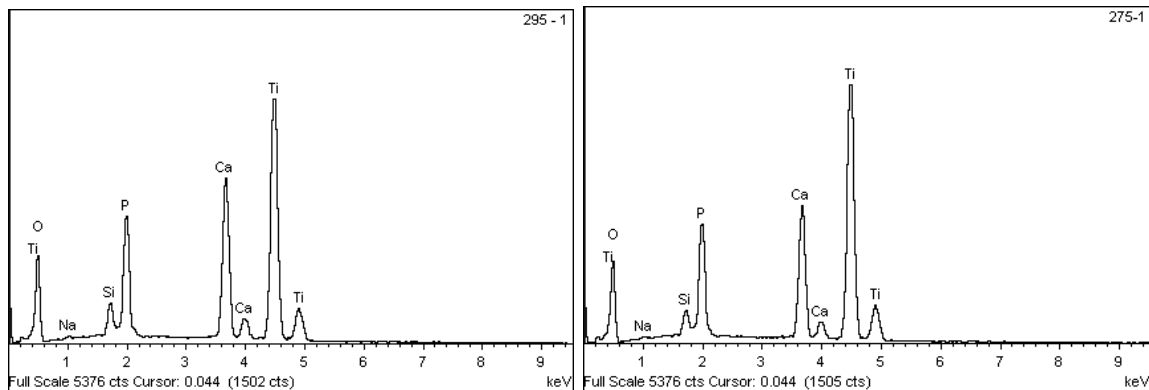a) Higher final voltage EDS results from 295V to 215V :

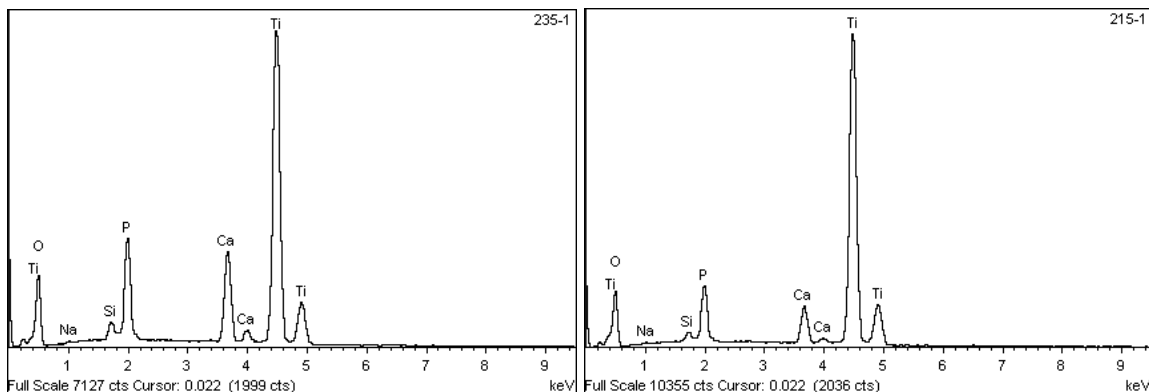**Fig 5.2.1** EDS analysis of 295.R   **Fig 5.2.2** EDS analysis of 275.R

Fig 5.2.3 EDS analysis of 235.R   **Fig 5.2.4** EDS analysis of 215.R

b) Lower final voltage EDS results from 205V to 155V:
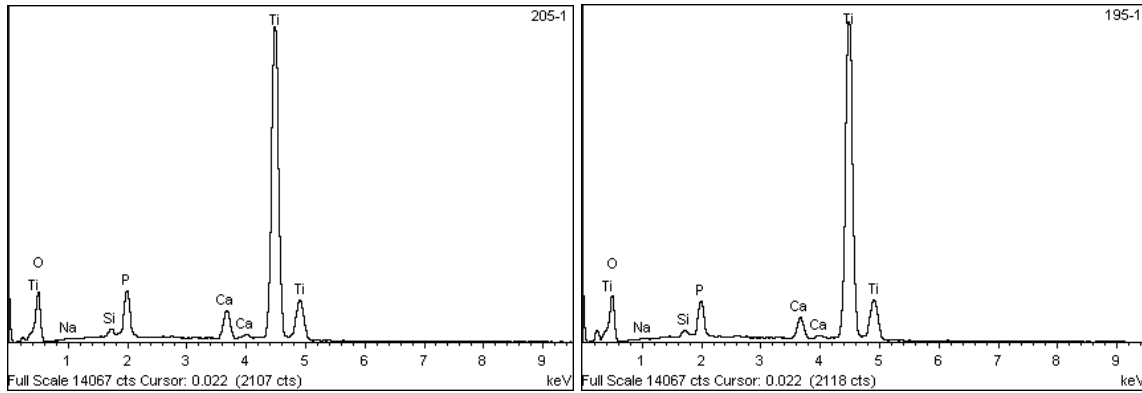

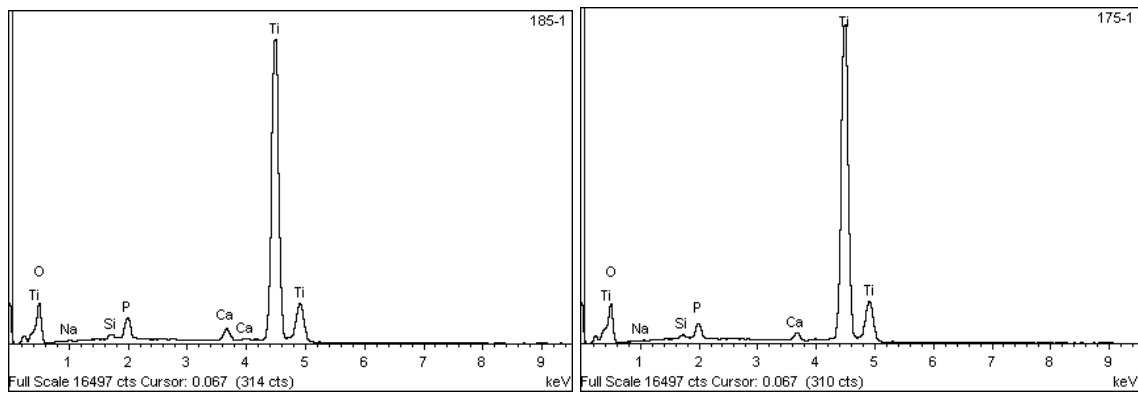**Fig 5.2.5** EDS analysis of 205.R

Fig 5.2.6 EDS analysis of 195.R

Fig 5.2.7 EDS analysis of 185.R

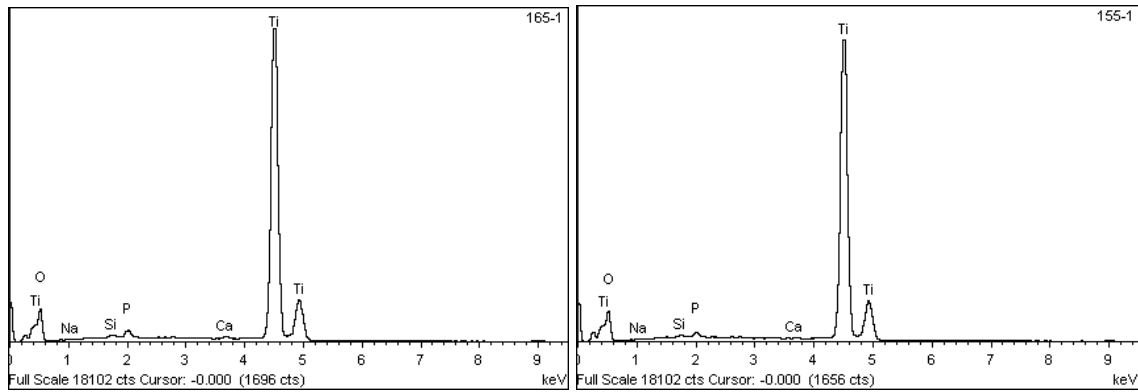**Fig 5.2.8** EDS analysis of 175.R

Fig 5.2.9 EDS analysis of 165.R

Fig 5.2.10 EDS analysis 155.R

The semi-quantitative results also can also be shown in Table 1.7, in which, all elements analysed (Normalised) and all results represented in weight %:

Spectrum	O	Na	Si	P	Ca	Total
295 - R	55.42	0.49	2.83	14.18	27.08	100.00
275-R	56.31	0.53	2.53	15.05	25.59	100.00
235-R	58.21	0.60	2.10	16.80	22.29	100.00
215-R	64.18	0.66	1.92	16.97	16.27	100.00
205-R	65.27	0.61	1.98	16.66	15.48	100.00
195-R	67.69	0.92	2.20	15.76	13.43	100.00
185-R	72.11	0.50	2.34	13.88	11.17	100.00
175-R	76.29	0.30	2.19	12.56	8.66	100.00
165-R	81.63	0.20	2.64	10.47	5.05	100.00
155-R	82.67	1.81	3.48	8.95	3.10	100.00

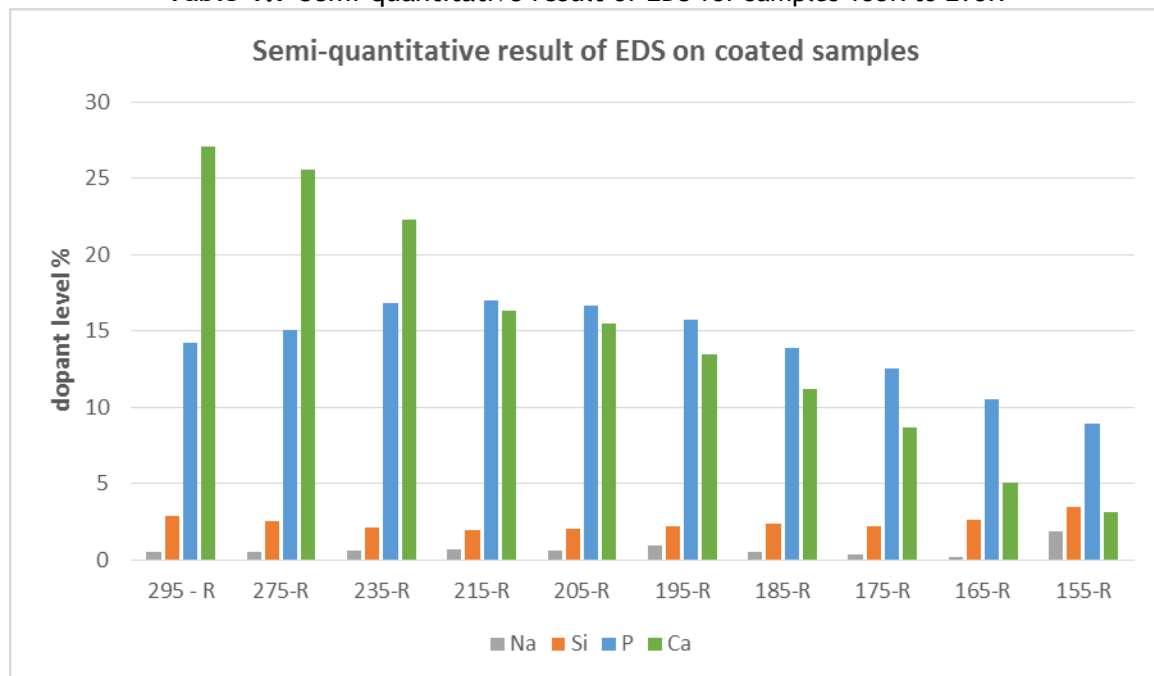**Table 1.7** Semi-quantitative result of EDS for samples 155R to 295R

Fig 5.2.11 Semi-quantitative result of EDS for samples 155R to 295R

As above Table (1.7) and Figure (5.2.11) show, on the surface of samples which treated in lower voltages, (starting from 215V downwards) the percentage of

Ca significantly decreases and this downward trends continues slightly until 155 V.

Moreover, P level shows a smooth fluctuation with a peak at 215 V, while Si remains almost stable over the voltages.

Besides, as no alkali treatment applied on the coatings, the Na level for all the samples are negligible.

5.3 Contact angle measurement

The measurements of the static contact angle are reported in Figures (5.3.A to 5.3.P)

The average values of water contact angle are also shown in Figure 5.3.2 for lower final voltages treated samples and in Figure 5.3.3 for higher final voltage treated samples.

It clearly shows the effect of alkali treatment in improvement of coatings wettability, compared to both untreated coated samples and Titanium grade II surface that is relatively more hydrophobic (Fig 5.3.1.) [94].

In particular, in lower voltage range, 175.D.Na and 185.D.Na surfaces possess the highest wettability with an average static contact angle lower than 45° (Figure 5.3.M and Fig 5.3.L), while 175.D possesses lowest one (80°), (P<0.01)

In the set of High voltage range, 255.R.Na and 295.R.Na show highest wettability with (40 °-50 °) values.

It is important to notice that , 175.D.Na and 185.D.Na in low voltage set and 255.R.Na and 295.R.Na   in higher voltage range have contact angle values lower than the so-called Berg's threshold (55°) which is considered to limit the denaturation of adsorbed plasma proteins.[103]

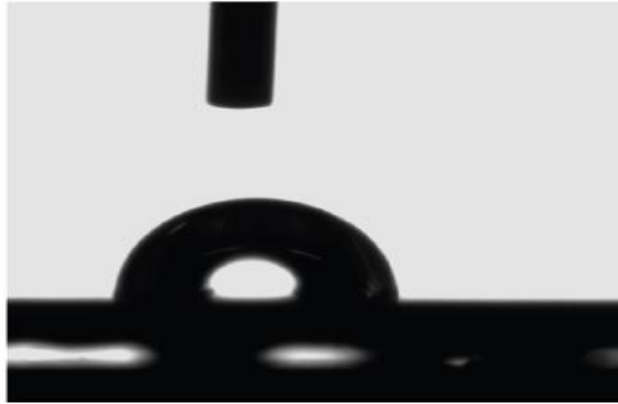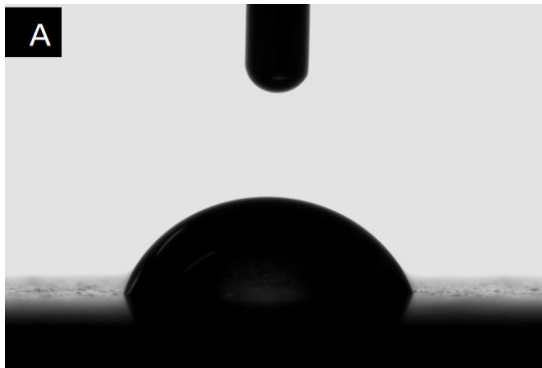**Fig 5.3.1** Water contact angle on untreated titanium surface

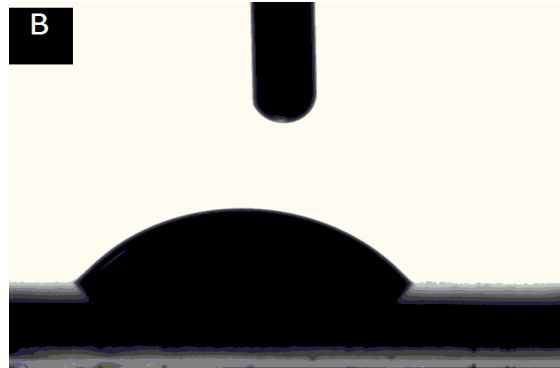**Fig 5.3.A** contact angle on 295.D

Fig 5.3.B contact angle on 295.D.Na

Fig 5.3.C contact angle on 275.D

Fig 5.3.D contact angle on 275.D.Na
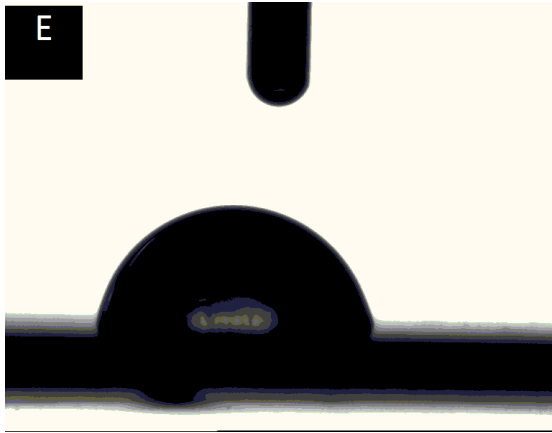
Fig 5.3.E contact angle on 255.D
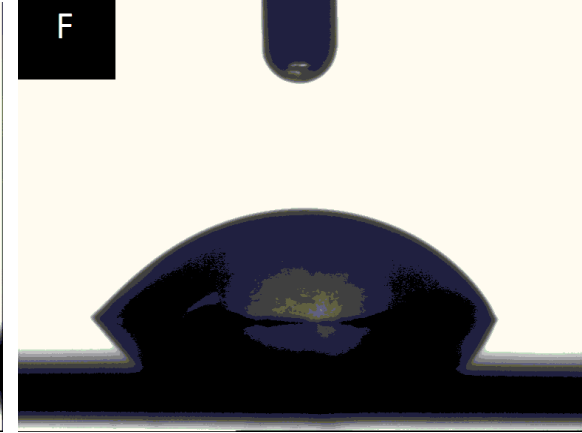
Fig 5.3.F contact angle on 255.D.Na
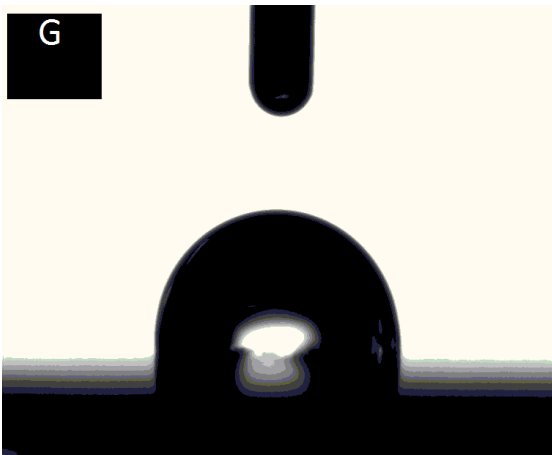
Fig 5.3.G contact angle on 235.D
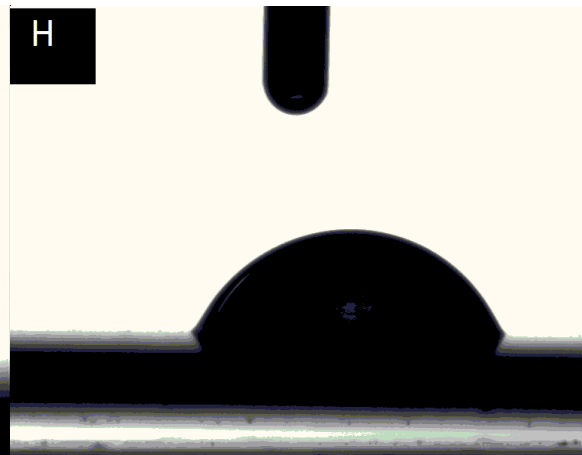
Fig 5.3.H contact angle on 235.D.Na
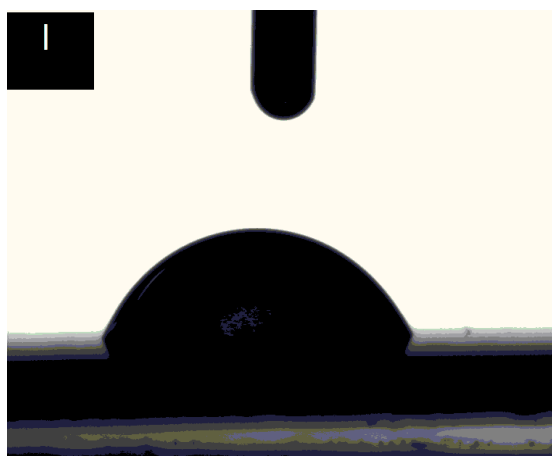
Fig 5.3.I contact angle on 205.D

Fig 5.3.J contact angle on 205.D.Na

Fig 5.3.K contact angle on 195.D.Na

Fig 5.3.L contact angle on 185.D.Na

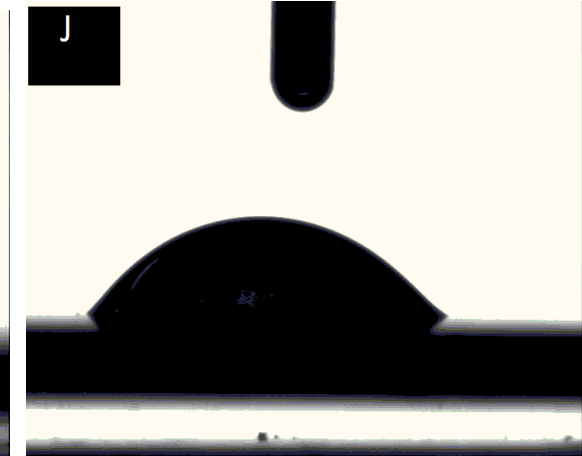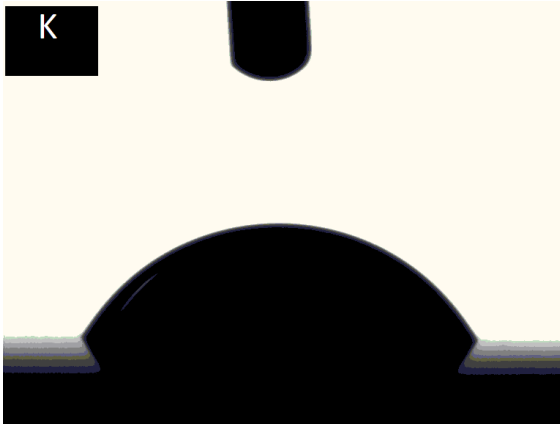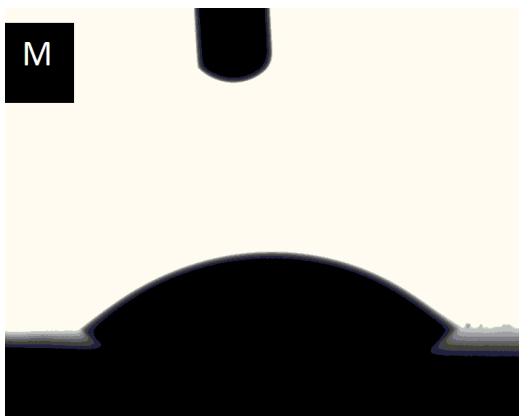**Fig 5.3.M** contact angle on 175.D.Na
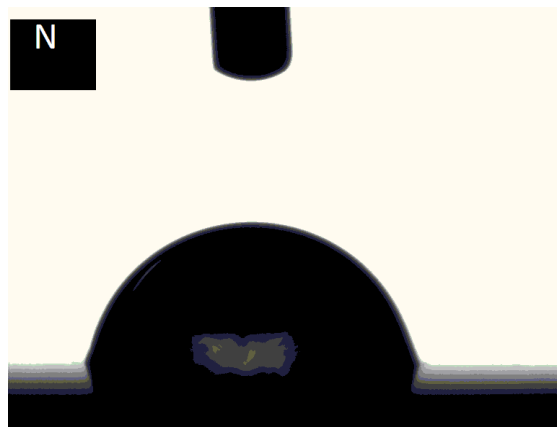

Fig 5.3.N contact angle on 175.D
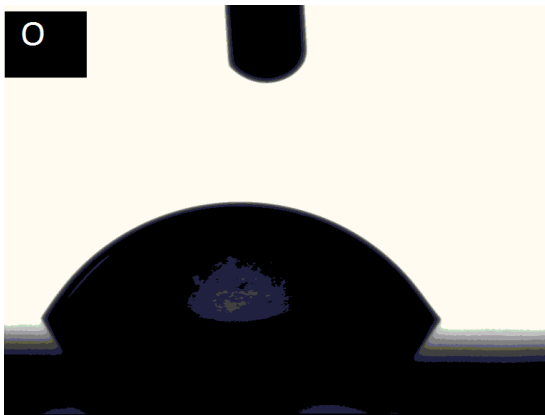
Fig 5.3.O contact angle on 165.D.Na

Fig 5.3.P contact angle on 155.D.Na
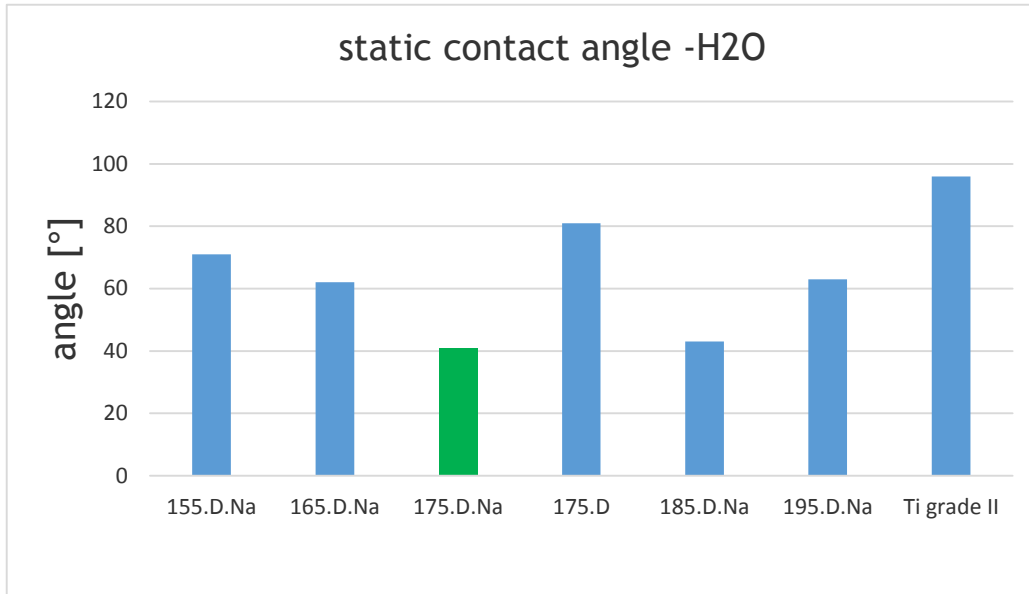
Fig 5.3.2 wettability of treated surface at lower final voltages (155V to 195V)
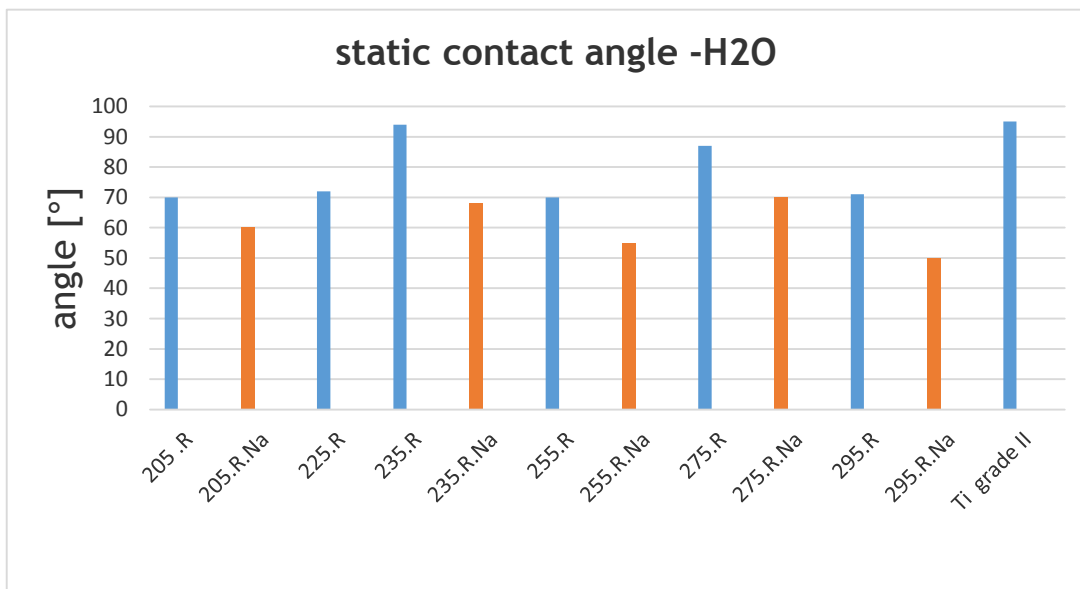
Fig 5.3.3 wettability of treated surface at higher final voltages (205V to 295V)

5.4 SEM after three point bending test

As previously cited in section 4.3.5, for the purpose of stent production, samples must endure high plastic deformation during balloon expansion without occurrence of any coating delamination or peeling.

In the Figure 5.4.1 to Figure 5.4.16 the SEM images of the ASD coating after the three point bending test by 12% -13 % applied strain (equal to $110°$ of bending) are reported.

Results of SEM illustrate the presence of big cracks and sever delamination on the coated samples at higher final voltage range. (Fig 5.4.1 to 5.4.10)

As the voltage decreases the amount of delamination significantly reduces, in a way that from 175 V downward (Fig 5.4.13, 5.4.15and 5.4.16) there is almost no sign of delamination, although cracks are still present on the surface of coating.

This behavior can be justified regarding to this fact that, by increasing the ASD treatment voltage, the thickness of the brittle oxide layer increases which makes the coating more prone to delaminate during bending test.

Besides, since by leveling up the voltage, the amount of doped elements on the oxide layer increases (fig 5.2.11), thus 175.R (samples treated as 175 V final voltage) can be regarded as nominated sample which serves the best both mechanical and physicochemical aspect of the project.

Further investigation carried out to observe morphology behavior of this coating in lower bending level (5% strain) which result in lower presence of micro cracks on the surface. (Fig 5.4.14)

Fig 5.4.17 sample during 3 point bending test
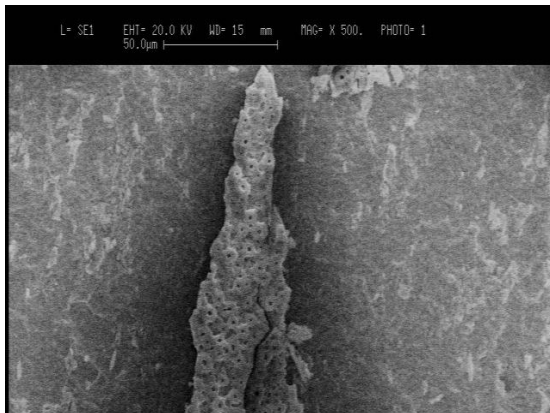
Fig 5.4.1 SEM 500X of Bended 295.R
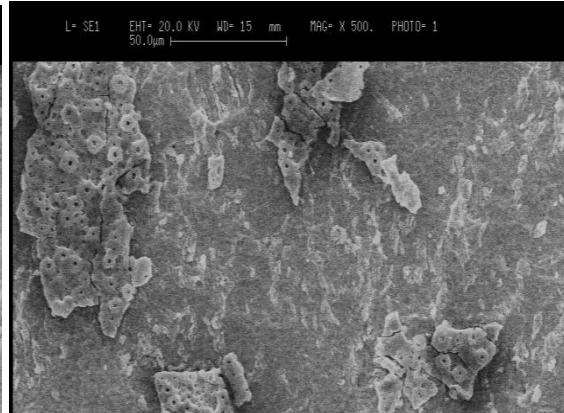
Fig 5.4.2 SEM 500X of Bended 285.R
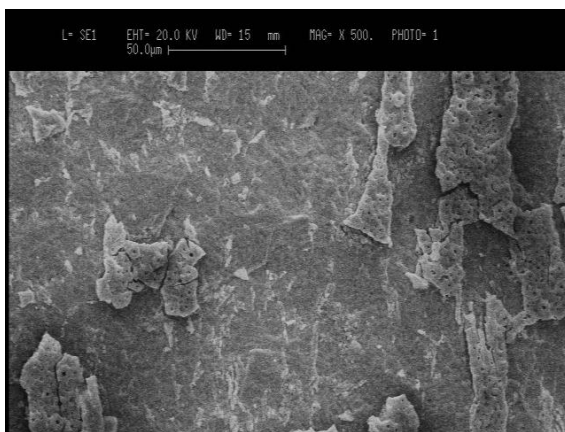
Fig 5.4.3 SEM 500X of Bended 275.R
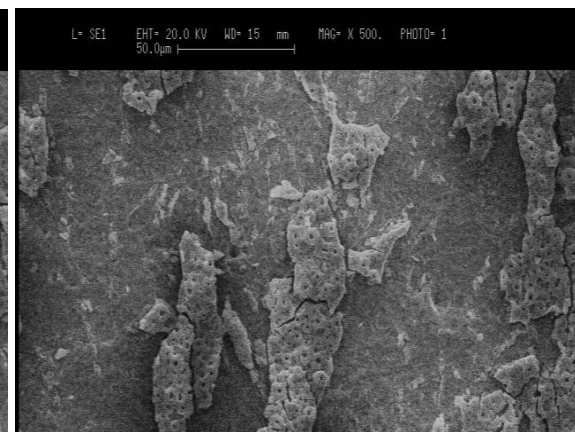
Fig 5.4.4 SEM 500X of Bended 265.R
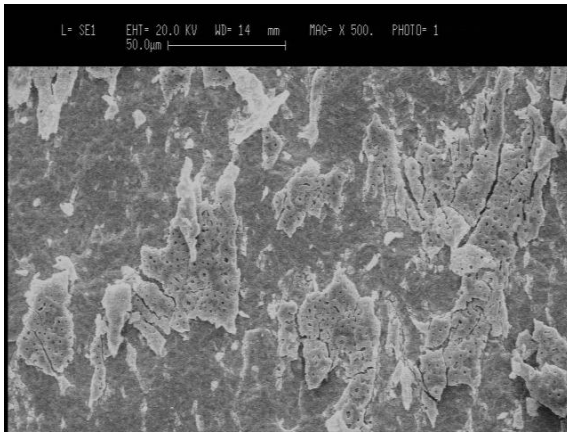
Fig 5.4.5 SEM 500X of Bended 255.R
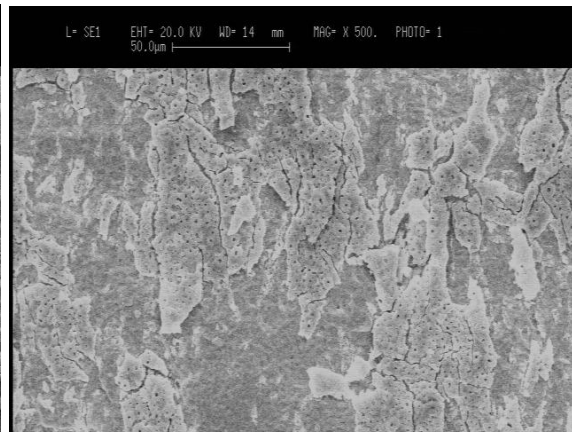
Fig 5.4.6 SEM 500X of Bended 245.R
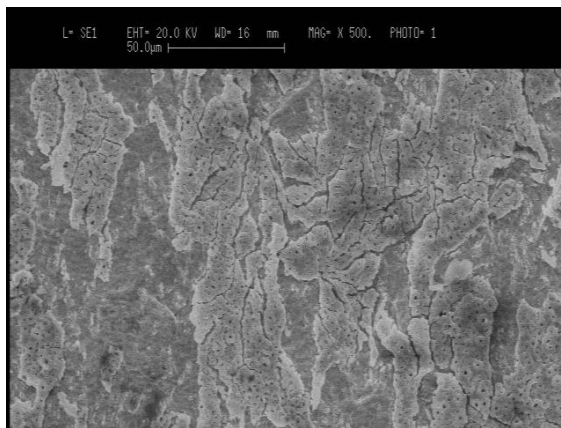
Fig 5.4.7 SEM 500X of Bended 235.R
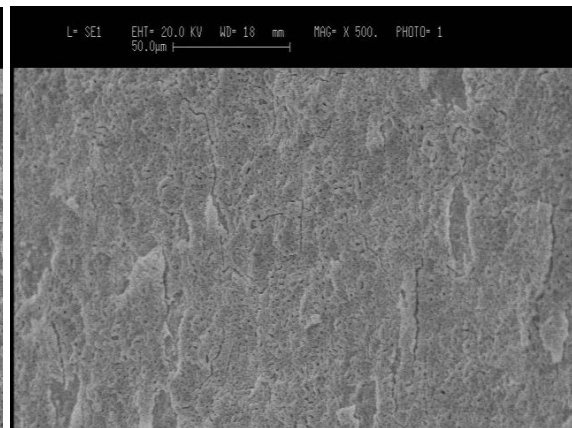
Fig 5.4.8 SEM 500X of Bended 225.R
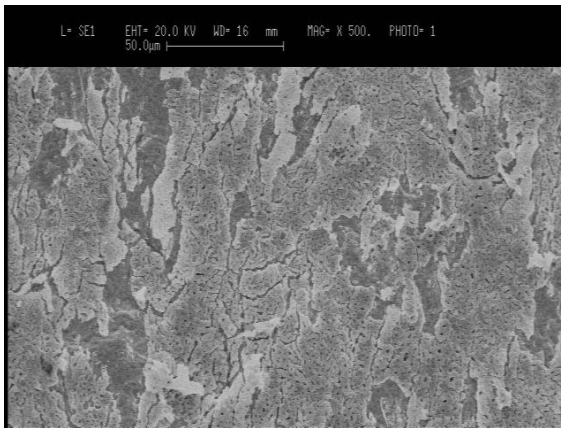
Fig 5.4.9 SEM 500X of Bended 215.R
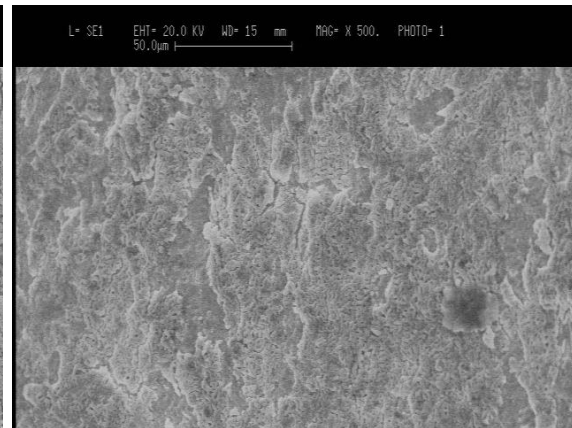
Fig 5.4.10 SEM 500X of Bended 205.R

And for lower voltage set, bended samples:
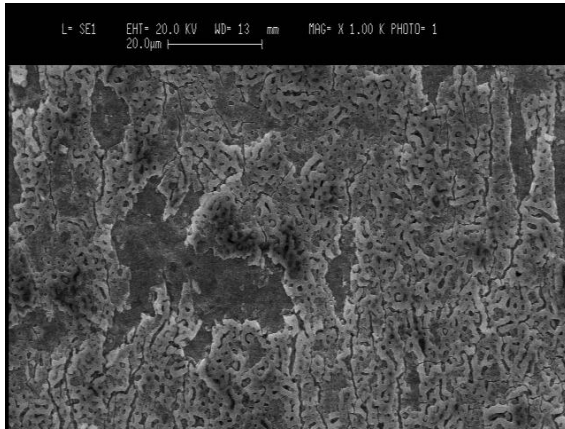
Fig 5.4.11 SEM 1K.X of Bended 195.R
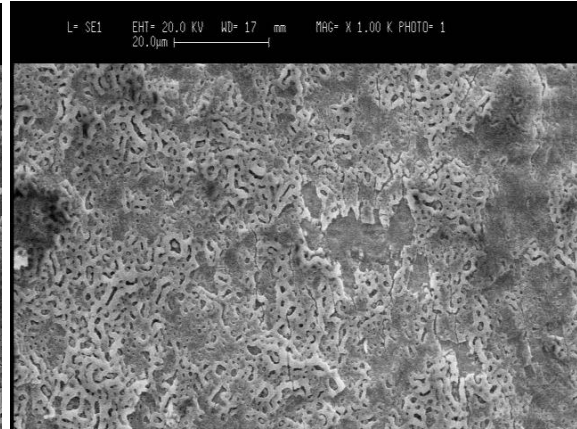
Fig 5.4.12 SEM 1K.X of Bended 185.R
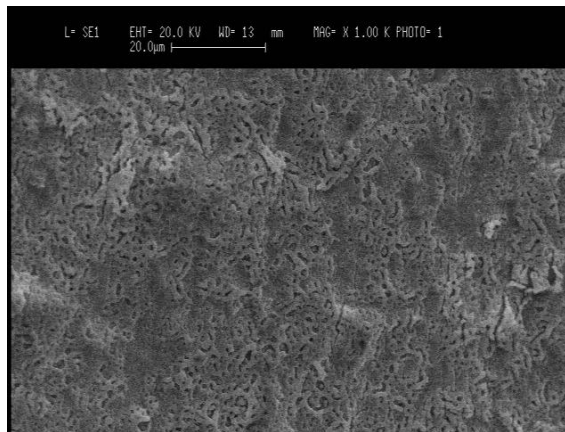
Fig 5.4.13 SEM 1K.X of Bended 175.R (12% ε)
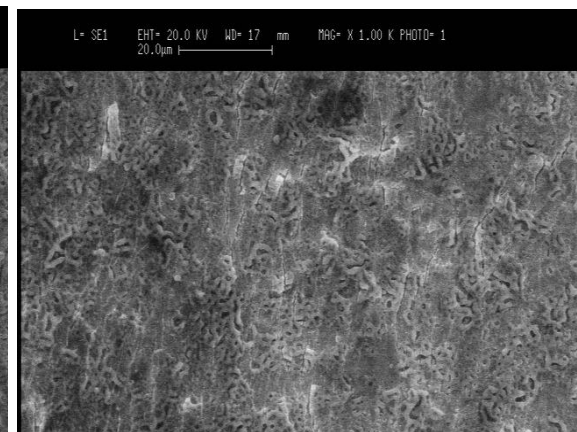
Fig 5.4.14 SEM 1K.X of Bended 175.R (5% ε)
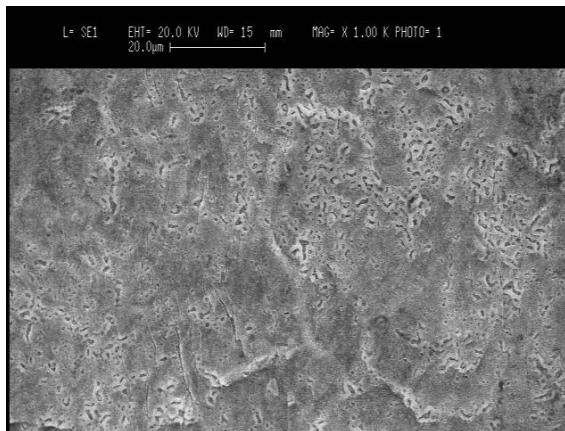
Fig 5.4.15 SEM 1K.X of Bended 165.R
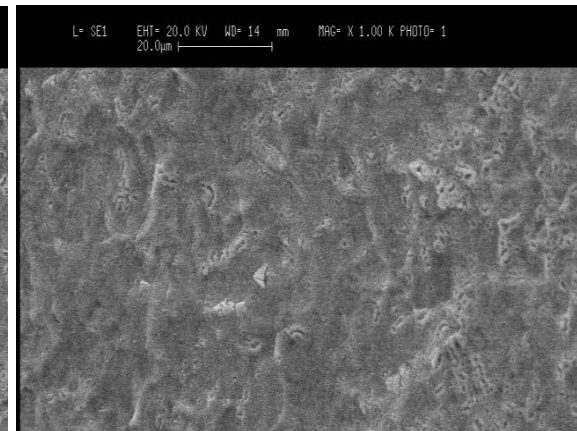
Fig 5.4.16 SEM 1K.X of Bended 155.R

5.5 ICP-OES

The ICP-OES analysis was carried out to evaluate the precise amount of important elements on the nominated coated samples (175.D.Na and 175.D).

It clearly demonstrates the effect of NaOH alkali treatment on alteration of chemical composition of coating. (Figure 5.5.1 and Figure 5.5.2)

Generally NaOH alkali treatment results in increase in Na level on the coated surface, meanwhile in our case it also leads to growth in Ca/P ratio.

Besides, no alteration on Si level observed during analysis.

Basically low level of doped elements on the coating deposited in lower final voltages was predictable due to previous semi-quantitative results of EDS. (Figure 5.2.11)

In Figure 5.5.3 Ca and Si amounts in 175V has been compared with 295V treated sample, regarding to the previous work which has been done to calculate chemical elements release from the surface of ASD treated titanium samples up to 21 days with the same electrolytic solution (SiB). [124]

Figure 5.5.3 demonstrates significant decrease in Ca level in 175 V up to one-fifth of its maximum value in 295 V.

The amount of Si in 175 V also falls down to almost half of its value in 295V treated samples.

ICP-OES result for 175.D
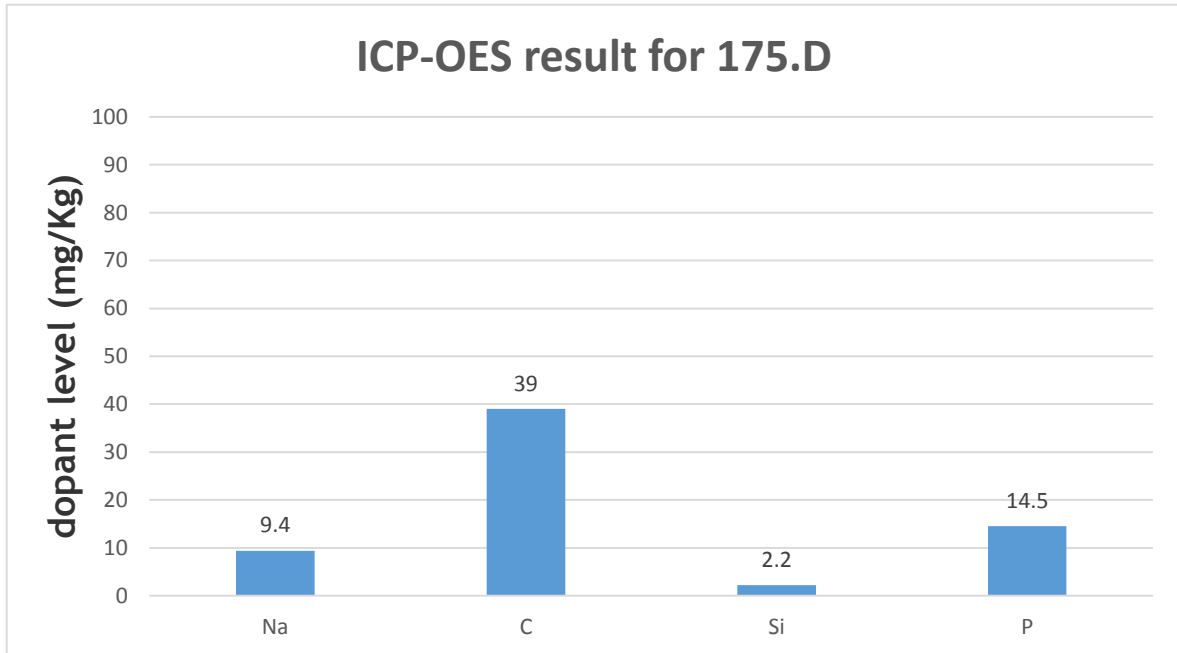
Fig 5.5.1 ICP-OES result for 327 mg non alkali treated 175.D

ICP-OES result for 175.D.Na
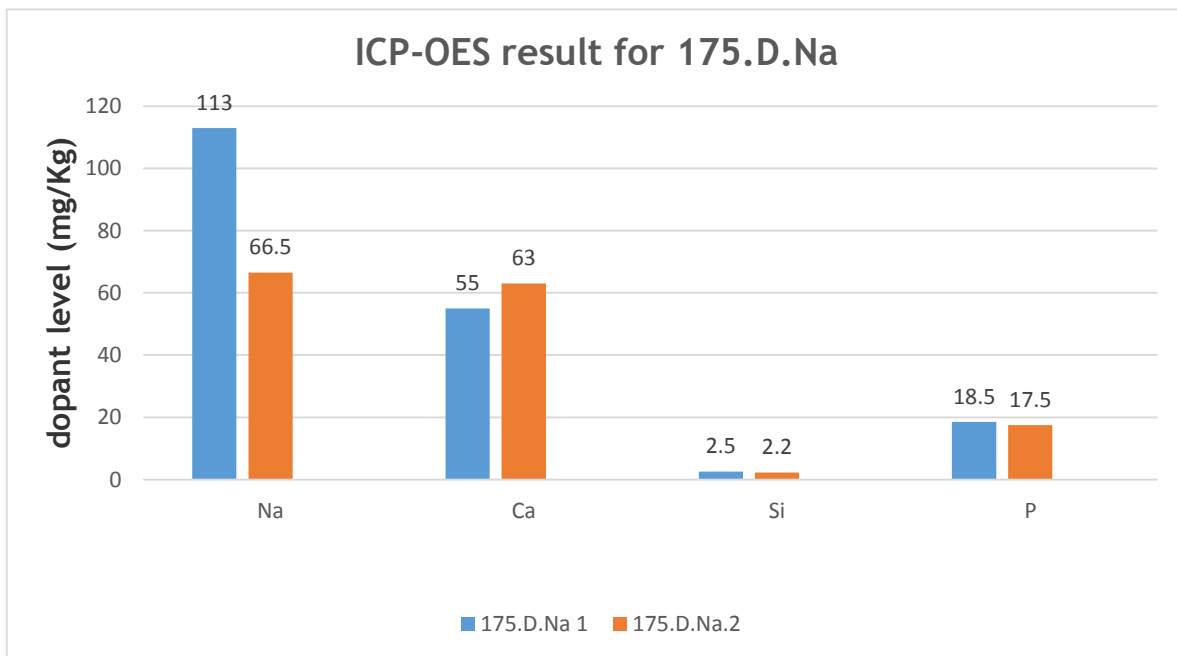
Fig 5.5.2 ICP-OES results for 328 mg and 329 mg alkali etched 175.D.Na
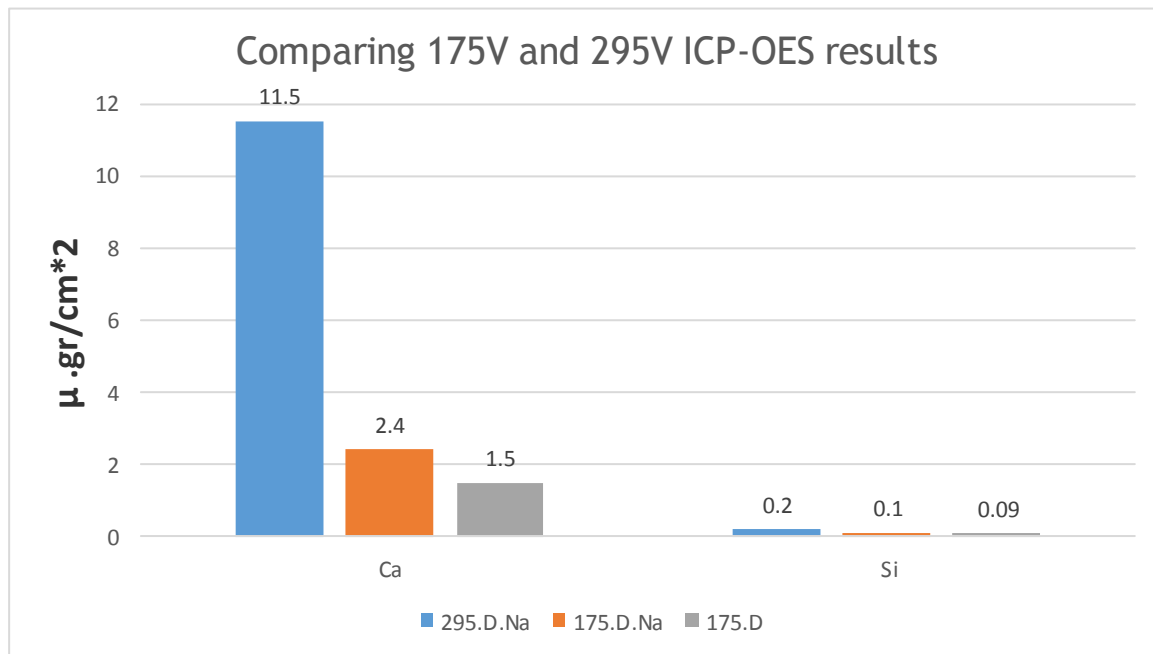
Fig 5.5.3 ICP-OES results for samples 295.D.Na, 175.D.Na and 175.D

5.6 Laser Profilometry (LP)

The surface average roughness (Ra), the maximum peak to valley height of the entire measurement area (Rz) and the kurtosis (K) parameter values are reported in Figure 5.5.4, Figure 5.5.5 and Figure 5.5.6 respectively.

The result for sample E (electropolished sample without ASD or any further treatment) has been taken from the previous thesis work done in Politecnico di Milano. [118]

Ra-Average roughness

Rz
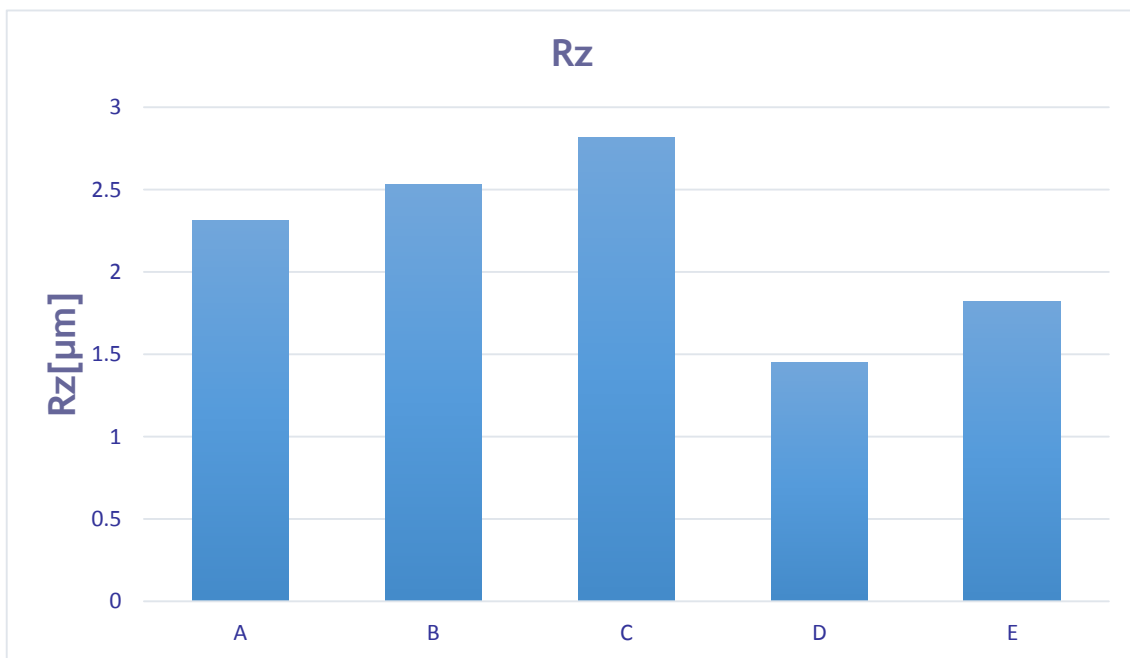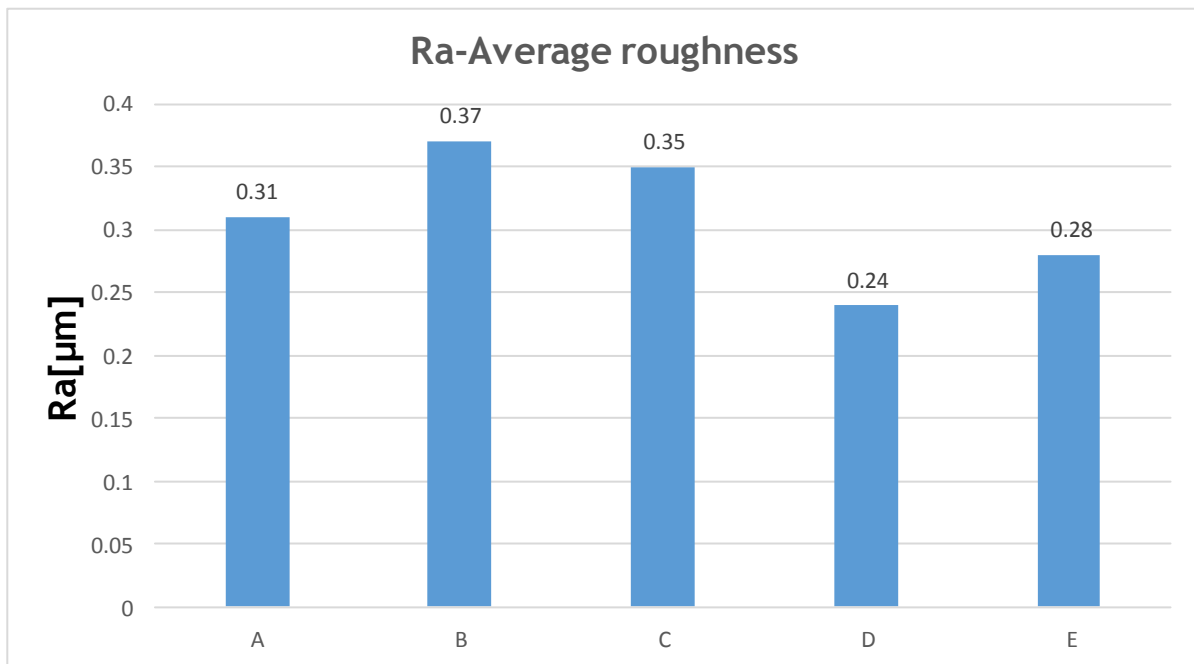
Fig 5.5.4 (first) and **Fig 5.5.5** (second) Surface average roughness Ra (first) and Rz (second) of the treated samples: A) Ti disk grade II without primary (HF-HNO3) etching & without ASD

treatment);B) 175.D sample primary (HF-HNO3) etched and ASD treated without alkali (NaOH) treatment); C) 175.D sample primary (HF-HNO3) etched and ASD treated followed by alkali (NaOH) treatment);D) 175.D sample primary electro-polished and then ASD treated without (HF-HNO3) and (NaOH) alkali treatment);E) Ti disk, electro-polished without ASD treatment, without (HF-HNO3) and (NaOH) alkali treatment
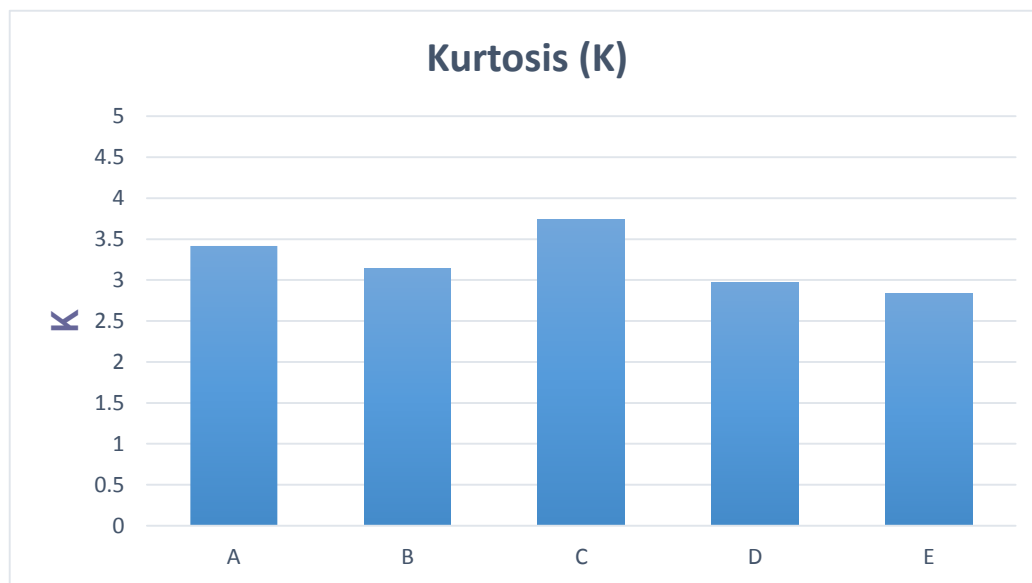
Fig 5.5.6 Surface roughness parameter K of the treated samples: A) Ti disk grade II without primary (HF-HNO3) etching & without ASD treatment); B) 175.D sample primary (HF-HNO3) etched and ASD treated without alkali (NaOH) treatment); C) 175.D sample primary (HF-HNO3) etched and ASD treated followed by alkali (NaOH) treatment) ;D) 175.D sample primary electro-polished and then ASD treated without (HF-HNO3) and (NaOH) alkali treatment) ;E) Ti disk, electro-polished without ASD treatment, without (HF-HNO3) and (NaOH) alkali treatment

	Ra	Rz (Din)	K
Sample A	0.31 ±0.02	2.31±0.40	3.41±0.84
Sample B	0.33±0.05	2.52±0.35	3.14±0.13
Sample C	0.35±0.06	2.81±1.09	3.74±0.86
Sample D	0.24±0.05	1.44±0.40	2.97±0.83
Sample E	0.28±0.06	1.82±0.55	5.34±1.81

Table1.8 Results of laser profilometry test in mean and standard deviation for: A) Ti disk grade II without primary (HF-HNO3) etching & without ASD treatment); B) 175.D sample primary (HF-HNO3) etched and ASD treated without alkali (NaOH) treatment); C) 175.D sample primary (HF-HNO3) etched and ASD treated followed by alkali (NaOH) treatment) ;D) 175.D sample primary electro-polished and then ASD treated without (HF-HNO3) and (NaOH) alkali treatment) ;E) Ti disk, electro-polished without ASD treatment, without (HF-HNO3) and (NaOH) alkali treatment

The results in Fig 5.5.4 demonstrate a slight increase in average surface roughness (Ra) for ASD treated surface (C) up to 0.35 µm in comparison with untreated titanium grade II (A) surface. (*0.31* µm) ($P < 0.05$)

Moreover, the surface roughness Ra is similar between ASD treated samples with alkali and non- alkali treatment. (Fig 5.5.4 B and C)

Electropolishing of the surface before ASD treatment (for the case D- electropolished sample followed by ASD treatment) remarkably decreases Ra parameter to almost 0.24 µm. (Table1.8)

It is worth mentioning that average Ra parameter for the electropolished sample which has not been treated by ASD (E), is about 0.28 µm and is moderately higher than the similar sample which firstly electropolished and then coated by ASD technique (D).($P < 0.05$)

Among analyzed samples, electropolished sample followed by ASD treatment (D) exhibits lowest value of Rz equal to 1.44 µm and ASD coated surfaces show higher value up to 2.5 µm.($P < 0.05$)

The kurtosis coefficient results similar among all the considered surfaces and is generally higher than 3 meaning that the surfaces are characterized by the presence of many peaks but in the case of electropolished and then ASD treated sample (D) the K parameter results significant lower than other cases; the K average values, for this surface, is less than 3, indicating a surface characterized by smooth surface profile. ($P < 0.05$)

Discussion

Nowadays, coronary angioplasty with deployment of stents is the most popular non-surgical treatment of coronary artery disease (CAD) which hold a coronary artery open to maintain blood flow after an angioplasty.

More than 2 million people get a stent each year all over the world, but unfortunately stenting is not a definitive answer to treatment of vessel occlusion symptoms.

In fact, In-Stent Restenosis (ISR) is the main limitation of coronary stenting,

Stenting with drug-eluting stents is a new promising method which delay to some extent the incidence of ISR pathology.

However, drug-coated stents are significantly more costly than other kinds of stents, so they are recommended only to patients who suffer a serious condition with predictable higher rates of ISR (diabetes, great lesion length, small caliber vessels, multiple stent implantations, etc.) [29]

In this work the possibility to coat titanium coronary stents with a layer of anodized titanium doped by different elements such as Ca, P, Na and Si is investigated, in the attempt of providing a titanium-core stent with a biocompatible coating, regarded as an alternative, cost-effective approach to drug-eluting stents for decreasing the incidence of ISR.

Titanium and titanium alloys considered as a first choice biomaterials for the majority of clinical treatments in the last few decades regarding to its unique combination of high mechanical properties, weightlessness, good workability and excellent resistance to corrosion.

Moreover, the low rates of corrosion and metallic ion release of titanium lead to very low degree of foreign body response.

previous studies showed the role of surface morphology modification of titanium dioxide layer on improvement of integration between stent surface and both vascular tissue and blood.[61][62]

Among vast surface modification techniques available to produce biocompatible coatings on titanium, the Anodic Spark Deposition technique (ASD) offers some notable advantages, such as the possibility to obtain mechanically stable and reproducible coatings on complex surfaces (like stents and dental implant) as well as feasibility to dope specific elements on the surface of metal by selecting a proper electrolytes.

In this Project SiB solution (containing $Na_2SiO_3*2H_2O$ 0.03M, b-GP 0.1M, $C_4H_6CaO_4*H_2O$ 0.3M, NaOH 0.036M) has been chosen as an electrolytic solution for ASD treatment and mechanical and physicochemical characterization of coating in wide range of deposition final voltage from (155 V to 295 V) has been investigated.

SEM analysis demonstrates that at higher voltage range ASD treated surfaces, pore size are circular and bigger in dimension, which are distributed more homogenously across the surface.

Meanwhile by lowering the voltage, pore size becomes smaller.

It also shows different morphology in lower voltage range from 235V downward to 155 V. (feasible minimum voltage in ASD treatment)

It mainly depicts elongated shape pores stretched out along the coated surface in a less homogeneous distribution pattern.

Three point Bending test then carried out by applying high plastic deformation (12%-13% of elongation) on coated samples.

The SEM analysis after three point bending test, showed sever delamination of coating treated at high final voltage range due to higher thickness of brittle oxide layer on titanium substrate.

However no peeling and delaminating occurred on the Ti–O film on lower voltage from 175 V downward which had undergone relatively high plastic deformation.

It demonstrates better adhesion of coating on 175V ASD treated substrate than other deposition method such as Sol-Gel coating method, which the maximum acceptable plastic deformation without any sign of Ti-O film delamination is less than 8%. [110]

The surfaces of all the samples which treated by NaOH alkali solution have water contact angle values lower than untreated titanium grade 2 indicating that the alkali etching after ASD treatment leads to a significant increase in surface hydrophilicity.

Among applied voltages, 175 V ,185 V,255 V and 295 V (which followed by alkali treatment)showed better wettability properties with average contact angle less than 55°(Berg's threshold) which is considered to limit the denaturation of adsorbed plasma proteins. (P<0.01) [103]

So the surface of titanium dioxide in these voltages show higher hydrophilic properties and regarding to this fact that hydrophilic surfaces enhance interactions with biological fluids, cells and tissues and have a better resistance to bacterial adhesion it is expected to lead to better biocompatibility in body environment. [126,127]

The EDS results demonstrate a decreasing trend for Ca level on the coating as treatment final voltage decreases.

On the other side, P level shows slight fluctuation.

It increases by increasing the treatment voltage and reaches to its peak at 205V then remains stable till 275 V where it follows by slight fall in P level.

It is important to mention that at around 215 V (treatment voltage), minimum difference between Ca and P level on the coating has been observed, so at 215 V, Ca/P ratio tends to almost 1.

Besides, Si level doesn't alter significantly by changing final treatment voltage. However, EDS results are semi-quantitative and are not precise so further analysis with ICP-OES has been carried out to calculate exact amount of dopants on the coating.

ICP-OES analyses indicates the effect of NaOH alkali treatment on alteration of Ca/P ratio for 175V ASD treated sample.

For 175 V non alkali treated sample Ca/P ratio is almost 2.69 while, after alkali treatment in 5M NaOH for 2h at 60 °C, Ca/P ratio increase and reach to approximately 3.6.

Besides, due to the nature of this kind of treatment, level of Na has been raised sharply on the alkali treated coatings.

Comparison between our ICP-OES results with the results for Ca and Si release from ASD treated sample at 295 V, (regarding to the previous work which has been done with the same electrolytic solution [124]) exhibit notable decrease in Ca level while Si level has not been changed remarkably.

The result of SEM analysis for the nominated sample (175V) which has been electropolished before ASD treatment displays the same morphological pattern as 175V deposited sample without any electropolishing.(Figure 5.1.H)

It demonstrates that electropolishing before ASD treatment is not changing the final surface morphology of the coating, but only modifies the surface roughness of the samples.

Nonetheless, the concern of the project was evaluation of non-electropolished samples, so electropolishing has been just done to compare the results.

In general, electropolishing reduces the roughness of the surface which influences the amount of protein adherence, as it determines the contact area of the stent with coronary artery. [131]

The results of laser profilometry analysis also demonstrates that electropolishing of the surface before ASD treatment (for the case D-electropolished sample followed by ASD treatment) remarkably decreases Ra parameter to almost 0.24 µm. (Table1.8)

Average Ra parameter for the electropolished sample which has not been treated by ASD (E), is about 0.28 µm and is moderately higher than the same sample which firstly electropolished and then coated by ASD technique (D). (P<0.05) (Table1.8)

Average micro roughness (Ra) of the available coronary stents covers range of 0.11 µm to 0.6 µm, [130] meanwhile, the results of laser profilometry analysis for all the ASD treated samples exhibit value lower than 0.36 µm.

Recent studies related to the effect of Ca and P dopant coated on the surface of stents exhibit less adhesion and activation of platelets in presence of each of these elements. [64, 73]

However when both of these elements are combined together and constitute the outer surface with Ca/P ratio of 1:10 (atomic concentration), it results in some inferior blood compatibility. [64]

Nevertheless, this project mainly focuses on mechanical and physicochemical characteristics of above mentioned coating with a different Ca/P ratio, and biological interaction of these elements with blood cells requires further in vitro investigations.

Conclusion and future works

In this project the possibility to coat titanium coronary stents with a layer of anodized titanium doped by different elements such as Ca, P, Na and Si by ASD treatment method was investigated, in the attempt of providing a Ti-core stent with a new biocompatible coating.

One of the main challenge of this project was to find maximum ASD treatment voltage needed to guarantee appropriate adherence of coating on titanium substrate at approximately high level of applied plastic deformation (12 %-13%).

The results of SEM analysis showed, 175 V is the optimum voltage which can be applied on the titanium rectangular shape substrate by ASD treatment, which result in (bended) coating without any trace of delamination or peeling.

Although lower voltages (below 175V) also satisfy mechanical aspect of the project, EDS analysis demonstrated that level of dopants deposited on their surfaces were much lower compared to 175V deposited coating .

Besides , 175V and 185V ASD treated samples which followed by chemical NaOH alkali treatment showed better wettability characterization than other samples with contact angle less than 55° (Berg's threshold) which is expected to lead to better biocompatibility in body environment due to the enhancement of interactions with biological fluids, cells and tissues.(P<0.01) [126,127]

Average micro roughness (Ra) of the available coronary stents covers range of 0.11 μm to 0.6 μm, [130] besides, results of laser profilometry analysis for all the ASD treated samples showed Ra values lower than 0.36 μm which are in the acceptable range of surface roughness for the stent production. (p<0.05)

Since this work, deals only with mechanical and physiochemical terms of stent production, further in vitro investigations are required for a better understanding body biological response to this new kind of coating for stents.

In light of these considerations, the ASD treatment on titanium with SIB electrolytic solution (containing Na2SiO3*2H2O 0.03M, b-GP 0.1M, C4H6CaO4*H2O 0.3M, NaOH 0.036M) which previously developed for dental and orthopedic applications can also be applicable (in term of mechanical and physiochemical aspects) in stent production and related fields such as endovascular surgery and stent placement in hemodialysis access. [129]

Since this work mainly focused on mechanical and physicochemical characteristics of coating deposited on titanium surface thus further in vitro investigations are required for a better understanding of body biological response to this new kind of stent coating.

Chapter X

References

[1] Paul A. Iaizzo, Handbook of Cardiac Anatomy, Physiology, and Devices

[2] Countries, Committee on Preventing the Global Epidemic of Cardiovascular Disease: Meeting the Challenges in Developing; Fuster, Board on Global Health ; Valentin; Academies, Bridget B. Kelly, editors ; Institute of Medicine of the National (2010)

[3] Fuster, V; Alexander RW; O'Rourke RA (2001). Hurst's the Heart (10th Ed.). McGraw-Hill. ISBN 0-07-135694-0.

[4] Santarone M, Boscarini M, Ghezzi I, Repetto S (June 1988). "Unusual origin and course of the first septal branch of the left coronary artery: angiographic recognition"

 [5] George Dangas and Frank Kuepper, Restenosis: Repeat Narrowing of a Coronary Artery- Prevention and Treatment, 2002

[6] Serruys PW, Luijten HE, Beatt KJ, et al. Incidence of restenosis after successful coronary angioplasty: a time- related phenomenon: a quantitative angiographic study in 342 consecutive patients at 1, 2, 3, and 4 months circulation. 1988; 77:361–371.

[7] Serruys PW, de Jaegere P, Kiemeneij F, et al. A comparison of balloon expandable-stent implantation with balloon angioplasty in patients with

coronary artery disease. Benestent Study Group. N Engl J Med. 1994; 331:489–495.

[8] Fischman DL, Leon MB, Baim DS, et al. A randomized comparison of Coronary-stent placement and balloon angioplasty in the treatment of Coronary artery disease. Stent Restenosis Study Investigators. N Engl J Med. 1994; 331:496–501.

[9] Lowe H, Oesterle S, Khachigian L; Coronary in stent restenosis: current status and future strategies; J Am Coll Cardiol 2002 39:183–93

[10] Woods TC, Marks AR. Drug-eluting stents. Annu Rev Med 2004; 55:169–178

[11] Approaches for Prevention of Restenosis, Amir Kraitzer, Yoel Kloog, Meital Zilberman, 2007

[12] Hofma SH, van Beusekom HM, Serruys PW, van Der Giessen WJ. Recent developments in coated stents. Curr Interv Cardiol Rep 2001; 3:28–36

[13] Haery C, Sachar R, Ellis SG. Drug-eluting stents: The beginning of the end of restenosis? Cleve Clin J Med 2004; 71815–824

[14] El-Omar M, Dangas G, Iakovou I, Mehran R; Update on In-stent Restenosis; Current Interventional Cardiology Reports 2001, 3:296–305

[15] Lau K.W, Johan A, Sigwart U, Hung J.S; A stent is not just a stent: stent construction and design do matter in its clinical performance; Singapore Med J 2004 Vol 45(7):305-312

[16] Indolfi C, Mongiardo A; Molecular mechanisms of in-stent restenosis and approach to therapy with eluting stents; Trends Cardiovasc Med 2003;13:142–148

[17] Abizaid A, Kornowski R, Mintz GS et al. The influence of diabetes mellitus on acute and late clinical outcomes following coronary stent implantation. J Am Coll Cardiol 1998; 32: 584–9.

[18] Elezi S, Kastrati A, Pache J et al. Diabetes mellitus and the clinical and angiographic outcome after coronary stent placement. J Am Coll Cardiol 1998; 32: 1866–73.

[19] Mittal S, Weiss DL, Hirshfeld JW, Kolansky DM, Herrmann HC. Restenotic lesions have a worse outcome after stenting. Circulation 1996; 94: I-331.

[20] Kastrati A, Scho¨mig A, Elezi S et al. Predictive factors of restenosis after coronary stent placement. J Am Coll Cardiol 1997; 30: 1428–36.

 [21] Elezi S, Kastrati A, Neumann FJ, Hadamitzky M, Dirschinger J, Scho¨mig A. Vessel size and long-term outcome after coronary stent placement. Circulation 1998; 98: 1875-80.

 [22] Kastrati A, Elezi S, Dischinger J, Hadamitzky M, Neumann FJ, Scho¨mig A. Influence of lesion length on restenosis after coronary stent placement. Am J Cardiol 1999; 83: 1617–22

[23] Marcus AJ. Thrombosis and inflammation as multicellular processes: Significance of cell-cell interactions.1994; PP 261–269

[24] Libby P, Simon DI. Inflammation and thrombosis: the clot thickens. Circulation. 2001; 103:1718–1720

[25] Santin M, Mikhalovska L, Lloyd A; In vitro host response assessment of biomaterials for cardiovascular stent manufacture; Journal of materials science: materials in medicine 15(2004), 473-477

[26] James N. George, TTP-HUS (Thrombotic Thrombocytopenic Purpura - Hemolytic Uremic Syndrome), 2014

[27] HARLAN J. M., THOMPSON P. J., ROSS R., BOWEN-POPE D. F. (1986) α-Thrombin induces release of platelet-derived growth factor-like molecule(s) by cultured human endothelial cells. J. Cell Biol. 103:1129–1133

[28] DANIEL T. O., GIBBS V. C., MILFAY D. F., GAROVOY M. R., WILLIAMS L. T. (1986) Thrombin stimulates c-sis gene expression in micro vascular endothelial cells. J. Biol. Chem. 261:9579–9582

 [29] Santin M, Colombo P, Bruschi G; Interfacial biology of in-stent restenosis; Expert Rev.Med. Devices 2(4), 2005

[30] Fukuda D, Shimada K; Circulating monocytes and in-stent neointima after coronary stent implantation; J Am Coll Cardiol 2004; 43: 18–23

[31] Libby P; Inflammation in atherosclerosis; Nature 2002, Vol. 420: 868-874

[32] Zhi-Ping Liu, Phenotypic Modulation of Smooth Muscle Cells through Interaction of Foxo and Myocardin 2005,

[33] Moiseeva E; Adhesion receptors of vascular smooth muscle cells and their functions; Cardiovascular Research 52 (2001) 372–386

[34] Evanko S, Johnson P; Platelet derived growth factor stimulates the formation of versican-hyaluronan aggregates and peri-cellular matrix expansion in arterial smooth muscle cells; Archives of Biochemistry and Biophysics Vol. 394, No. 1, October 1, pp. 29–38, 2001

[35] Bruce Alberts, Alexander Johnson Molecular Biology of the Cell, Fifth Edition.

[36] Laurent TC, Fraser JR Hyaluronan. 1992 Apr; 6(7):2397-404

[37] Moore J.E; Effects of stent design on arterial mechanics: implications for thrombosis and restenosis; BED-Vol. 50, Bioengineering Conference, 2001

[38] Thomas N Wight Versican: a versatile extracellular matrix proteoglycan in cell biology, 2002

[39] Santin M, Colombo P, Bruschi G; Interfacial biology of in-stent restenosis; Expert Rev.Med. Devices 2(4), 2005

[40] Lisa T. Newsome; A Protocol for the Perioperative Management of Patients With Intracoronary Drug-Eluting Stents, 2007

[41] Windecker S, Mayer I, De Pasquale G; Stent coating with titanium-nitride-oxide for reduction of neointimal hyperplasia; Circulation. 2001; 104:928-933

[42] Arjomand H, Turi Z, McCormick D, et al. Percutaneous coronary intervention: historical perspectives, current status, and future direction. Am Heart J 2003; 146:787-96.

[43] Serruys PW, Kutryk MJB, Ong ATL. Coronary-artery stents. N Engl J Med 2006; 354:483-95.

[44] Moliterno DJ. Healing Achilles—sirolimus versus paclitaxel. N Engl J Med 2005; 353:724-6.

[45] Jeffrey Caren; Stents and Coronary Angioplasty, 2014

[46] Greenberg D, Cohen D.J; Examining the economic impact of restenosis: implications for the cost-effectiveness of an antiproliferative stent; Z Kardiol 91: Suppl 3, III/137 – III/143(2002)

[47] Sultan F, Kazmi K, Dhakam S, Quraishi A; Late in-stent restenosis in a patient with drug-eluting stent; JCPSP 2005, Vol. 15(10): 648-649

[48] L.L. Hench, "Biomaterials", Science 208 (1980) 826–831.

[49] Sanjay Pant Geometry parameterization and multidisciplinary constrained Optimization of coronary stents

[50] Bertrand O.F, Sipehia R, Mongrain R; Biocompatibility aspects of new stent technology; J Am Coll Cardiol 1998;32:562–71

[51] Pache J, Intracoronary stenting and

Angiographic results: strut thickness effect on restenosis outcome

(isar-stereo-2) trial. J Am Coll Cardiol 41(8):1283–1288

[52] Alderson H, Zamir M; Mechanical aspects of stenting on local haemodynamics.2003

[53] Curcio A, Torella D, Coppola C, Mongiardo A; Coated stents: a novel approach to prevent in-stent restenosis; Ital Heart J 2002; 3(Suppl 4): 16S-19S

[54] Raval A, Choubey A, Engineer C, Kothwala D; Development and assessment of 316LVM cardiovascular stents; Materials Science and Engineering A 386(2004) 331–343

[55] T Duerig, An overview of nitinol medical applications 10.1016/S0921 .1999

[56] Nicoud F; Haemodynamic changes induced by stenting in elastic arteries; Center for turbulence research, Annual research briefs. 2002

[57] Taylor A. Metals. In: Sigwart U, ed. Endoluminal Stenting. London,

Philadelphia, Toronto, Sydney, Tokyo: WB Saunders, 1996:28 –33.

[58]Ratner B, Hoffman A, Schoen F, Lemons J, eds. An introduction to

Materials in medicine. San Diego, London, Boston, New York, Sydney, Tokyo, Toronto: Academic Press, 1996.

[59]. Park JB. Metallic Biomaterials. In: Branzino JD, Ed. The Biomedical Engineering Handbook. Boca Raton: CRC Press, 1995:537–71.

[60] S. W. Robertson1, CYCLIC FATIGUE OF NITINOL International Conference on Shape Memory and Super elastic Technologies October 2004,

[61] De Scheerder I, Wang K, Zhao H, Sohier J; Metallic surface treatment using electrochemical polishing decreases thrombogenicity and neointimal hyperplasia; JACC February 1998

[62] k.wang; Biocampatibilsation of coronary artery stents ,Leuven ,1997

[63] B.michaels Stents: Traditional Metals Reign, But Bioresorbables are rising, 2014

[64] S.C.H. Kwok, Biocompatibility of calcium and phosphorus doped diamond-like carbon thin films synthesized by plasma immersion ion implantation and deposition. 2005

[65] Paolo Moroni; "Development and in vitro characterization of titanium surfaces".2005

[66] Web source: Aneurysm Surgery - Aortic Aneurysms by the society of thoracic surgeons. http://www.sts.org

[67] Robin Reichert, Titanium Stents vs. Magnetic Therapy

[68] Web source: http://karweigoay.blogspot.it/2013/10/coronary-heart-disease-updates-in.html

[69] Tanguay J, Zidar J, Phillips H, Stack R. Current status of biodegradable stents. Cardiol Clin. 1994; 12: 699–713.

[70] van der Giessen W, Lincoff A, Schwartz R, van Beusekom H, Serruys PW, Holmes D, Ellis S, Topol EJ. Marked inflammatory sequelae to implantation of biodegradable and nonbiodegradable polymers in porcine coronary arteries. Circulation. 1996; 94: 1690–1607.

[71] Zartner P, Cesjnevar R, Singer H, Weyand M. First successful implantation of a biodegradable metal stent into the left pulmonary artery of a preterm baby. Catheter Cardiovasc Interv. 2005; 66: 590–594.

[72] Kimura T, Abe K, Shizuta S, Odashiro K, Yoshida Y, Sakai K, Kaitani K, Inoue K, M. Long-term clinical and angiographic followup after coronary stent placement in native coronary arteries. Circulation. 2002; 105: 2986–2991.

[73] P.D. Maguire; Mechanical stability, corrosion performance and bio response of amorphous diamond-like carbon for medical stents and guide wires, 2005.

[74] Boris Michael Holzapfel, Johannes Christian Reichert, Jan-Thorsten Schantz, Maximilian Rudert, Jürgen Groll, Dietmar Werner Hutmacher, "How smart do biomaterials need to be? A translational science and clinical point of view", Elsevier, ADR-12336

[75] N. Huebsch, D.J. Mooney, Inspiration and application in the evolution of biomaterials,Nature 462 (2009) 426–432.

[76] L. De Nardo, L. Altomare, B. Del Curto, A. Cigada and L. Draghi, "Electrochemical surface modifications of titanium and titanium alloys for biomedical applications", in R.Driver (Ed.), Coatings for biomedical applications, Cambridge: 106-111.

[77] Long M, Rack HJ, "Titanium alloys in total joint replacement--a materials science perspective", Biomaterials. 1998 Sep; 19(18):1621-39.

[78] Wang, K. The use of titanium for medical applications in the USA. Mater. Sci. Eng. A 1996, 213, 134–137.

[79] Navarro M, Michiardi A, Castaño O, Planell JA. "Biomaterials in orthopaedics" J R Soc Interface. 2008 Oct 6; 5(27):1137-58.

[80] CRC Handbook of Chemistry and Physics, CRC Press, 92nd Edition, 2011. G. W. C. Kaye and T. H. Laby Tables of Physical and Chemical Constants, Longman, 16th Edition, 1995.

[81] Titanium Alloys and Their Characteristics: Part Two web source

http://www.keytometals.com/

[82] Corrosion, web source http://www.gc3.com/

[83] Pourbaix diagram of titanium; web source http://www.sigmaaldrich.com

[84] Brunette M.D; Titanium in medicine; Springer biomaterials book, 2001

[85] Libby P; Inflammation in atherosclerosis; Nature 2002, Vol. 420: 868-874

[86] Lim I.A; Biocompatibility of stent materials; MURJ Vol.11 (2004)

[89] Textor M(2001), "Properties and biological significance of natural oxide films on titanium and its alloys", in Brunette D M, Tengvall P, Textor M and Thomsen P, Titanium in medicine: material science, surface science, engineering, biological responses, and medical applications, Berlin; New York, Springer: 171-230

[90] Vu N.H, Le H.V, Cao T.M, Pham V.V, Le H.M, Nguyen-Manh, "D.Anatase-rutile phase transformation of titanium dioxide bulk material: a DFT + U approach", J Phys Condens Matter. 2012 Oct 10; 24(40):405501. doi: 10.1088/0953-8984/24/40/405501. Epub 2012 Sep 6

[91] Xuanyong Liu, Paul K. Chu, Chuanxian Ding, "Surface modification of titanium, titanium alloys, and related materials for biomedical applications", Materials Science and Engineering R 47 (2004) 49–121

[92] TITANIA NANOTUBES FOR ENHANCED SOLAR ENERGY HARVESTING Web source: http://thurj.org/

[93] R, Sandrini E, Santin M, Rondelli G, Cigada A, "Osteointegration of titanium and its alloys by anodic spark deposition and other electrochemical techniques: a review", Biomater Biomech. 2003 May-Aug; 1(2):91-107.

[94] Della Valle C, Rondelli G, Cigada A, Bianchi A.E, Chiesa R, "A novel silicon-based electrochemical treatment to improve osteointegration of titanium implants" , J Appl Biomater Function Mater. 2012

[95] Titanium oxidation ,web source http://micropat.ch/

[96] X. Lu, B Leng, "Nano-Ag-loaded hydroxyapatite coatings on titanium surfaces by electrochemical deposition", Journal of the Royal Society, Interface / the Royal Society, vol. 8, Apr. 2011

[97] X. Zhu, K.H. Kim, J.L. Ong, and S. Kim, "Surface characteristics and structure of anodic oxide films containing Ca e P on a titanium implant material", Journal of Biomedical Materials Research, vol. 60, 2002

[98] H. Ishizawa and M. Ogino, "Formation and characterization of anodic titanium oxide films containing Ca e O", Journal of Biomedical Materials Research, vol. 29, 1995, pp.65-72.

[99] L. De Nardo, L. Altomare, B. Del Curto, A. Cigada and L. Draghi, "Electrochemical surface modifications of titanium and titanium alloys for biomedical applications", in R. Driver (Ed.), Coatings for biomedical applications, Cambridge: Woodhead: 106-111.

[100] PTCA with stent implantation web source: http://vedmedi.ru

[101] R. Chiesa, A. Cigada, C. Della Valle, G. Rondelli, G. Candiani, and C. Giordano, "Silicon-based biomimetic treatment for the osteointegration of metal substrates," WO/2010/013120, 2010.

[102] C. Della Valle, "Sviluppo di Trattamenti Biomimetici a base di Silicio per l' osteointegrazione Del Titanio," Politecnico di Milano Thesis, 2007.

[103] Simone Panzuto, Development and characterization of antibacterial treatments for titanium obtained by anodic spark deposition

[104] G.P. Wirtz, S.D. Brown & W.M. Kriven, "Ceramic Coatings by Anodic Spark Deposition",Pages 87-115 in Materials and Manufacturing Processes Volume 6, Issue 1, 1991.

[105] Chiesa R, Cigada A, Della Valle C, Rondelli G, Candiani G, Giordano G: "Metal substrates modified with silicon-based biomimetic treatment for the osteointegration thereof". EP2479318-A1 (2012)

[106] Sverzut A.T, de Albuquerque G.C, Crippa G.E, Chiesa R, Della Valle C, de Oliveira P.T, Beloti M.M, Rosa A.L, "Bone tissue, cellular, and molecular responses to titanium implants treated by anodic spark deposition", J Biomed Mater Res A. 2012 Nov;100(11):3092-8.

[107] Sandrini E, Morris C, Chiesa R, Cigada A., Santin E, "In vitro Assessment of the Osteointegrative Potential of a novel Multiphase Anodic Spark Deposition Coating for Orthopaedic and Dental Implants", J. Biomed. Mater. Res. B Appl. Biomater. 2005 May; 73(2):392-9.

[108] J. Goldstein, D. Newbury, D. Joy, C. Lyman, P. Echlin, and E. Lifshin, Scanning Electron Microscopy and X-Ray Microanalysis, Springer, 2003.

[109]   Contact   angle   scheme,   web   source: http://en.wikipedia.org/wiki/Contact_angle

[110] Dong Xie, Deformation and corrosion behaviors of Ti–O film deposited 316L stainless steel by plasma immersion ion implantation and deposition,2013

[111] ASTM D790, Standard Test Method for Elastic Modulus by Thermo mechanical Analysis Using Three-Point Bending and Controlled Rate of Loading.

[112] Xiandeng Hou and Bradley T. Jones; Inductively Coupled Plasma/Optical Emission Spectrometry.

[113] inductively coupled plasma atomic emission spectroscopy, from web source Wikipedia

[114] B. L. Sawhney and D. E. Stilwell; Dissolution and Elemental Analysis of Minerals, Soils and Environmental Samples, 1994.

[115] wettability, web source; http://en.wikipedia.org/wiki/Wetting

[116] Coronary artery, web source: www.crosslogicproductions.com

[117] web source: http://www.astm.org

[118] Alfonso Marchetti ,Angelo Vozza,Modifiche di Superficies u substrati di titanio per applicazioni casiovascolari,2014

[120] Angioplasty, web source; http://www.ask4healthcare.com

[121] Thomas J Vander Salm,What constitutes optimal surgical revascularization?: Answers from the bypass angioplasty revascularization investigation (BARI) ,2002

[122] Tanishita Web soruce : https://staff.aist.go.jp

[123] web source: http://www.bostonscientific.com

[124] Cinzia Della Valle, Development of antibacterial surface modification treatments for titanium to improve the osteointegration, 2012

[125] (66 old) Lim I.A; Biocompatibility of stent materials; MURJ Vol.11 (2004)

[126] K. Merrit and Y.H. An, "Factors Influencing Bacterial Adhesion," Handbook of Bacterial Adhesion: Principles, Methods, and Applications, Y.H. An and R.J. Friedman, eds., Totowa, NJ, USA: Humana Press Inc., 2000

[127] G. Zhao, Z. Schwartz, M. Wieland, F. Rupp, J. Geis-Gerstorfer, and D.L. Cochran, "High surface energy enhances cell response to titanium substrate microstructure," Journal of Biomedical Materials Research, vol. 74, 2005, pp. 49-58.

[128] Virmani R, Farb A; Pathology of in-stent restenosis; Curr Opin Lipidol 1999, 10(6): 499-506

[129] Alexander Yevzlin, Arif Asif, Stent Placement in Hemodialysis Access: Historical Lessons, the State of the Art and Future Directions, 2009

[130] 4th European Conference of the International Federation for Medical and Biological Engineering.Nov 2008 Belgium,PP 2241

[131] Andrade, J.D. and Hlady, V., Plasma Protein Adsorbtion: The Big Twelve, In: Leonard, E.F., Turitto, V.T. and Vroman, I. (Eds), Blood in Contact with Natural and Artificial Surfaces, Annals of the New York Academy of Sciences, NY,1983, 153.